JOURNAL OF GEOPHYSICAL RESEARCH

The continuation of

ERRESTRIAL MAGNETISM AND ATMOSPHERIC ELECTRICITY

(1896-1948)

An International Quarterly

OLUME 57 December, 1952 NUMBER 4

CONTENTS

(Contents concluded on outside back cover)

Part one of two parts

PUBLISHED BY

THE WILLIAM BYRD PRESS, INC.

P. O. Box 2-W—Sherwood Ave. and Durham St., Richmond 5, Virginia

FOR THE JOHNS HOPKINS PRESS, BALTIMORE 18, MARYLAND

EDITORIAL OFFICE:

5241 Broad Branch Road, Northwest, Washington 15, D.C., U.S.A.

THREE DOLLARS AND FIFTY CENTS A YEAR SINGLE NUMBERS, ONE DOLLAR

JOURNAL OF GEOPHYSICAL RESEARCH

The continuation of

Terrestrial Magnetism and Atmospheric Electricity

(1896-1948)

An International Quarterly

Founded 1896 by L. A. BAUER *Continued 1928–1948 by* J. A. FLEMING

Fields of Interest

Terrestrial Magnetism
Atmospheric Electricity
The Ionosphere
Solar and Terrestrial Relationships
Aurora, Night Sky, and Zodiacal Light
The Ozone Layer
Meteorology of Highest Atmospheric Levels
The Constitution and Physical States of the Upper Atmosphere
Special Investigations of the Earth's Crust and Interior, including experimental seismic waves, physics of the deep ocean and ocean bottom, physics in geology
And similar topics

This Journal serves the interests of investigators concerned with terrestrial magnetism and electricity, the upper atmosphere, the earth's crust and interior by presenting papers of new analysis and interpretation or new experimental or observational approach, and contributions to international collaboration. It is not in a position to print, primarily for archive purposes, extensive tables of data from observatories or surveys, the significance of which has not been analyzed.

Forward *manuscripts* to the editorial office of the Journal at 5241 Broad Branch Road, Northwest, Washington 15, D. C., U.S.A., or to one of the Associate Editors. It is preferred that manuscripts be submitted in English, but communications in French, German, Italian, or Spanish are also acceptable. A brief abstract, preferably in English, must accompany each manuscript. A *publication charge* of $4 per page will be billed by the Editor to the institution which sponsors the work of any author; private individuals are not assessed page charges. Manuscripts from outside the United States are invited, and should not be withheld or delayed because of currency restrictions or other special difficulties relating to page charges. Costs of publication are roughly twice the total income from page charges and subscriptions, and are met by subsidies from the Carnegie Institution of Washington and international and private sources.

Back issues and *reprints* are handled by the Editorial Office, 5241 Broad Branch Road, N.W., Washington 15, D.C., U.S.A.

Subscriptions are handled by The Johns Hopkins Press, Baltimore 18, Maryland, U.S.A.

THE JOHNS HOPKINS PRESS

Baltimore 18, Maryland

Entered as second-class matter at the Post Office at Richmond, Virginia, under the act of March 3, 1879.

Journal of

GEOPHYSICAL RESEARCH

The continuation of

Terrestrial Magnetism and Atmospheric Electricity

VOLUME 57 DECEMBER, 1952 No. 4

AN INVESTIGATION OF THE IONIZING EFFECT IN THE *E*-LAYER NEAR SUNRISE*

BY RUNE LINDQUIST**

Ionosphere Research Laboratory, The Pennsylvania State College, State College, Pennsylvania

(Received April 18, 1952)

ABSTRACT

This paper discusses the pre-sunrise decrease in height of the reflection point noted in 150 kc/sec vertical incidence group height recordings. It is shown that the local time of this decrease has a pronounced seasonal variation. The total number of particles along the sun ray to the reflection point where the height decrease begins has been computed. This number is almost constant throughout the year, yielding a value of about 3.3×10^{20} atmospheric particles.

By considering the composition of the upper atmosphere, it is shown that the only constituent which might possibly be subject to the pre-sunrise ionization is O_2 . The corresponding solar radiation should have $\lambda > 910$Å. The value for the absorption coefficient of O_2 obtained from these considerations is $K_{O_2} = (3.3 \pm 2.1) \times 10^{-19}$ cm^2.

It is shown that the pre-sunrise ionization is not due to a pure screening effect.

*The research reported in this paper has been supported by the Geophysics Research Division of the Air Force Cambridge Research Center under Contract AF19(122)-44 and by the Department of State under Contract SCC-2680.

**On leave from the Chalmers University of Technology, Gothenburg, Sweden.

1—INTRODUCTION

The problem considered in this paper is to attempt to obtain information concerning the upper atmosphere from the observed behavior, near sunrise, of vertical incidence group height recordings on a frequency of 150 kc/sec.

Reflection of the 150 kc/sec pulse signals takes place in the lower portion of the *E*-layer. It, therefore, seems likely that these reflections would be very sensitive to the increase in ionization in the ionosphere occurring near sunrise. In earlier investigations at this Laboratory [see 1 and 2 of "References" at end of paper], it was reported that the above-mentioned virtual height *versus* time recordings show a sudden decrease in height before or near ground sunrise. That this transition point was under solar control was proved by plotting its seasonal variation. This seasonal variation, in time, showed the same general trend as the time of ground sunrise. No further conclusions were drawn at that time.

We have, therefore, carried out this investigation in more detail for records obtained throughout the years 1950 and 1951. As will be shown later, the seasonal variation of the time of the height transition can be referred to a pure geometrical problem involving the earth and the sun. The conclusion can be drawn that the sunrise effect always takes place before ground sunrise. This is in agreement with effects on higher frequencies as reported by other workers [3, 4, 5, 6, 7].

Some of the sunrise effects noted earlier have been attributed to a screening effect of some kind; see, for example, S. K. Mitra [4]. Other proposed explanations have been based on the atmospheric absorption of the effective solar radiation. We shall consider both theories in this paper.

2—SEASONAL VARIATIONS OF THE SUNRISE EFFECT

As mentioned in the introduction, the sunrise effect to be considered is noted as a height transition in 150 kc/sec vertical incidence group height recordings near this diurnal time. The study of this phenomena involves a detailed investigation of the connection between the time of the height transition and the time of sunrise at various heights. As an initial approach to this problem, all of the height records available during the interval January 1950 through December 1951 were scaled for sunrise effects. A typical height record showing the characteristic drop in height commonly noted near ground sunrise is shown in Figure 1. The most important parameters scaled were the time when the height drop started and the height of the reflection point at that time.

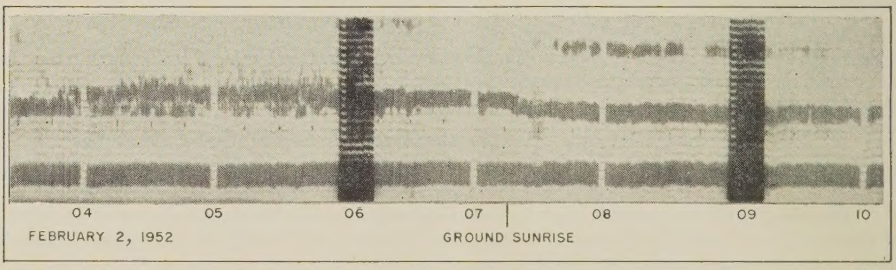

FIG. 1—SHOWING A TYPICAL HEIGHT TRANSITION NEAR GROUND SUNRISE

The exact time for ground sunrise can, very accurately, be obtained from the "Tables Crepusculaires" by Jean Lugeon [8]. From these tables, we can find the time of ground sunrise without taking account of the effect of refraction in the earth's atmosphere. We can most certainly overlook refraction corrections for the range of heights of interest in the present work.

The monthly median experimental values of the differences between the time of the height drop and the time of ground sunrise have been computed. These values are given in Table 1 and are plotted in Figure 2. The plots show reasonably

TABLE 1—*Monthly median values of the time in minutes that the drop in height preceded ground sunrise; numbers in parentheses are considered doubtful because of lack of sufficient data*

Year	Jan.	Feb.	Mar.	Apr.	May	June	July	Aug.	Sep.	Oct.	Nov.	Dec.
1950	6.5	1	3.5	5.5	17.5	13	27	15	8	(−1.5)	9	13
1951	6.5	11	6	15	14	..	18	7	10	2	3	3.5

good agreement between the two years investigated. They also show that the sunrise effect, in general, takes place before ground sunrise. The difference in time is seen to be a maximum near the solstices, decreasing to a minimum near the equinoxes.

This shape of the curves immediately suggests that the time of the sunrise drop should be compared with the actual sunrise time in the layer rather than at the ground. The time of sunrise at a certain height, compared to ground sunrise, can also be found in the Lugeon tables. When this comparison is made, it is immediately evident that the seasonal trend is the same for both phenomena.

For this reason, it seemed necessary to include the height of the layer in every individual computation. This is done by comparing the time of the height transition with the time for sunrise in the layer instead of ground sunrise as before. In this connection, it is worth emphasizing that all heights used in this paper are virtual heights. The probable correction to be applied to these heights is discussed later.

The time of sunrise in the layer is computed for every individual record by using the Lugeon tables. We can then determine the time difference between the time of sunrise at the reflection level and the time of the height drop. This has been done for all the available records, and the monthly median values of the time differences are listed in Table 2. The individual values, together with the

TABLE 2—*Monthly median values of the time in minutes that the sunrise height drop occurs after sunrise in the layer; numbers in parentheses are considered doubtful because of lack of sufficient data*

Year	Jan.	Feb.	Mar.	Apr.	May	June	July	Aug.	Sep.	Oct.	Nov.	Dec.
1950	53	53	53	51	(49)	53	(41)	50	49	(62)	(47)	50
1951	51	45	50	(43)	49	..	49	54	48	53	54	58

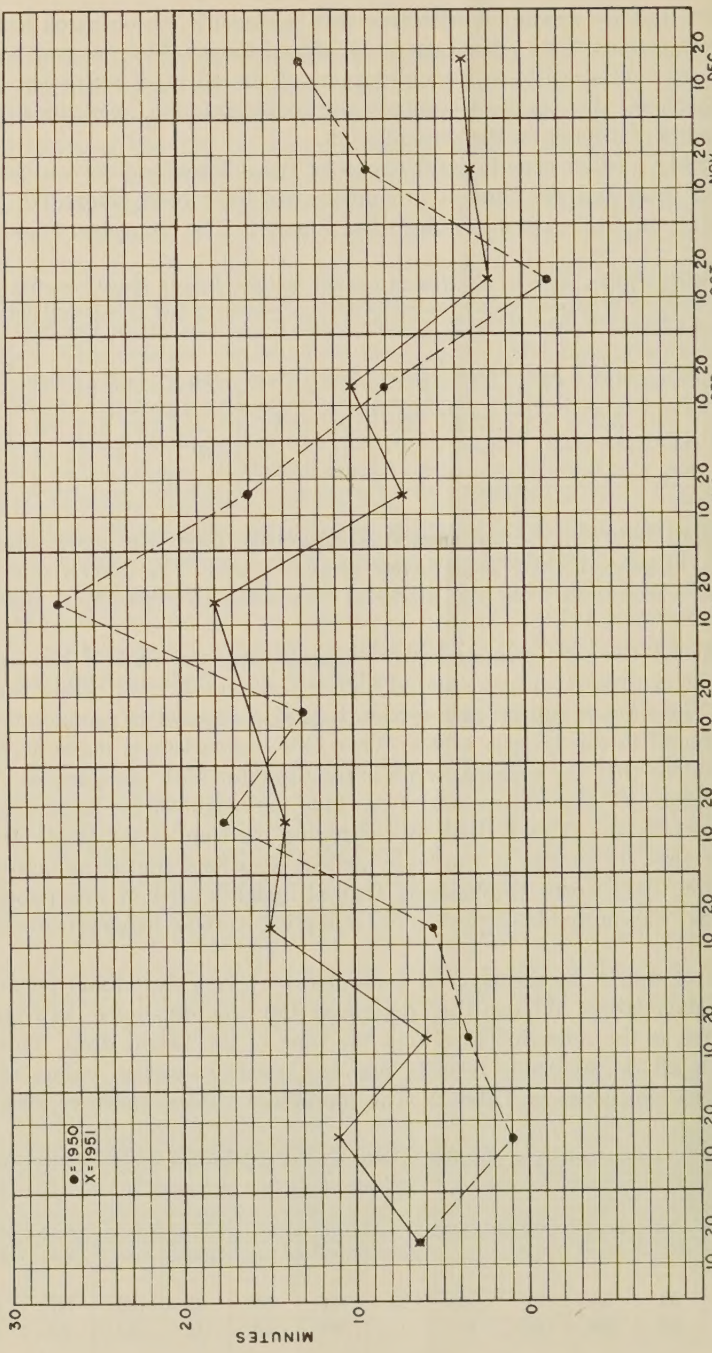

FIG. 2—MONTHLY MEDIAN VALUES OF TIME DIFFERENCE BETWEEN THE TRANSITION POINT AND GROUND SUNRISE

two-year monthly median values, are plotted in Figure 3. These plots show that, except for random fluctuations, this difference in time remains constant, independent of the season.

3—THE EFFECT OF A SCREENING LAYER

At this point in the investigation the question arises: Is this sunrise effect due to the influence of a screening layer effective at the ground sunrise point? Or is it due to a pure absorption effect? By absorption is meant the atomic or molecular absorption in the upper atmosphere of the ionizing solar radiation.

In order to study these two questions, we have first to return to the geometry of the earth's rotation. This question is discussed in detail in Appendix A.

From Figures 8 and 9, and the following discussion in Appendix A, we can see that it is sufficient, and most convenient for our purpose, to reduce our data to a great circle plane. This great circle plane contains the sun, the center of the earth, and our observation point on the earth. By doing so, we can confine all of our numerical calculations to this plane.

For transforming the measured difference in time between the height drop and ground sunrise, $\Delta\phi$, into the angular distance in the great circle plane, α, we use the following equation from Appendix A:

$$\Delta\phi = \cos^{-1}\left(-\frac{\tan\delta}{\tan\theta} - \frac{\sin\alpha}{\cos\delta\sin\theta}\right) - \cos^{-1}\left(-\frac{\tan\delta}{\tan\theta}\right) \quad \ldots\ldots\ldots (1)$$

where $\Delta\phi$ is measured in radians, δ is the declination of the sun, and θ is the latitude of our observational point measured from the North Pole. A positive $\Delta\phi$ (and consequently positive α) corresponds to the height transition on the dark side of the earth.

Once we have transformed our experimental data to the great circle plane, we can find the height of a screening layer which might be effective at the ground sunrise point. (The method is discussed in Appendix A.) This has been done for all of our experimental points. The monthly median values of the height, in kilometers, of such a screening layer are listed in Table 3. From this Table, we find

TABLE 3—*Monthly median values of the height of a screening layer; numbers in parentheses are considered doubtful because of lack of sufficient data*

Year	Jan.	Feb.	Mar.	Apr.	May	June	July	Aug.	Sep.	Oct.	Nov.	Dec.
1950	99.5	99	103.5	101	(92)	100	(86)	102	105	102	97	103
1951	101.5	100	104	(100.5)	104.5	...	98	105	108.5	103	101	103

that the height of the screening layer should be about 100 km, with no characteristic seasonal variations. This result leads to the belief that our height drop near sunrise more likely is an absorption effect than a pure screening effect. It would be difficult to explain a layer of about 100 km height with this screening property.

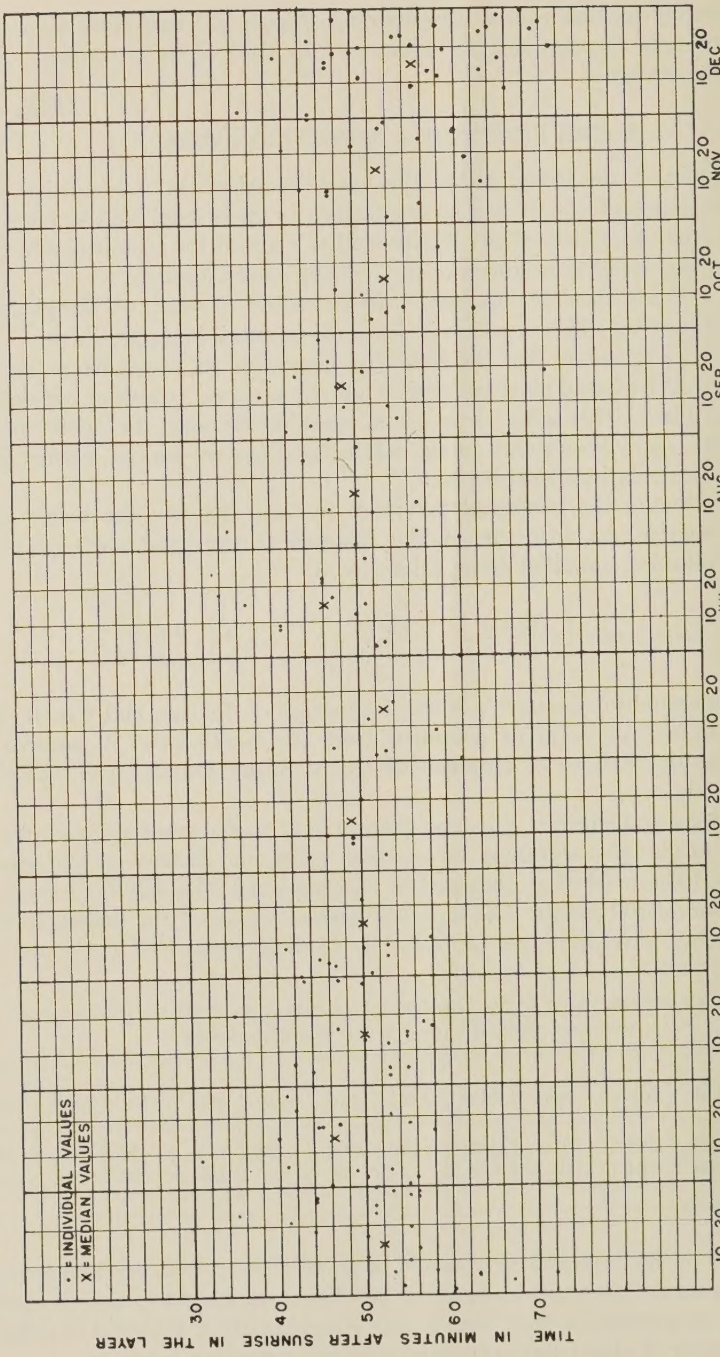

FIG. 3—INDIVIDUAL AND MONTHLY MEDIAN VALUES OF THE DIFFERENCE IN TIME BETWEEN THE SUNRISE POINT IN THE LAYER AND THE TRANSITION POINT

4—THE EFFECT OF ATMOSPHERIC ABSORPTION

The other possible explanation for our pre-sunrise increase in ionization is to be sought in the atomic or molecular absorption of solar radiation in the upper atmosphere. We will still confine our computations to the great circle plane referred to earlier. Let us, further, assume that the vertical distribution of the atmosphere is independent of latitude. The important question is now to find a suitable atmospheric model to be used in our computations.

M. Nicolet has suggested a complete model for the atmosphere covering the height interval of interest in this work [9, 10, 11, 12]. We follow the method used

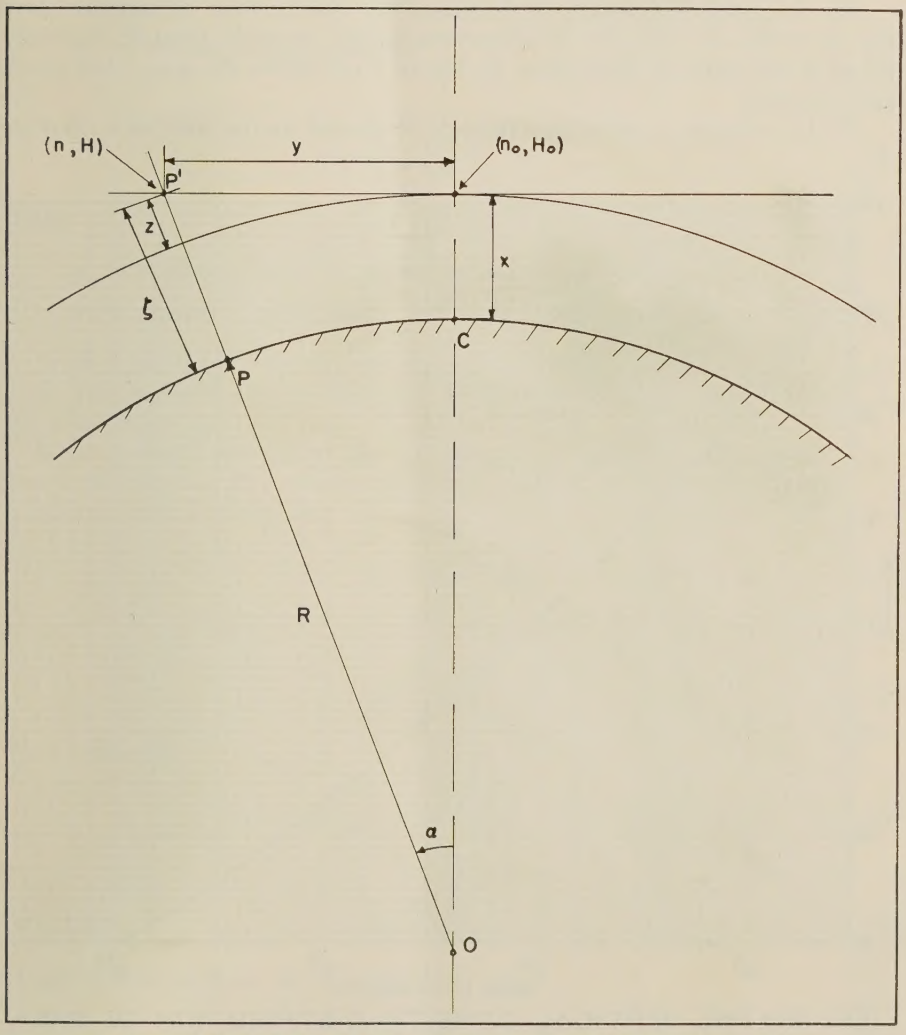

FIG. 4—PARAMETERS USED FOR COMPUTING $\bar{n}$

in his papers, for example [9]. In accordance with his suggestion, we use a slightly simplified version of his model [12] which agrees with the rocket data of the Naval Research Laboratory. However, the simplifications are relatively insignificant, so our results should be quite accurate.

Our atmospheric model is based on the following assumptions:

(1) The total number of particles at the level of 120 km, n_* , is 10^{12} particles/cm^3.

(2) The scale height at 120 km, H_* , is 10 km.

(3) The scale height gradient, β, is 0.2 above and 0.1 below the 120 km level.

The immediate problem is to determine the total number of particles along any ray of the sun. This is to be taken from infinity up to the point P', vertically ahead of our point of observation. In Figure 4 are shown the parameters which are of interest.

We have chosen a vertical line through the ground sunrise point as a reference

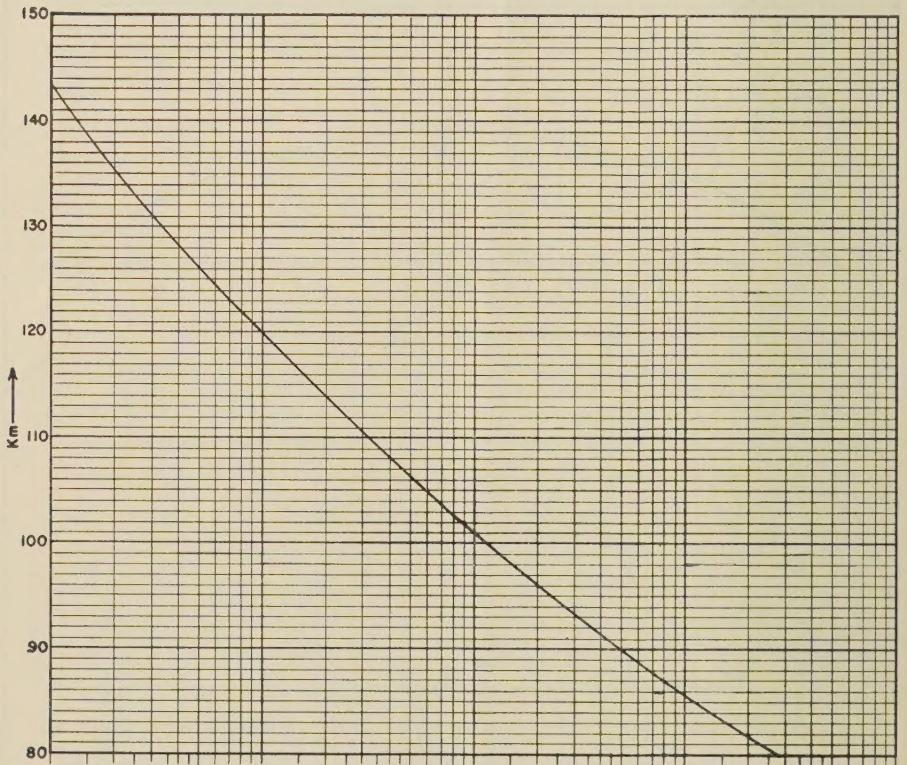

FIG. 5—THE VERTICAL DENSITY DISTRIBUTION OF PARTICLES

line for the computations. The vertical distribution of the particle concentration along this line has been computed as indicated below.

According to the theory, previously mentioned, by Nicolet for an atmosphere with a varying scale height, we have the following expressions:

$$H_0 = H_* + \beta \cdot z \quad \ldots\ldots (2)$$

where

H_* = scale height at the reference level

H_0 = scale height at the height z above the reference level

β = the scale height gradient

and

$$n_0 = n_* \cdot \left(\frac{H_0}{H_*}\right)^{-[(1+\beta)/\beta]} \quad \ldots\ldots (3)$$

where

n_* = number of particles per cm^3 at the reference level

n_0 = number of particles per cm^3 at the height z above this reference level

From equations (2) and (3), we can compute the vertical distribution of particles. This has been done in the height interval 80 to 140 km, and the result is shown in Figure 5.

We now wish to determine the total number of particles $\bar{n}$ along a ray from the sun to the point, P', passing at the height x above the ground sunrise point.

This number is given by

$$\bar{n} = 10^5 \int_{P'}^{\infty} n \, dy \quad \ldots\ldots (4)$$

where

$$n = n_0 \left(1 + \frac{\beta \cdot z}{H_0}\right)^{-[(1+\beta)/\beta]} \quad \ldots\ldots (5)$$

From Figure (4)

$$z = (R + x)\left\{\sqrt{1 + \frac{y^2}{(R + x)^2}} - 1\right\} \approx \frac{1}{2} \cdot \frac{y^2}{R + x} \quad \ldots\ldots (6)$$

for

$$\frac{y^2}{(R + x)^2} \ll 1 \quad \ldots\ldots (7)$$

Substitution of equation (6) in equation (4) gives

$$\bar{n} = n_0 \times 10^5 \left[\int_0^{\infty} \{1 + ay^2\}^{-[(1+\beta)/\beta]} \, dy \pm \int_0^{y} \{1 + ay^2\}^{-[(1+\beta)/\beta]} \, dy\right] \ldots (8)$$

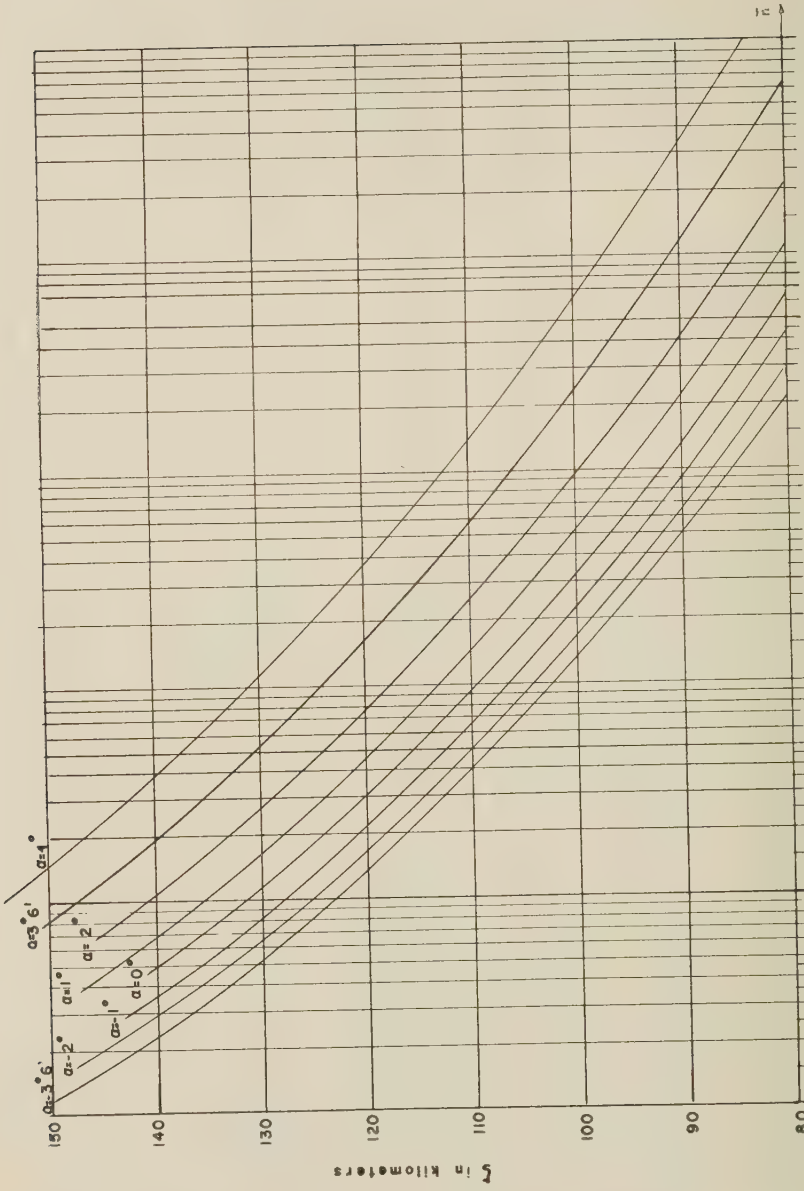

FIG. 6— $\bar{n}(\zeta)$ WITH α AS PARAMETER

where

$$a = \frac{\beta}{H_0} \cdot \frac{1}{2} \cdot \frac{y^2}{R + x} \qquad (9)$$

The plus sign refers to P and P' on the dark side and the minus sign to P on the sunlit side of the earth. All distances are expressed in kilometers.

We have now to separate our computations for the two cases $x \geq 120$ km and $x < 120$ km. These correspond to an exponent of -6 and -11, respectively. The integrals can be evaluated by using repeated integration and then computed numerically.

The only trouble that arises in the evaluation of these integrals occurs when the upper limit is infinity. The assumption $[y^2/(R + x)^2] \ll 1$ will not be valid in this case. However, the original integral can be expressed as a function of α; namely (for $\beta = 0.2$)

$$\bar{n} = \frac{n_0 \cdot (R + x)}{A^6} \cdot \left\{ \int_0^{\alpha} \frac{\cos^4 \alpha \cdot d\alpha}{\{1 - (A - 1)/A \cos \alpha\}^6} + \int_{\alpha}^{\pi/2} \frac{\cos^4 \alpha \cdot d\alpha}{\{1 - (A - 1)/A \cos \alpha\}^6} \right\} \quad \ldots (10)$$

where

$$A = \frac{0.2 \cdot (R + x)}{H_0} \quad \ldots (11)$$

The first integral can be evaluated up to a certain value of the parameter, α_1, where the assumption in equation (7) is still valid. The maximum value of the second integral can then be evaluated by using the mean value theorem.

Let us put $\alpha_1 = 25°$, $x = 120$ km, and $n_0 = 10^{12}$. We then obtain

$$\bar{n} \leq (3.1141 \times 10^7 + 3.9 \times 10) n_0 = 3.1141 \times 10^{19} \text{ cm}^{-2} \quad \ldots (12)$$

If we evaluate the original integral in its approximate form, as given by equation (8), we obtain

$$\bar{n} = \int_0^{\infty} n \cdot dy = 3.1142 \times 10^{19} \text{ cm}^{-2} \quad \ldots (13)$$

We can, thus, conclude that the error introduced by the approximation, equation (7), can be neglected throughout the relevant range of y. It might be added here that we also could have computed the exact value of equation (10) by using residue calculus (13). However, this would have involved a long numerical computation without a noticeable difference in the final result.

The numerical values of equation (8) have been computed for various values of α falling within the range $-3°$ to $+4°$. In all these computations, we have used $R = 6{,}370$ km and $\theta = 49°$. The results of these computations are plotted in Figure 6, giving $\bar{n}$ as a function of the local vertical height with α as the parameter.

Using these $h - \bar{n}$ curves, it is now possible to determine the total number of particles up to the point in the ionosphere where the sunrise drop in height occurred. This has been done for all of our experimental points of the sunrise drop in virtual height of reflection. By these means, the monthly median values of $\bar{n}$ have been computed and are shown in Figure 7. As can be seen from this Figure, there is no predominate seasonal variation. The conclusion can, therefore, be drawn that $\bar{n}$ is probably independent of season. We, consequently, can use all of our data

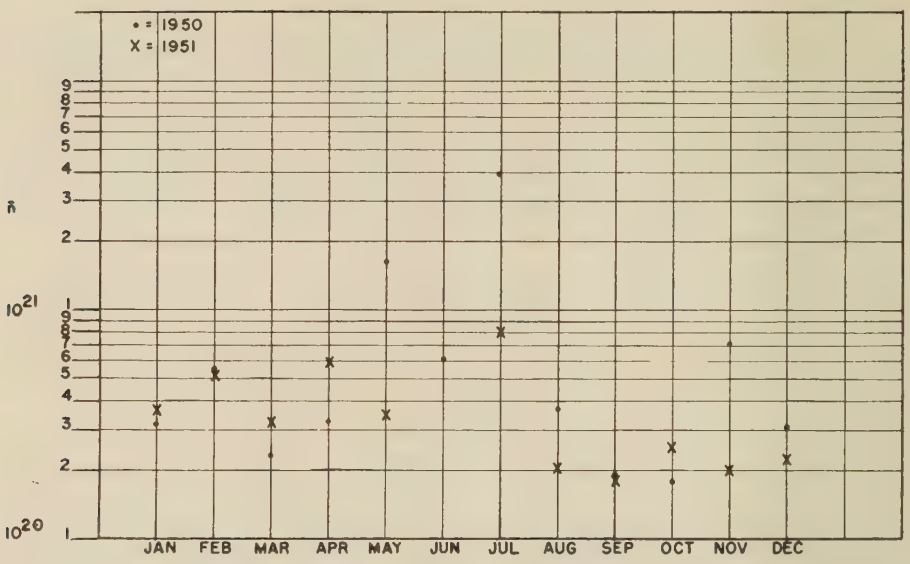

FIG. 7—MEDIAN VALUES DURING 1950 AND 1951 OF $\bar{n}$

to compute a median value. The median value obtained is $\bar{n}_{median} = 3.3 \times 10^{20}$ particles. The major portion of the individual values of $\bar{n}$ are seen to fall within the range 1.8×10^{20} to 8.0×10^{20} particles.

5—AN APPROXIMATE DETERMINATION OF THE ABSORPTION COEFFICIENT

We return now to the original theory by M. Nicolet on the ionization in an atmosphere with a varying scale height (see, for example, [10]). Nicolet has shown that the total number of particles in a vertical column is given by

$$\int_z^\infty n \cdot dz = n_0 \cdot H_0^{(1+\beta)/\beta} \cdot (H_0 + \beta z)^{-1/\beta} \quad \ldots\ldots\ldots\ldots\ldots\ldots (14)$$

where z is the vertical height above a certain reference level, $z = 0$. At $z = 0$, we have the particle concentration n_0 and the scale height H_0.

The electron production, q, is given by

$$q = n_0 \cdot K \cdot Q_\infty \cdot H_0^{(1+\beta)/\beta} \cdot (H_0 + \beta z)^{-[(1+\beta)/\beta]} \cdot \exp\left[-\sec\chi \cdot n_0 \cdot K \cdot H_0^{(1+\beta)/\beta} \cdot (H_0 + \beta z)^{-1/\beta}\right] \quad \ldots\ldots (15)$$

where χ = the sun's zenith distance, Q_∞ = the number of quanta available at the top of the atmosphere, and K = the molecular or atomic absorption coefficient.

The condition of a maximum in electron production is given by $dq/dz = 0$. This yields

$$K = \frac{1 + \beta}{n_0 \cdot H_0^{(1+\beta)/\beta} \cdot (H_0 + \beta z)^{-1/\beta} \cdot 1/(\cos\chi)} \quad \ldots\ldots\ldots\ldots\ldots\ldots (16)$$

or, from equation (14),

$$K = \frac{1 + \beta}{\int_z^\infty 1/(\cos \chi) \cdot n \cdot dz} \quad \ldots\ldots\ldots\ldots\ldots\ldots\ldots\ldots (17)$$

Equation (17) can be rewritten in our notation as

$$\int_z^\infty \frac{1}{\cos \chi} \cdot n \cdot dz = \int_y^\infty n \, dy = \bar{n} \quad \ldots\ldots\ldots\ldots\ldots\ldots\ldots\ldots (18)$$

or

$$K = \frac{1 + \beta}{\bar{n}} \quad \ldots\ldots\ldots\ldots\ldots\ldots\ldots\ldots\ldots\ldots (19)$$

We now make the assumption that the electron production has a maximum at the local time and height where we first note the sudden decrease in virtual height near sunrise. This assumption may not, in general, be fully justified, but is valid for our purpose. We can obtain an estimate of the error involved by examining the electron production function, equation (15). The absolute value of this equation is rather sensitive to the order of magnitude of K. If we, for example, increase K by a factor of 10 [from its value given by equation (19)], we see that equation (15) decreases in value by a factor of 10^3. On the other hand, if we decrease the value of K, the variation of equation (15) is not quite as fast. This means that the values we obtain for K must be looked upon as the maximum values to be expected. This will, however, be sufficient for our purpose.

It remains now to consider separately the number densities of the constituents of interest relative to the total particle densities. An examination of Figure 6 shows immediately that the main contribution to the total number of particles along a certain ray falls within a limited range of α around the ground sunrise point. We have shown earlier that the equivalent screen height is of the order of 100 km, throughout the year. From this we can, therefore, see that the main contribution to our integrals, equation (8), is originating in a limited height range around the 100 km level.

We can, further, assume that the mixing of the atmospheric constituents is complete in the above height region. Various authors have discussed the vertical composition of the atmosphere, and the major undetermined question appears to be where the bordering region between atomic and molecular oxygen is located. This question is still not definitely settled, but we can consider that, in the region of interest in this work, both atomic and molecular oxygen are present. We may also assume the presence of molecular nitrogen with the same ratio to total particle number as a ground level.

According to the atmosphere model proposed by M. Nicolet [14], we have, approximately, the following ratios between some of the constituents and the total particle density, n, in the height range of interest:

$$\frac{n_O}{n} = \frac{1}{3} \qquad \frac{n_{N_2}}{n} = \frac{2}{3} \qquad \frac{n_{O_2}}{n} = \frac{1}{100} \quad \ldots\ldots\ldots\ldots\ldots\ldots (20)$$

where n_O , n_{N_2} and n_{O_2} are the particle densities of O, N_2 , and O_2 . It will be noted that this assumes practically total dissociation of O_2 into O in the height range of interest, as justified in [14].

Nicolet has also shown that these ratios can be considered constant within the height interval of interest; that is,

$$\frac{\bar{n}_O}{\bar{n}} = \frac{1}{3} \qquad \frac{\bar{n}_{N_2}}{\bar{n}} = \frac{2}{3} \qquad \frac{\bar{n}_{O_2}}{\bar{n}} = \frac{1}{100} \quad \ldots\ldots\ldots\ldots\ldots\ldots (21)$$

where $\bar{n}_O$, $\bar{n}_{N_2}$, and $\bar{n}_{O_2}$ are the total number of particles along the integration line for the respective constituents, and $\bar{n}$ is the total number of particles.

We can, therefore, compute the K-values which would correspond to O, N_2 , and O_2 as the absorbing constituents.

We get from equations (19) and (21)

$$K_O = \frac{1+\beta}{\bar{n}} \cdot 3 \qquad K_{N_2} = \frac{1+\beta}{\bar{n}} \cdot \frac{3}{2} \qquad K_{O_2} = \frac{1+\beta}{\bar{n}} \cdot 100 \ldots\ldots\ldots (22)$$

Using the median value we determined for $\bar{n}$, $\bar{n} = 3.3 \times 10^{20}$, we obtain the following results

$$K_O = 10^{-20} \text{ cm}^2; \qquad K_{N_2} = 5 \times 10^{-21} \text{ cm}^2; \qquad K_{O_2} = 3.3 \times 10^{-19} \text{ cm}^2$$

Comparing these results with the absorption coefficients accepted in recent investigations, namely, $K_O \geq 2.6 \times 10^{-18}$ cm^2 [15] and $K_{N_2} \simeq 10^{-17}$ cm^2 [16], shows that K_O and K_{N_2} as deduced from the observational data are too small by a factor of 10^2 and 10^4, respectively. We can, therefore, draw the conclusion that the increase in electron density which accounts for the decrease in virtual height observed near sunrise is not caused by ionization of atomic oxygen or molecular nitrogen.

The absorption coefficient of the remaining constituent, molecular oxygen, is seen to be of the proper order of magnitude [16]. We may, consequently, conclude that the observed ionization could very likely be caused by photoionization of O_2 . In a survey by M. Nicolet [10], the origin of the different layers has been discussed. He suggests the possibility of O_2 comprising the major ionized constituent in the E-layer by assuming pre-ionized O_2-molecules. This explanation appears to make our result acceptable from a physical point of view.

Nevertheless, we must consider the absorption from another point of view, namely, absorption of X-rays.

At 100 km, with a total number of absorbing particles $\bar{n} = 3.3 \times 10^{20}$, we have

$$\bar{n}_O = 1.1 \times 10^{20} \text{ cm}^{-2}$$

$$\bar{n}_{N_2} = 2.2 \times 10^{20} \text{ cm}^{-2}$$

compared to normal air composition without dissociation of O_2

$$\bar{n} = \bar{n}_{air} = 2.2 \times 10^{20} + 0.55 \times 10^{20} = 2.75 \times 10^{20} \text{ cm}^{-2}$$

This gives

$$K_{air} = \frac{1+\beta}{2.75 \cdot 10^{20}} = 4.0 \times 10^{-21} \text{ cm}^2$$

In the X-region, of Nicolet [14], this corresponds to a wave-length of about 4 Å. Choosing a region where the coefficient is ten times greater (8 to 9 Å), the X-radiation reaches only, according to theoretical determinations by Nicolet, a maximum of 2.5×10^4 and a minimum of 10^2 photons per second and cm^2. For the region 5 to 10 Å, we have a rocket measurement of 4×10^4 photons per second and cm^2 [17]. Thus, theoretical and observational results concerning X-rays are consistent and the absorption of X-radiation may occur at the correct level.

However, we must try to determine what radiation is effective in producing ionization at sunrise at about 100 km.

We know [18] that the number of electrons necessary for the reflection of 150 kc/sec waves is about 3,000 electrons/cm^3. Thus, the solar radiation available in the height range of interest must produce, in less than five minutes, of the order of 3,000 electrons.

For X-ray ionization, we have a production of electrons per second and cm^3

$$\frac{dn_e}{dt} = \frac{(1+\beta)\cdot Q_1}{H \cdot e^{(1+\beta)}} = \frac{1.1 \cdot 2.5 \cdot 10^4}{8 \cdot 10^5 \cdot e^{1.1}} = 1.1 \times 10^{-2} \text{ cm}^{-3} \text{ sec}^{-1} \ldots\ldots (23)$$

Ignoring the effect of recombination, the number of electrons produced in five minutes is only 3.3 per cm^3, a value much less than the necessary value of 3×10^3 electrons per cm^3.

If we on the other hand consider X-radiation at $\lambda > 10$ Å, where the radiation definitely is more intense, it would be possible to obtain an effect. This would require a radiation at least 10^3 times greater. But the absorption ($K \simeq 10^{-19}$) should occur at about 130 km, which is definitely too high. The other possibility is an effect of radiation in the range of 30 to 33 Å where the coefficient is the same. But the penetration at 100 km level is not sufficient. We may, therefore, neglect this possibility.

For the ultraviolet radiation resulting in the ionization of O_2, we apply the same formula with the proper value of Q.

At $\lambda > 910$ Å, the limit of absorption by atomic absorption, O_2 is able to absorb the incident solar radiation. The number of photons per second and cm^2 is certainly more than 10^9. Thus, we find

$$\frac{dn_e}{dt} \geq \frac{1.1 \cdot 10^9}{8 \cdot 10^5 \cdot 3.0} = 4.6 \times 10^2 \text{ cm}^{-3} \text{ sec}^{-1}$$

This number is more than sufficient to increase the electronic concentration to the required value in the length of time of interest. It is not, however, possible to find the exact value because the variation with wave-length of the absorption coefficient of O_2 is not known and, also, the recombination coefficient should be determined.

We, therefore, can conclude that the sunrise effect might be attributed to ultraviolet radiation ($\lambda > 910$ Å) ionizing O_2.

The method used in this investigation is based on the knowledge of the actual height of the reflection point in the layer. We have used the group heights as the actual heights. This is in accordance with work of N. Davids [19]. It is shown in this work that the corrections to be applied, at the times in question, are, at the most, a few kilometers. Obviously, the slight differences involved can be neglected.

6—CONCLUSIONS AND SUGGESTIONS

The main conclusion to be reached from this investigation is that the pre-sunrise increase of ionization which produces the sunrise decrease in 150 kc/sec virtual height, in the lower portion of the *E*-layer, can be explained by computing the total molecular absorption of the relevant solar radiation. It does not seem to be controlled by a screening layer above the ground sunrise point. Consideration of the absorption coefficients permits the exclusion of O and N_2 as the atmospheric constituents ionized by ultraviolet solar radiation at sunrise in the *E*-layer height range of interest. With an ultraviolet solar radiation effect, the only possibility is the photoionization of a constituent whose concentration is small compared to the total concentration. O_2 is a possible constituent and in this case the absorption coefficient would be $K_{O_2} = (3.3 \pm 2.1) \times 10^{-19}$ cm^2. Unfortunately, the available experimental values of the absorption coefficient of O_2 are not very reliable and it is highly desirable that they should be determined in the laboratory in this important spectral range.

Ionization produced by X-radiation is possible but at greater heights than we consider.

Finally, it must be stressed that the careful analysis of sunrise effects is a method by which important results regarding the physical constitution and the chemical composition of the ionospheric layers may be determined. Our conclusions based only on 150 kc/sec virtual height measurements do not, of course, completely resolve the problem. Investigations on frequencies below and up to the critical frequency of the *E*-layer should be conducted in order to give a complete answer.

7—ACKNOWLEDGMENTS

The author wishes to express his sincere thanks and appreciation to Dr. M. Nicolet, Dr. A. H. Waynick, and other members of the Ionosphere Research Laboratory for their many helpful suggestions and valuable criticism. The author also wishes to thank Dr. M. Nicolet especially for the opportunity of using some of his unpublished results.

References

[1] P. G. Sulzer and B. B. Underhill, Preliminary vertical incidence equivalent height versus time recordings on 150 Kc/s, Technical Report No. 8, Ionosphere Research Laboratory, Pennsylvania State College (1949).

[2] D. Van Meter, Vertical incidence equivalent height versus time recordings on 150 Kc/s, Technical Report No. 12, Ionosphere Research Laboratory, Pennsylvania State College (1950).

[3] E. O. Hulburt, The *E*-region of the ionosphere, Phys. Rev., 55, 639–645 (1939).

[4] S. K. Mitra, The ozonsphere and the early morning increase of the *E*-layer ionization of the ionosphere, Science and Culture, **3**, 496–497 (1938).
[5] H. W. Wells, Sunrise effects in *F* region from high speed ionospheric recordings, J. Geophys. Res., **54**, 277–280 (1949).
[6] R. A. Helliwell, *et al.*, Pulse studies of the ionosphere at low frequencies, Report from Stanford University, Calif. (March 15, 1950).
[7] E. Theissen, Pre-sunrise ionization in the daily formed layers of the ionosphere, Naturwiss., **34**, 371–372 (1947).
[8] J. Lugeon, Tables Crepusculaires, Office Meteorologique Pologna, Warsaw (1934).
[9] M. Nicolet et L. Bossy, Sur l'absorption des ondes courtes dans l'ionosphère, Ann. Géophys., **5**, 275–292 (1949).
[10] M. Nicolet, Contribution à l'étude de la structure de l'ionosphère, Inst. R. Met. Belgique, Mém. 19, 74 (1945).
[11] M. Nicolet, Effects of the atmospheric scale height gradient on the variation of ionization and short wave absorption, J. Atmos. Terr. Phys., **1**, 141–146 (1951).
[12] M. Nicolet, The collisional frequency of electrons in the ionosphere, Scientific Report No. 32, Ionosphere Research Laboratory, Pennsylvania State College (1952).
[13] H. Jeffreys and B. S. Jeffreys, Methods of mathematical physics, Cambridge, University Press, 375–377 (1950).
[14] M. Nicolet, Ann. Géophys. (in preparation for publication, 1952).
[15] D. R. Bates and M. J. Seaton, Theoretical considerations regarding the formation of the ionized layers, Proc. Phys. Soc., **63**, 129–140 (1950).
[16] G. L. Weissler, Liege, Mém. Soc. roy. sci., **12**, Fasc. 1–2, 281 (1952).
[17] E. O. Hulburt, Physical characteristics of the upper atmosphere of the earth: paper presented at the Air Force Symposium on the Physics and Medicine of the Upper Atmosphere, November 6–9, 1951, San Antonio, Texas.
[18] J. J. Gibbons and R. J. Nertney, Wave solutions, including coupling, of ionospherically reflected long radio waves for a particular *E*-region model, J. Geophys. Res., **57**, 323–338 (1952).
[19] N. Davids, Dispersion effects at 150 Kc/s for a particular *E*-layer model, Scientific Report No. 31, Ionosphere Research Laboratory, Pennsylvania State College (1952).

Appendix A—Geometrical considerations

In Figure 8, we have depicted the earth with the sun at infinity. This means that we are treating the sun's rays as parallel rays. The sunrise line will be defined as the great circle produced by the intersection of the earth's surface and a plane perpendicular to the sun's rays. The angle of tilt of this plane with respect to the equatorial plane is $90 - \delta$, where δ is the declination.

Let P be the point on the earth where we are making our observations. The ground sunrise point for this place is the intersection between the latitude line and the sunrise line, point B. We wish to study the solar effect on the ionosphere before ground sunrise. From Figure 8, it can be clearly seen that it is sufficient to confine our investigations to the great circle plane containing the points POC. This plane contains all the rays affecting the different heights above P. Figure 9 shows this plane with the quantities in which we are interested.

The relation between the zenith distance of the sun, χ, and the corresponding angular distance in the great circle plane, α, is given by

$$\alpha = \chi - 90^\circ \quad (24)$$

Remembering the well-known identity,

$$\cos \chi = \sin \delta \cos \theta + \cos \delta \sin \theta \cos \phi \quad (25)$$

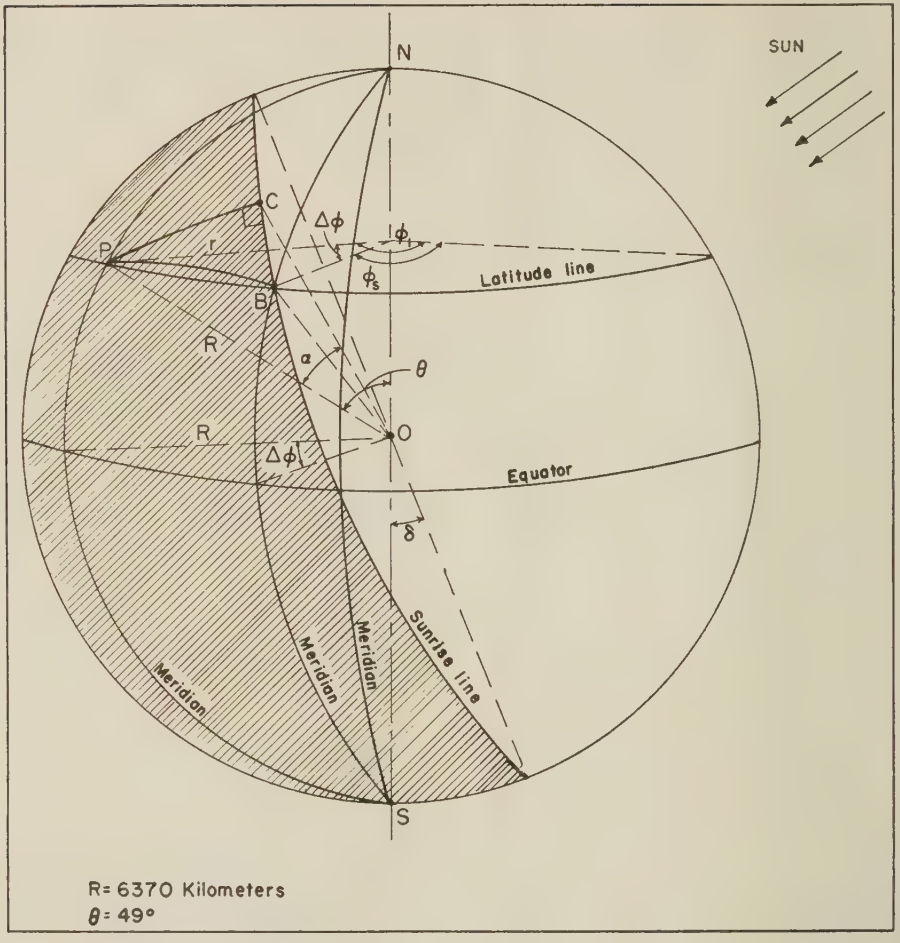

FIG. 8—THE EARTH WITH THE SUNRISE LINE

where θ = the latitude of the point P measured from the North Pole, δ = the declination of the sun, and ϕ = the time measured from local noon.

We are mainly interested in

$$\Delta\phi = \phi - \phi_S \quad \ldots\ldots\ldots\ldots\ldots\ldots\ldots\ldots\ldots\ldots (26)$$

where ϕ_S = the time of ground sunrise at P and ϕ = the time when the virtual height drop occurred.

From equations (24), (25), and (26), we find

$$\Delta\phi = \cos^{-1}\left(-\frac{\tan\delta}{\tan\theta} - \frac{\sin\alpha}{\cos\delta\sin\theta}\right) - \cos^{-1}\left(-\frac{\tan\delta}{\tan\theta}\right) \quad \ldots\ldots\ldots (27)$$

From this relation, we may plot α *versus* $\Delta\phi$ as a function of the season. By using a plot of this relation, we can now refer all of our experimental results to the great circle plane shown on Figure 9. This is simply a matter of converting the time difference into the angular distance, α.

In order to study the effect of a possible screening layer, we must also use the great circle plane *POC*. Let us presume the existence of a screening layer of height h_1 in the great circle plane *BOC*. The point in the ionosphere we are studying is at the height h_2 . From Figure 9, we find

$$\cos \alpha = \frac{R + h_1}{R + h_2} \quad \ldots\ldots\ldots\ldots\ldots\ldots\ldots\ldots\ldots\ldots (28)$$

Thus, by knowing the time $\Delta\phi$ when the height drop occurred and the height of the layer at that time, we can compute the height of the corresponding screen.

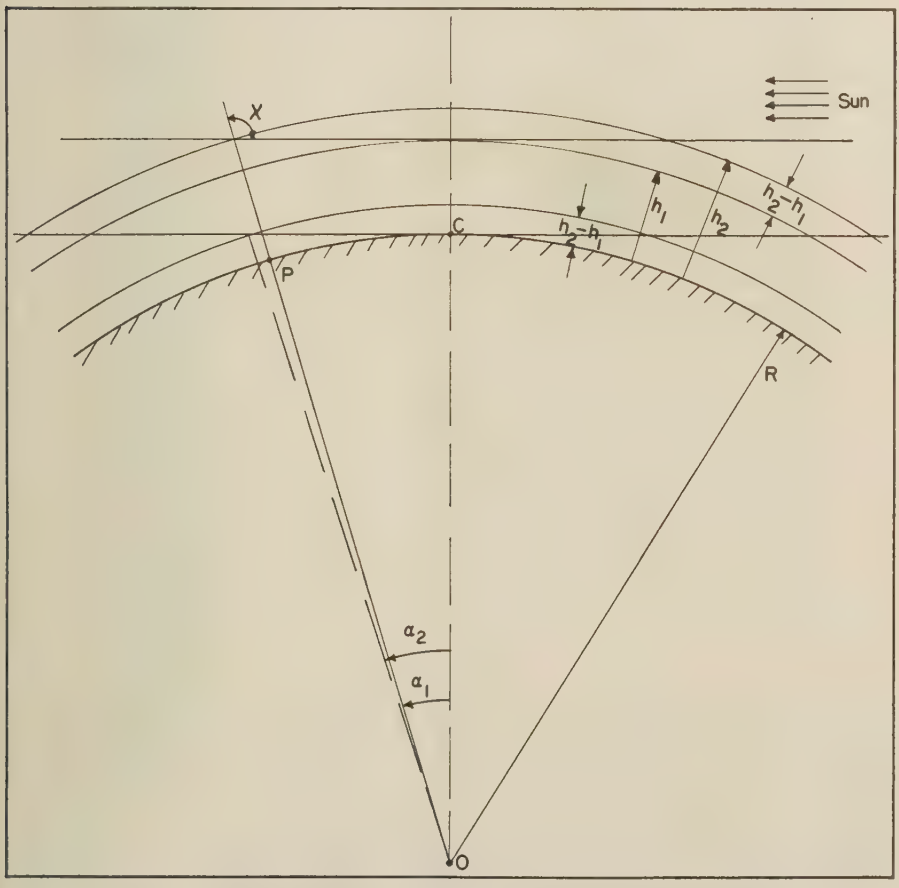

FIG. 9—THE EFFECT OF A SCREENING LAYER

However, we can more easily find the screening height by using the Lugeon tables, without having to perform this computation.

Let us assume we have computed h_1 by using equation (28). What α-value would then correspond to sunrise at the height $(h_2 - h_1)$?

From Figure 9, we find

$$\cos \alpha_2 = \frac{R}{R + h_2 - h_1} \quad \ldots\ldots\ldots\ldots\ldots\ldots\ldots\ldots (29)$$

Equations (28) and (29) yield

$$\cos \alpha - \cos \alpha_2 = \frac{R + h_1}{R + h_2} - \frac{R}{R + h_2 - h_1} \approx \frac{h_1^2}{R^2} \ll 1 \approx \frac{h_1 h_2}{(R + h_2)^2} \quad \ldots (30)$$

The greatest error can be expected for $h_1 = h_2 \approx 60$ km. This gives

$$\cos \alpha - \cos \alpha_2 \approx \frac{1}{(1 + R/h_1)^2} \leq 10^{-4} \quad \ldots\ldots\ldots\ldots\ldots\ldots (31)$$

This error can be neglected, and we can therefore use the Lugeon tables for finding the height of the screen.

ELECTRIFICATION OF SMALL AIR BUBBLES IN WATER

By Waldo E. Whybrew, Gilbert D. Kinzer, and Ross Gunn

Physical Research Division, United States Weather Bureau, Washington, D. C.

(Received June 6, 1952)

ABSTRACT

Steady velocities of an air bubble moving along the axis of rotation of a glass cell filled with water were measured at two angles of tilt from a horizontal direction and at several rotational speeds. These velocities, many times smaller than Stokes' law would predict, can be explained by taking into consideration hydrodynamic forces which depend on density and the speed of rotation. An experimental determination of the law of resistance to the movement of a bubble in this rotating system leads to revised estimates of apparent surface electrical charge density inferred from measurements of electrical mobilities. These estimates, approximating 0.8 esu cm^{-2}, are ten or more times larger than formerly reported. Furthermore, the surface charge density appears to be nearly independent of the bubble diameter. The electrification has been measured in a different manner with the same apparatus by establishing a static balance between the force of an electric field parallel to the axis of rotation and a component of the force of buoyancy. The charge carried by the bubble is not dependent upon its motion.

The electrification of bubbles of air rising freely in water was measured also, and the magnitude of the apparent surface charge density has been found to be only about one-third that obtained with the rotating system under similar chemical conditions. This discrepancy is believed to be due to a lack of sufficient time for the rising air bubbles to attain an equilibrium electrified state. The observed effect of CO_2 as a water impurity is to reduce the electrification of an air bubble, in agreement with the measurements of other investigators.

Introduction

Electrification associated with an air-water interface has been investigated by McTaggart [see 1 of "References" at end of paper], Alty [2], and Currie and Alty [3] by measuring the mobility of an air bubble supported in water in a glass cylinder rotating with its axis parallel to the horizontal direction. Estimates of apparent interfacial electrical charge density have been made from these measurements by assuming that the bubble motion obeys Stokes' law. These experiments which may bear a relation to the problem of atmospheric electricity have been

reexamined and, in addition, it has been found that when the rotating cylinder is tipped through an angle of several degrees the velocity produced by the force of buoyancy is much smaller than that given by Stokes' law. When the law of resistance to movement is evaluated experimentally, it becomes clear that published electrical surface charge densities are at least an order of magnitude too small. Two new experiments have been performed which give values of the apparent charge density. One uses the rotating cylinder of water to support a bubble in static balance between a force of buoyancy and a force produced by an electric field, and the other measures the free charge transported upward by a bubble

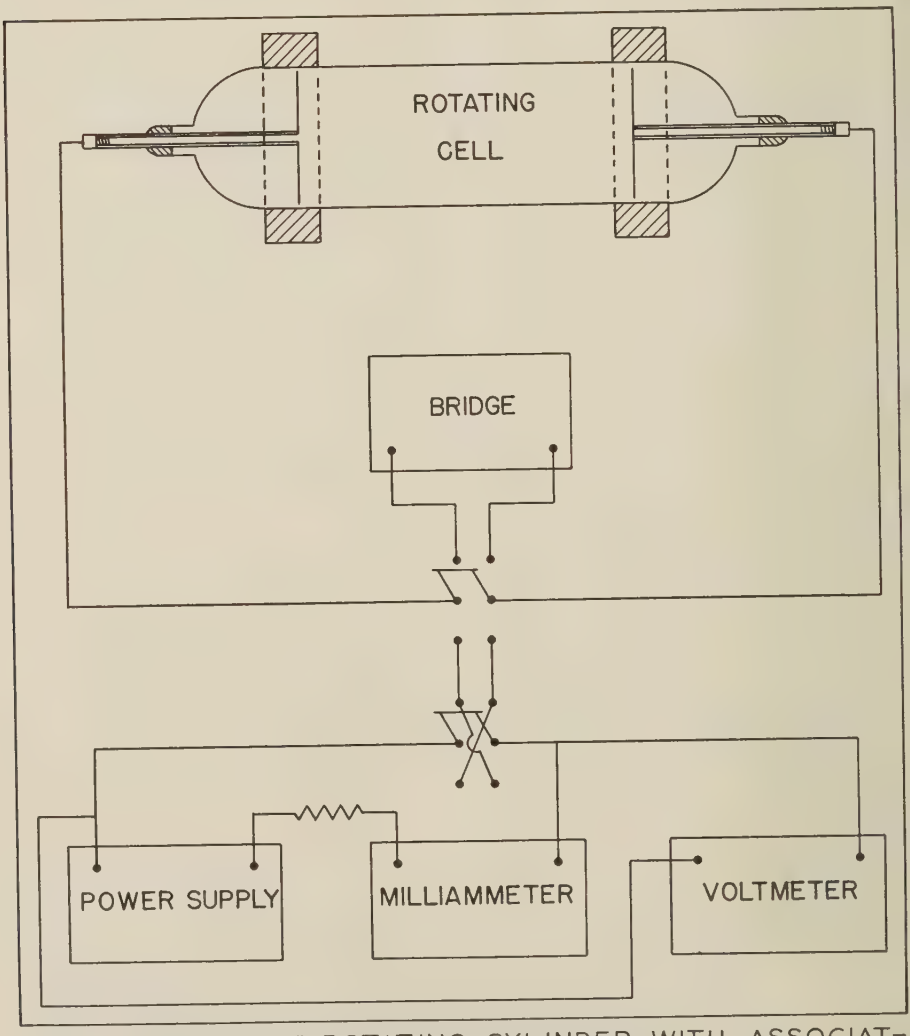

FIG. 1—DIAGRAM OF ROTATING CYLINDER WITH ASSOCIATED ELECTRICAL CIRCUITS

rising freely in a vertical column of water. Both give values of charge density consistent with the revised estimates made from mobility measurements.

It is well known that impurities dissolved in water modify the physical constants of the surface whether it be between water and air, water and another liquid, or water and a solid, and CO_2 is an impurity which seems to have a marked effect on electrification. Dinger and Gunn [4] found, for example, that dissolved CO_2 reduces electrification from melting ice, and McTaggart and Alty found that CO_2 diminishes the mobilities of air bubbles. This effect has been examined and qualitative results are given.

Apparatus

A bubble of air was supported in a water-filled rotating Pyrex glass cylinder shown in Figure 1. The cylinder was accurately ground inside and out with an internal diameter of 3.6 cm and a length of 15 cm. A separation of 13.1 cm between flat circular platinum electrodes, closely fitted at the ends, gave a conductivity cell constant of 1.286 cm^{-1}. Heavy platinum tubing welded to the electrodes came through drawn down sections of the glass cylinder at the ends along the axis of rotation. A small annular space between the platinum tubing and the glass was sealed by deKhotinsky cement. Short pieces of threaded platinum wire were screwed into threaded segments at the outer ends of the platinum tubes. A tungsten wire, 5 mils in diameter, was attached to each platinum wire, and the tungsten wire, in turn, penetrated small cups filled with mercury. This made a rotating electrical connection which was free of any detectable contact irregularity. Two short aluminum alloy rings, slightly larger than the glass cylinder, were cemented outside close to the ends. One ring had a series of notches around its outer circumference so that the tube could be rotated by jets of compressed air.

The cylinder and rings were mounted on an insulating frame and supported by two air bearings. The cylinder was kept centered by air jets directed longitudinally on the sides of the rings. The assembly, frame, and a traveling microscope were set on a sturdy wooden base, which could be tilted through an angle of 7° each way from horizontal. The speed of rotation was measured with a Strobotac light, and the resistance of the water in the cylinder was measured by both a DC bridge and a 1,000-cycle AC bridge. The electrical connections, shown in Figure 1, included a switch for reversing the voltage between the platinum electrodes.

The cylinder and its parts were assembled on a glass lathe and, though not precisely balanced, they would rotate smoothly at certain speeds. The electrical mobility data were taken at a speed of 445 radians sec^{-1}, although quiet operation could be obtained at 223 and 173 radians sec^{-1}. There were a few places along the axis of rotation where a bubble would tend to remain stationary when the tube was tipped through an angle up to 7°. The most pronounced places where this occurred were about 2 cm from each electrode and close to a region midway between.

A diagram of a different system by which the electric charge transported by rising bubbles of air was measured is shown in Figure 2. This method might be called a negative sedimentation method. Soft borosilicate glass was used throughout in the construction because of its marked resistance to the solvent action of water. Three platinum electrodes, separated by 50-cm intervals, and a conductivity cell

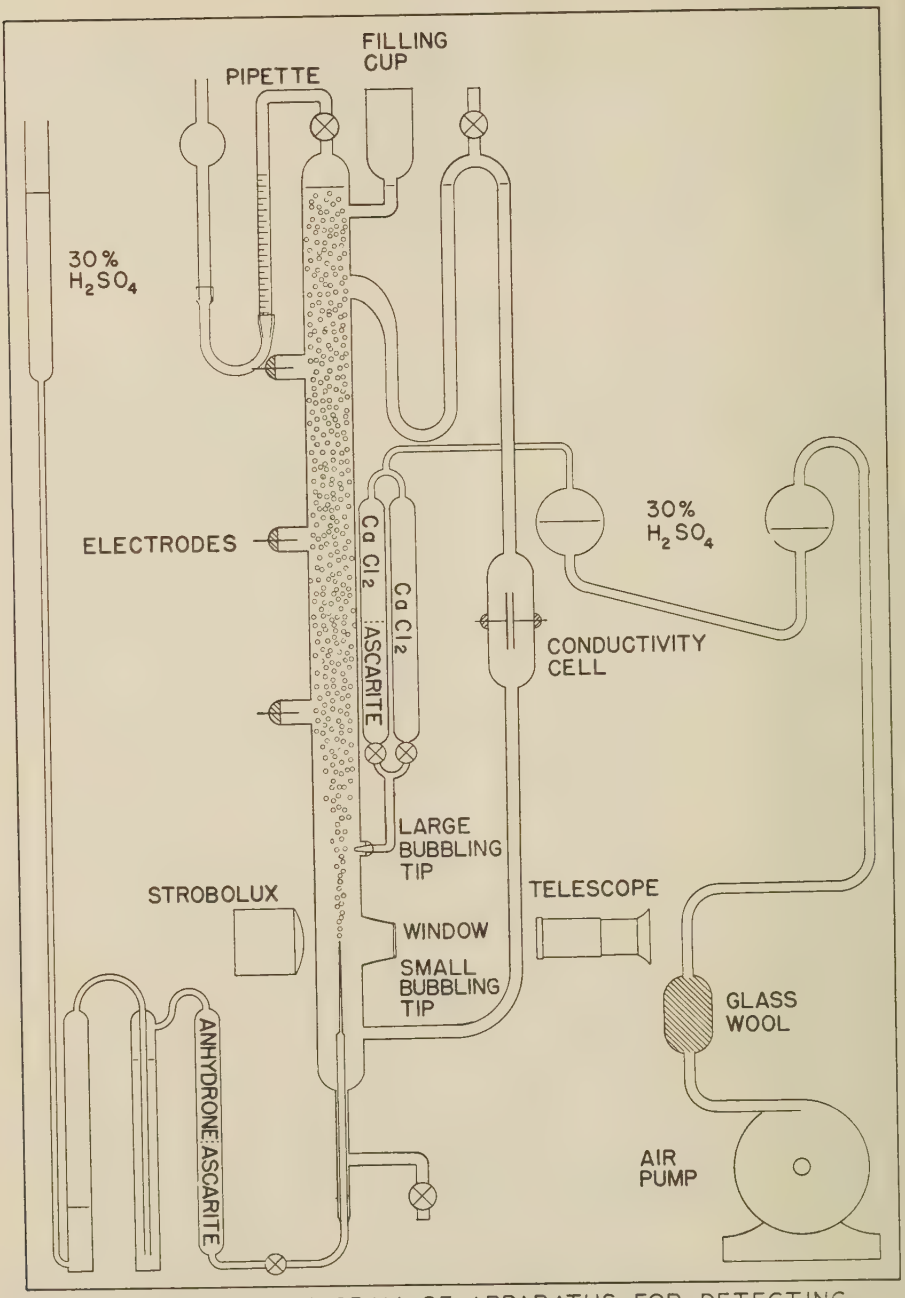

FIG. 2—SCHEMATIC DIAGRAM OF APPARATUS FOR DETECTING ELECTRIFICATION OF BUBBLES OF AIR RISING FREELY IN WATER

were sealed into the system. The electrodes were covered with platinum black to stabilize their potentials. A small bubbling tip, made by drawing down glass tubing, was mounted back of a plain window so that the diameter of newly-formed bubbles, illuminated by a Strobotac light, could be measured with a reading telescope. Bubbles having a diameter of 0.030 ± 0.002 cm were produced at a rate varying from 100 to 150 per second. The rate was measured by letting the bubbles collect to form an air-filled space at the top for a certain length of time, usually about 20 minutes, and then drawing off the air through the upper stop-cock, into a graduated pipette. It was found that the rate was essentially constant for a given pressure differential, temperature, and cleanliness of nozzle.

Two needle-valves were attached to an auxiliary bubbling tip above the glass window. Air to one valve was bubbled through a 30 per cent H_2SO_4 solution, then dried, and passed through ascarite to remove CO_2 . Air to the other valve was bubbled through a 30 per cent H_2SO_4 solution, and dried, leaving in the small amount of CO_2 present in room air. The air mixing ratio from the two valves controlled the resistivity of the water in the tube through a range of from 0.8 to 5.0×10^6 ohm cm. The bubbles from the auxiliary tip forced circulation of the water up the tube and down the side arm through the conductivity cell.

The tube and associated components were housed in a copper-shielded room, covered outside with Celotex to provide a constant temperature air bath. The room contained four fans for circulating the air and a controlled heating element for maintaining a desired temperature.

The voltage produced between electrodes by rising bubbles was measured with

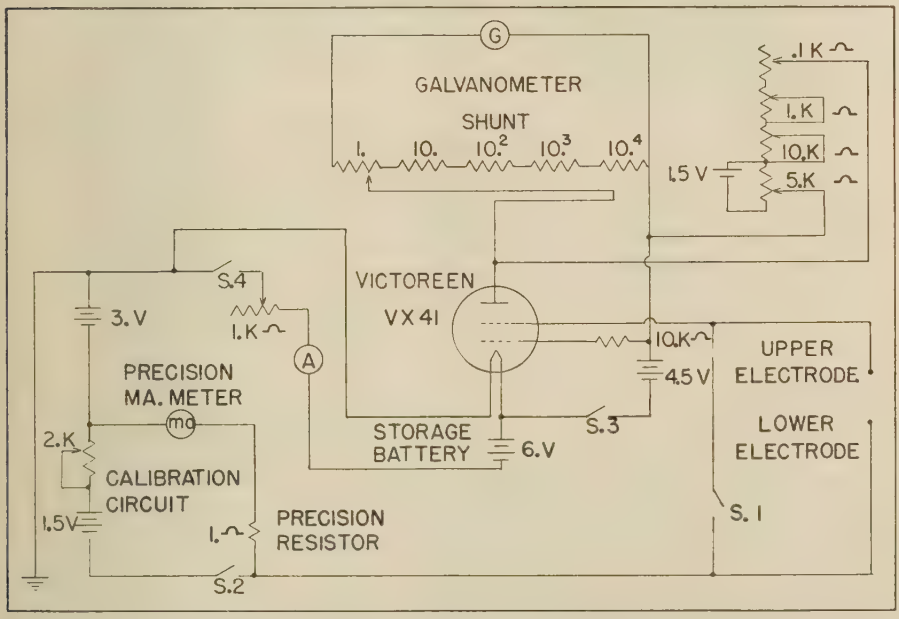

FIG. 3—ELECTRICAL CIRCUIT USED TO MEASURE THE ELECTRICITY ON BUBBLES OF AIR RISING FREELY IN WATER

the vacuum-tube circuit shown in Figure 3. The galvanometer deflections were calibrated by a standardizing voltage applied to the calibrating circuit. When the polarity of the calibrating battery was in the direction shown, the galvanometer deflections were in the same direction as that produced by rising bubbles. This showed that the bubbles transported a negative charge. The electrometer tube and circuit, and the conductivity bridge for measuring the resistance of the conductivity cell, were housed in an adjoining shielded room.

Experiments

Measurements of the velocity of travel of a bubble along the axis of rotation of the cylinder when the latter was tipped at two different angles to the horizontal direction are shown in Figure 4, with Stokes' law velocities included for comparison

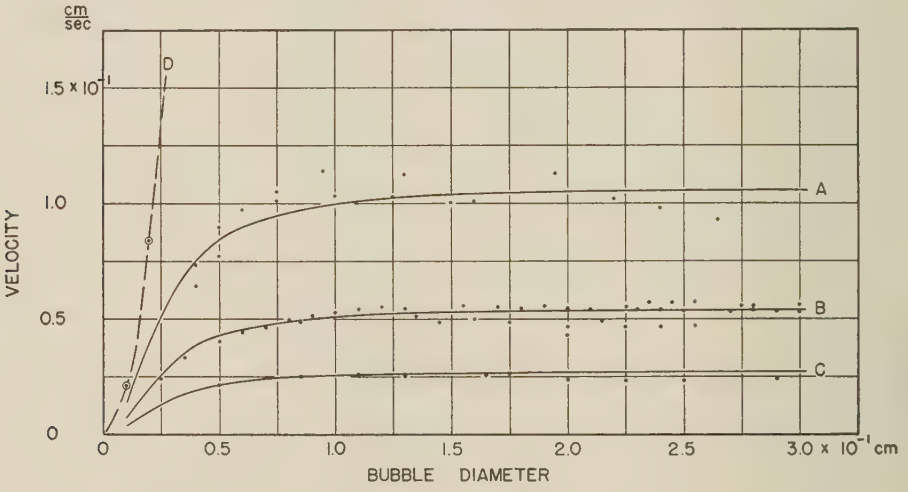

FIG. 4—BUBBLE VELOCITIES ALONG THE ROTATING AXIS OF A WATER-FILLED CYLINDER TILTED AT AN ANGLE θ WITH THE HORIZONTAL DIRECTION: (A) ROTATIONAL SPEED 173 RADIANS SEC^{-1}, SIN θ = 0.038; (B) ROTATIONAL SPEED 445 RADIANS SEC^{-1}, SIN θ = 0.038; (C) ROTATIONAL SPEED 450 RADIANS SEC^{-1}, SIN θ = 0.019; (D) STOKES' LAW VELOCITY, SIN θ = 0.038

at small diameters and for one set of conditions. Angles of tilt were used which gave bubble velocities convenient for later mobility measurements. The equilibrium bubble velocity along the tilted axis is insensitive to the diameter of the bubble for a large range of diameters, although it varies inversely as the speed of rotation.

The procedure followed in measuring the electric mobility of an air bubble was the same as that described by McTaggart, except that no attempt was made to keep the axis of rotation horizontal. In fact, the axis was tilted purposely to produce a steady migration velocity on which the effects of an axial electric field were measured, first with the field in one direction and then in the opposite direction. One-half the change in velocity divided by the electrical potential gradient gave the

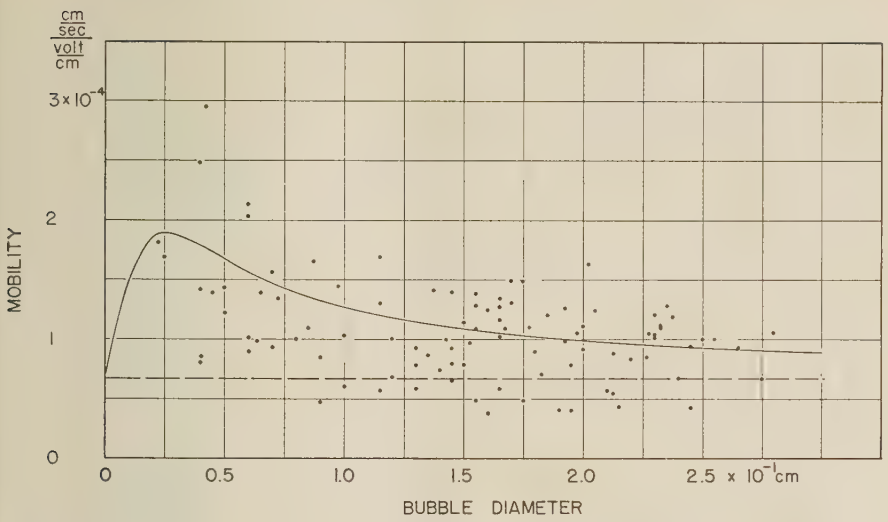

FIG. 5—ELECTRICAL MOBILITIES OF AIR BUBBLES IN WATER CONTAINING CO_2 IN EQUILIBRIUM WITH THE AIR

mobilities in water containing CO_2 in equilibrium with room air shown in Figure 5 and in water free of CO_2 in Figure 6. The direction of the velocity change relative to the direction of the electric field was as if there were negative electricity on the bubbles. The water in the cylinder was partially freed of dissolved air, so that a bubble introduced initially with a diameter of 0.3 cm would dissolve and grow smaller at a rate that would give enough time for a careful set of measurements

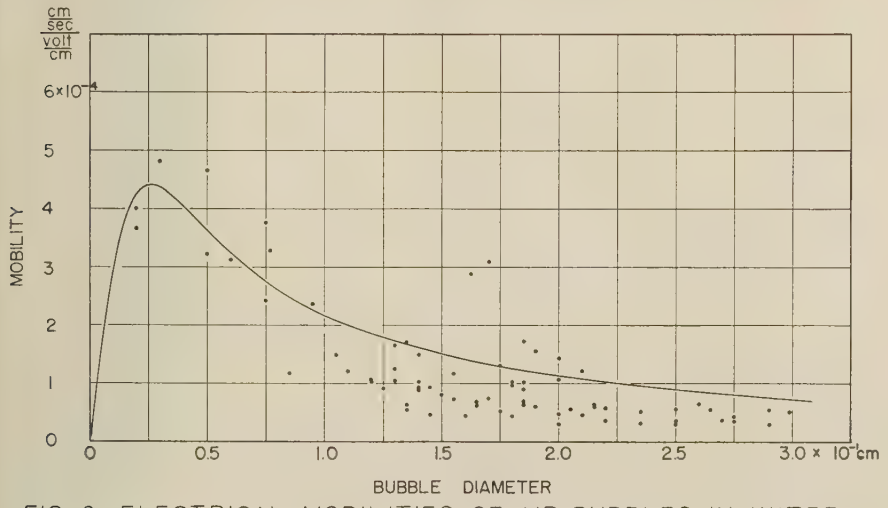

FIG. 6—ELECTRICAL MOBILITIES OF AIR BUBBLES IN WATER FREE OF DISSOLVED CO_2

to be made at selected diameters. No attempt was made to allow for aging or for the effect of the rate of shrinkage which Alty and Currie found to be a significant factor affecting the electric mobility. The neglect of these effects unquestionably introduced scatter in the data in Figures 5 and 6.

Currie [5] has found that an axial endosmotic counter-flow of 0.67×10^{-4} $cm^2\ sec^{-1}\ volt^{-1}$ is to be expected in rotating Pyrex tubes when the water has a conductivity of between 1 and 1.6×10^{-6} $ohm^{-1}\ cm^{-1}$. This flow should be in opposition to the movement of the bubbles and must be taken into account before true values of the mobilities are known. The water containing CO_2 had a conductivity of 1.3×10^{-6} $ohm^{-1}\ cm^{-1}$, which is just midway in the range specified by Currie, so it is appropriate to correct for the counter-flow in Figure 5 by subtracting a constant value of 0.67×10^{-4} $cm^2\ sec^{-1}\ volt^{-1}$ from each mobility. This corresponds to raising the zero reference axis to a new position, indicated by the horizontal dashed line. The water free of CO_2, on the other hand, had a much smaller conductivity of 2.5×10^{-7} $ohms^{-1}\ cm^{-1}$, and no appropriate counter-flow correction is known. It would appear that the correction must be appreciably less than that used above, since measured mobilities at larger diameters fall below this value. The correction, whatever it may be, must be relatively small and has been neglected in Figure 6.

The force on a bubble of air in water produced by an electric field was measured by static balance with a known buoyancy force in the rotating tube. This condition

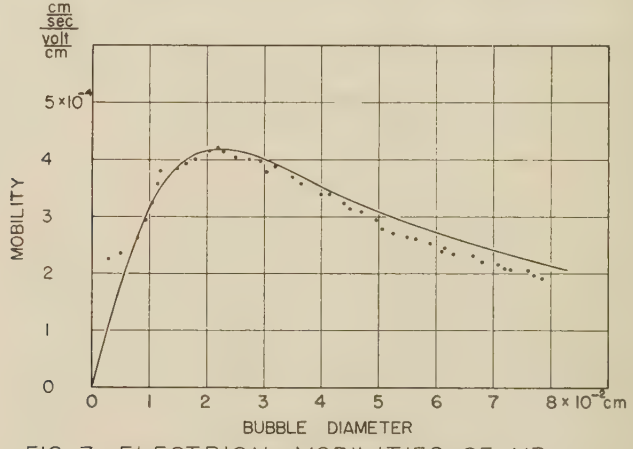

FIG. 7—ELECTRICAL MOBILITIES OF AIR BUBBLES MEASURED BY ALTY IN WATER FREE OF DISSOLVED CO_2

was not easy to obtain because of interference with positions along the axis where the bubble had a tendency to remain stationary. A sufficient number of measurements, shown in Figure 8, were made even though they were individually scattered to obtain an average value for the apparent surface charge density, σ in esu cm^{-2}, from the force equilibrium equation

$$\frac{\pi D^3}{6}(\rho - \rho')\, g \sin\theta = \pi D^2 \frac{E\sigma}{300 \times s} \text{ dynes} \quad \ldots\ldots\ldots\ldots\ldots (1)$$

where D is the bubble diameter in centimeters, ρ and ρ' are the densities in gms cm^{-3} of water and air, respectively, at atmospheric pressure and at room temperature, g is the acceleration of gravity in cm sec^{-2}, θ is the angle between the axis of rotation and the horizontal direction, E is the electric potential difference in volts between the end electrodes, and s is their separation in centimeters.

The procedures followed in the second measurement of the electrification of

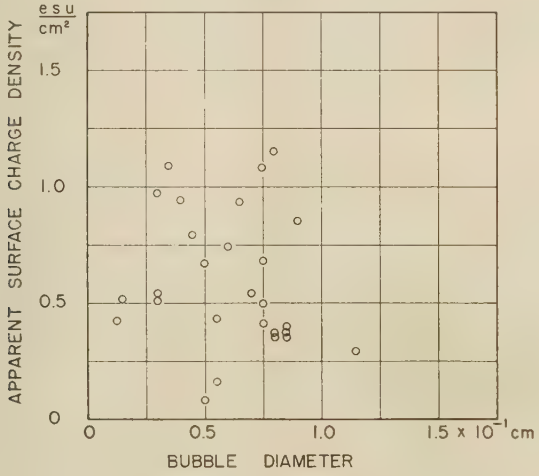

FIG. 8—APPARENT SURFACE DENSITY OF ELECTRICAL CHARGE ON BUBBLES OF AIR STATICALLY BALANCED IN A ROTATING TUBE

air bubbles, where the bubbles were rising in a column of water, were typical of those employed in investigations requiring chemical cleanliness. The glass system was cleaned with $K_2Cr_2O_7$ dissolved in H_2SO_4 and then rinsed several times with distilled water. The final filling was with water having a resistivity of 0.9×10^6 ohm cm at 24C. The two needle-valves leading to the tip above the viewing window were adjusted to give vigorous bubbling, which would increase the resistivity of the water by taking out dissolved CO_2 present at the start. After the resistance and temperature of the air bath were brought to desired values, the large bubbles were shut-off, and the water in the side arm was drained down to break the path of circulation. The deflections were calibrated by opening S_1 and closing S_2, Figure 3, and noting the deflection for a known electrical current through the 1.0-ohm precision resistor. Small bubbles were then produced with air that had been bubbled through a 30 per cent H_2SO_4 solution, then passed through a dryer and ascarite. After a short time, S_1 was opened, the flow of small bubbles was stopped, and the change in the galvanometer deflection was observed. This was repeated again and again, until about 12 readings had been taken, and, at the end, the rate of flow

of the bubbles and the resistance of the conductivity cell were measured. The difference in the deflections of the galvanometer, first with a flow of bubbles and then without, was proportional to the rate of transport of electric charge, and the apparent surface charge density in esu cm^{-2} was obtained from the equation

$$\sigma = \frac{E_v dt D}{2kR_c v C_d} \times 10^9 \quad \ldots\ldots\ldots\ldots\ldots\ldots\ldots\ldots (2)$$

where E_v is the calibration voltage in volts, d is the average of the difference in galvanometer deflections obtained during a given set of conditions, C_d is the calibration deflection, v is the volume of air in milliliters collected at the top of the tube in t seconds, D is the diameter of the bubbles in centimeters, R_c is the resistance of the conductivity cell in ohms, and k is the ratio of the resistance of the tube between electrodes to the resistance of the conductivity cell. The measurements of σ are shown in Figure 9.

Results

The measured equilibrium velocity of a bubble along the axis of rotation of a supporting water-filled tube inclined at a given angle with the horizontal direction appears, in Figure 4, to be independent of the bubble diameter when the diameter is greater than 0.1 cm. It does vary, on the other hand, inversely as the speed of rotation. For diameters smaller than 0.1 cm, the velocity decreases, but does not necessarily approach Stokes' law as McTaggart has suggested. An investigation

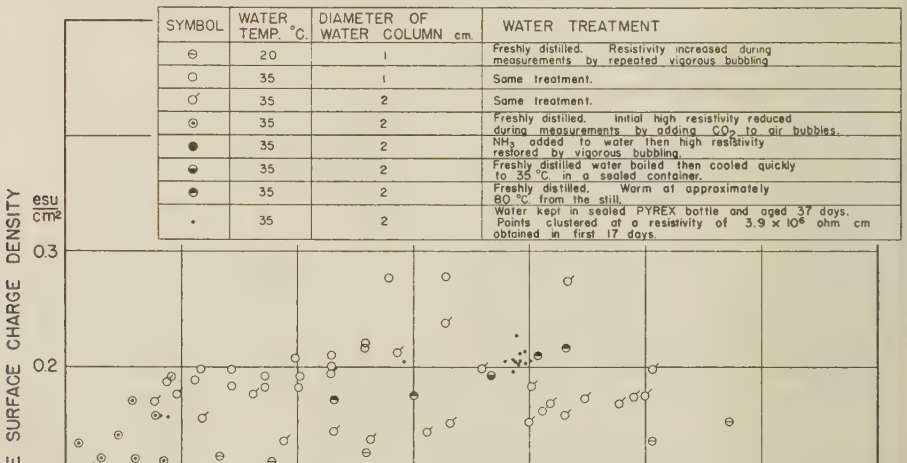

FIG. 9—APPARENT SURFACE DENSITY OF ELECTRICAL CHARGE ON AIR BUBBLES RISING FREELY IN WATER

by Stewartson [6] on the velocity V of a sphere of diameter D, moving along the axis of rotation of a non-viscid fluid of density ρ, having an angular speed Ω, showed the force resisting the motion to be $(2/3)\rho D^3\Omega V$.

Water, of course, has a coefficient of viscosity, η, which is not zero, and the expression obtained by Stewartson cannot be used directly. Careful study of Figure 4 shows, however, that Stewartson's form, combined linearly with that of Stokes', inserting two experimental factors, K_1 and K_2, permits a good description of the resisting force to be given by the expression

$$[(2/3)D^3\rho\Omega K_1 + 3\pi\eta DK_2]V$$

Equating the liquid resistance to the buoyant force gives the formula

$$V = \frac{\pi D^2(\rho - \rho')g \sin\theta}{4D^2\rho\Omega K_1 + 18\pi\eta K_2} \quad \ldots\ldots(3)$$

which for large values of D reduces to

$$V = \frac{\pi}{4}\left(1 - \frac{\rho'}{\rho}\right)g\frac{\sin\theta}{\Omega K_1} \simeq \frac{\pi}{4}\frac{g\sin\theta}{\Omega K_1} \quad \ldots\ldots(4)$$

Empirical fitting of the curves in Figure 4 to the experimental points gives the values of the factors, K_1 and K_2, listed in Table 1. It will be seen that, as the

TABLE 1—*Experimental coefficients K_1 and K_2 used in equation (3) in order to give the calculated velocities shown as solid curves in Figure 4*

Angular speed	K_1	K_2
radians sec^{-1}		
445	1.23	2.8
173	1.60	1.4

angular speed Ω is increased, the constant, K_1, approaches unity, and when Ω is decreased the value of K_2 approaches unity. This is interpreted to mean that forces depending on the density of the fluid, and the angular speed and forces which depend on the viscosity of the fluid, must act simultaneously. The dynamic forces predominate when the speed of rotation is large, but the viscous forces take over and become controlling when the angular speed approaches zero.

A force produced by an electric potential gradient of E/s volts cm^{-1}, parallel to the axis of rotation and acting on a charge Q esu associated with the bubble, will produce a velocity

$$V = \frac{Q}{(2/3)D^3\rho\Omega K_1 + 3\pi\eta DK_2} \times \frac{E}{300 \times s} \quad \ldots\ldots(5)$$

Thus, if an apparent surface density of charge, σ esu cm^{-2}, be specified in place of Q, the electric mobility of the bubble can be written as

$$U_e = \frac{\pi D\sigma}{[(2/3)D^2\rho\Omega K_1 + 3\pi\eta K_2][300 \times s]} \quad \ldots\ldots(6)$$

and if σ may be treated as being a constant, a maximum value of this mobility will be found at a diameter

$$D_{max} = \left(\frac{9\pi\eta K_2}{2\rho\Omega K_1}\right)^{1/2} \quad \ldots\ldots\ldots\ldots\ldots\ldots\ldots\ldots\ldots\ldots (7)$$

The measured mobilities in Figures 5 and 6 suggest the occurrence of maxima, but the points are scattered and do not extend to small diameters. However, the published results of Alty in his paper of 1924, Figure 2, have been replotted in Figure 7 and show a clearly defined maximum. Alty's data were obtained at a rotational speed of 628 radians sec^{-1}. It should be emphasized that the explanation of the experimentally-determined fluid resistance encountered by the bubble as a combination of dynamic and viscous forces, and the assumption that the surface charge density is independent of the bubble diameter, accounts by means of (6) and (7) for both the existence and the position of the maxima in Figures 5, 6, and 7. There is a tendency for the calculated mobilities to exceed the measured mobilities at larger diameters, and this could be interpreted as an indication that the surface charge density is not entirely independent of the diameter.

The computations of the mobilities were made using the values of K_1 and K_2 in the first row of Table 1, and by assigning a value of 0.80 esu cm^{-2} to the apparent free surface charge density for the case where water was free of CO_2 , and 0.22 esu cm^{-2} for the surface density when water contained CO_2 . The coefficient of viscosity was taken to be 0.0089 poise in these computations. The curve plotted in Figure 7 with Alty's data was obtained in the same way by assigning a value of 0.91 esu cm^{-2} to the surface charge density. The value, 0.80 esu cm^{-2}, assigned to the charge density for water free of CO_2 with a resistivity of 4×10^6 ohm cm, is large compared to the value 0.039 esu cm^{-2} computed from Currie and Alty's [3] estimate of a charge of 5.4×10^{-4} esu on a bubble of 0.033-cm radius in water having a resistivity of 1.4×10^6 ohm cm. Furthermore, while former interpretations [2], [3] of mobilities, assuming Stokes' law to give the resistance to the motion of the bubble, have indicated a dependency of the apparent surface charge density on the bubble diameter beyond a certain critical size, the new interpretation reported here is that the charge density is practically independent of bubble diameter.

A group of legends are shown in Figure 9 which describe the experimental parameters that were changed during the measurement of the effective surface charge density of rising air bubbles. The voltage produced by the rising bubbles was found to be proportional to the distance between electrodes and to the number of bubbles rising per second, or to the rate of flow of air, since the bubbles always had the same diameter of 0.3 cm. The bubbles, small enough to obey Stokes' law, always spread out uniformly in the cross-section of the tube between the upper and lower electrodes and did not associate to form larger bubbles.

Two features should be noted about these measurements. The first is that the wall effects appear to be small; at least no measurable difference can be assigned to values of surface charge density σ obtained under identical conditions, using either a large or the small diameter column of water. Second, σ appears to be insensitive to the resistivity of the water above 1×10^6 ohms cm, where its value is taken to be 0.19 esu cm^{-2}. Below a resistivity of 1×10^6 ohm cm, σ decreases.

The point of view that the electricity on a bubble acts as if it were a free charge and not an attached neutral double layer is supported not only by the interpretation given above of mobility measurements, but also by the fact that the electric force on a suspended bubble could be statically balanced by an opposite force of buoyancy. The average value of the apparent surface density of charge obtained by static balance and shown in Figure 8 is 0.66 esu cm^{-2}, and this is in fair agreement with the value 0.80 required to satisfy the mobility measurements. Finally, a simple direct interpretation of the electrification of rising bubbles of air is to picture a net free surface charge. The discrepancy between the 0.19 esu cm^{-2} found in this experiment, and the 0.66 and 0.80 values found for a bubble suspended in the rotating liquid, is thought to be due to the time required for charge on a bubble to reach surface equilibrium. The time of rise of the bubbles in the floatation tube never exceeded 20 seconds, while the bubbles suspended in the rotating liquid usually existed for 15 minutes before any mobility data were taken, and Currie and Alty [3] found that the final constant charge may not be reached for as long as 200 seconds after an air bubble is formed.

When CO_2 is dissolved in water, it not only lowers the resistivity of the water, but it also reduces the electric mobilities of air bubbles from those found in Figure 6 to those in Figure 5, or in terms of apparent surface charge density, dissolved CO_2 in equilibrium with room air reduces the density from 0.80 esu cm^{-2} to 0.22 esu cm^{-2}.

References

[1] H. A. McTaggart, The electrification at liquid-gas surfaces, Phil. Mag., **27**, 297–314 (1914).

[2] T. Alty, The cataphoresis of gas bubbles in water, Proc. R. Soc. London, **106**, 315–340 (1924).

[3] B. W. Currie and T. Alty, Absorption at a water surface, Proc. R. Soc. London, **122**, 622–633 (1929).

[4] J. E. Dinger and R. Gunn, Electrical effects associated with a change of state of water, Terr. Mag., **51**, 477–494 (1946).

[5] B. W. Currie, Electro-endosmosis in closed cylindrical tubes of large diameter, Phil. Mag., **12**, 7th Ser., 429–438 (1931).

[6] K. Stewartson, On the slow motion of a sphere along the axis of a rotating fluid, Proc. Cambridge Phil. Soc., **48**, Pt. 1, 168–177 (1952).

THE DIFFERENCES IN THE RELATIONSHIP BETWEEN IONOSPHERIC CRITICAL FREQUENCIES AND SUNSPOT NUMBER FOR DIFFERENT SUNSPOT CYCLES

By S. M. Ostrow and M. PoKempner

Central Radio Propagation Laboratory, National Bureau of Standards, Washington 25, D. C.

(Received June 26, 1952)

ABSTRACT

Analysis of data for Washington and Watheroo indicates differences in the relationship between $f^{\circ}F2$ and sunspot number for the current and preceding sunspot cycles. The sunspot number is therefore not entirely satisfactory as an index for ionospheric variations. Consequently, ionospheric data for the current cycle only should be used in preparing ionospheric radio propagation predictions whenever possible.

1—INTRODUCTION

The approximately linear relationship between ionospheric critical frequencies and sunspot number is well known and is the basis for the predictions of ionospheric radio communications frequencies issued regularly by the National Bureau of Standards and by similar laboratories in other countries [see 1 of "References" at end of paper]. Since the physical mechanisms of the formation and variations of the ionospheric layers have not been established, and also since the sunspot number is an arbitrary, though very useful, index of solar activity, it is of considerable practical and scientific interest to determine whether the same relationship holds between critical frequencies and sunspot numbers over more than one sunspot cycle.

Only a very few ionosphere stations have been in operation long enough to cover substantial parts of two sunspot cycles. Even in these few cases, considerable care must be exercised in the use of the data in order to avoid drawing erroneous conclusions. The earliest observations are few in number per month as compared with the relatively complete daily hourly coverage of modern stations. In addition, over the years, record-scaling techniques have changed with increasing understanding and experience and with international standardization of practices. The older records have seldom been rescaled in accordance with current standards largely because, for most purposes, the increased uniformity and consistency of the data do not justify the excessive labor involved. However, when the data must be as statistically homogeneous as possible, it is important that all records be scaled and the data processed in a uniform manner.

The detailed data and original records from Washington, D. C., and Watheroo, Australia, were the only ones immediately available for this study from the small

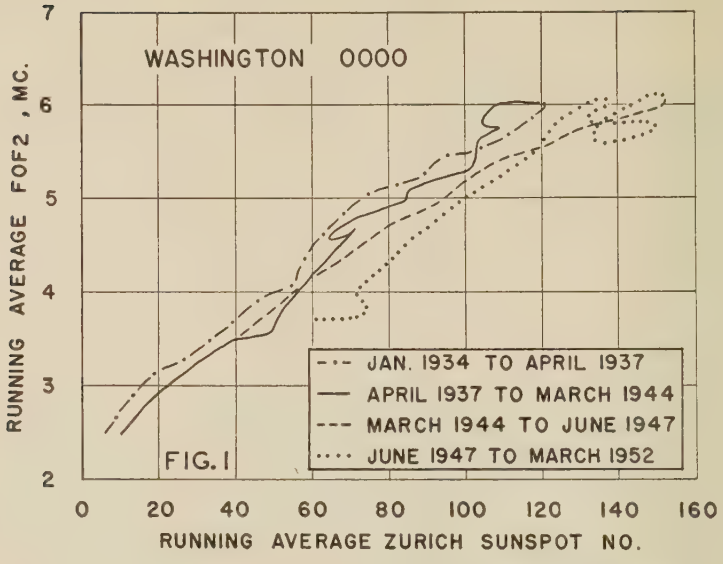

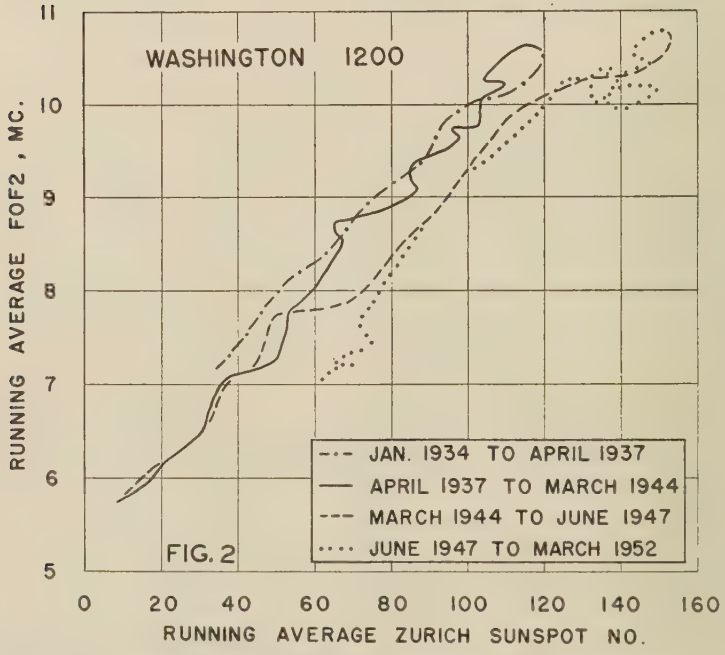

FIGS. 1 AND 2—PLOT OF 12-MONTH RUNNING AVERAGE OF MONTHLY MEDIAN f^0F2 AGAINST 12-MONTH RUNNING AVERAGE OF MONTHLY ZURICH SUNSPOT NUMBER, LOCAL TIME

group of stations making observations for a sufficient length of time. The hours 0000 and 1200 local time were selected for the study as being representative of night and day, and also because in the earlier years observations were often made only at these times. The original records prior to 1946 were examined carefully and often rescaled to conform to current standard scaling practices. Data since 1946 were accepted as tabulated. Monthly medians of $f^{\circ}F2$ were then computed by current standard practice. In this way, the data used were made as nearly uniform as possible, though the earlier medians usually were based on relatively fewer observations per month.

2—RESULTS

The 12-month running averages of monthly median $f^{\circ}F2$ were computed and plotted against the 12-month running averages of monthly Zurich sunspot numbers. The results for Washington and Watheroo are shown in Figures 1, 2, 3, and 4. The graphs show differences between the curves for the two sunspot cycles. It should be noted in passing that early in 1947, operation of the Watheroo station was transferred from the Department of Terrestrial Magnetism, Carnegie Institution of Washington, to the Australian Department of Supply and Shipping. It is possible, though not likely, that some of the differences shown between prior and subsequent data may be due to small systematic differences in interpretation of records between the two organizations. It should be mentioned that the differences between the two cycles shown in Figures 1, 2, 3, and 4 are smaller than those that were observed before the older data were corrected.

The question of the significance of these differences now arises. Conventional statistics are based on assumptions of independence of the data considered, and little work has been done on the validity of their application to cases where the data are not independent. Since at any given time the state of the ionosphere depends, to some extent not yet known, on its prior states, successive observations of ionospheric characteristics are not completely independent. Since statistical tests of significance of relationships of dependent or partially dependent data are not available, it was decided to use standard procedures on the relationship between monthly median $f^{\circ}F2$ and monthly average sunspot numbers, assuming the data for the same month for successive years to be relatively independent.

Another difficulty to be taken into consideration is the relatively small sample size of the data involved. In no case do we have more than 11 years per cycle for a given month, and, in most cases, we have only eight or nine. The small sample size is reflected statistically in correspondingly large standard errors of estimate.

Using the hours 0000 and 1200 for Washington and 1200 for Watheroo, "least squares" lines of regression of monthly median $f^{\circ}F2$ against monthly Zurich sunspot number were computed separately for data subsequent to March 1944 and data prior to that time. It was found that, in all but one case, the correlation coefficient was greater than 0.8. In the great majority of cases, it was better than 0.9. Figures 5, 6, and 7 give examples typical of most of the year, showing little difference in the slopes for the two cycles. However, a few months showed fairly large differences in slope, two of which are illustrated in Figure 8.

Applying Student's t test, for the significance of the difference between the

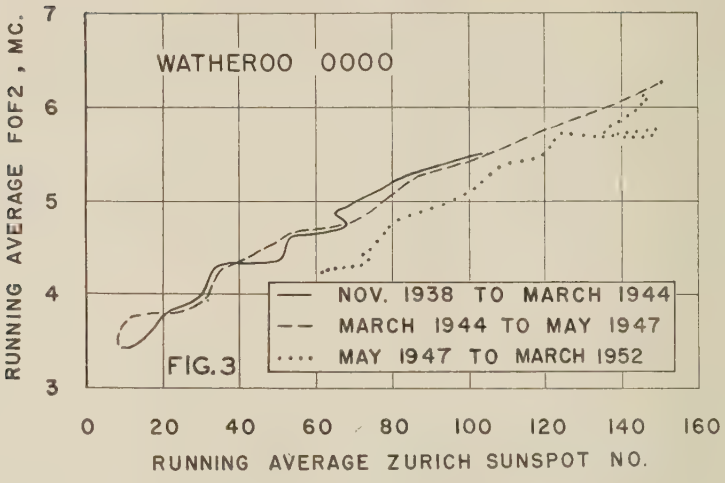

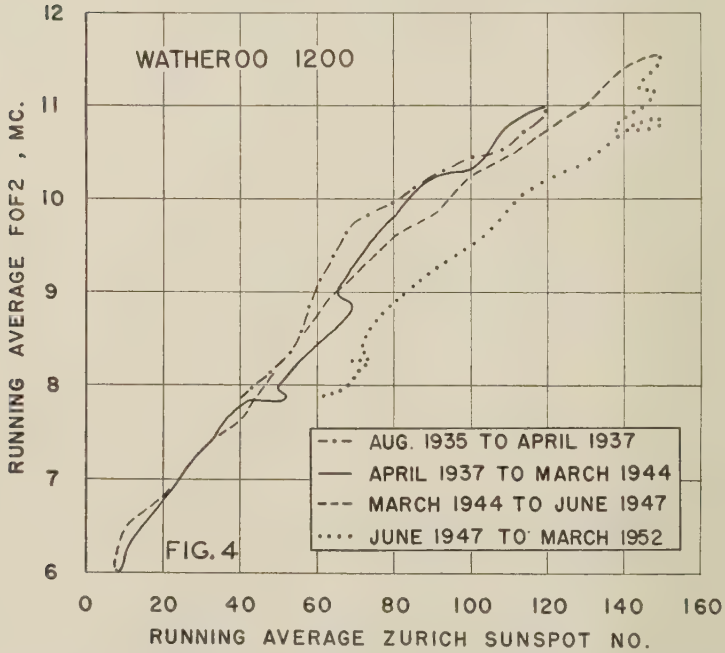

FIGS. 3 AND 4—PLOT OF 12-MONTH RUNNING AVERAGE OF MONTHLY MEDIAN $f^{o}F2$ AGAINST 12-MONTH RUNNING AVERAGE OF MONTHLY ZURICH SUNSPOT NUMBER, LOCAL TIME

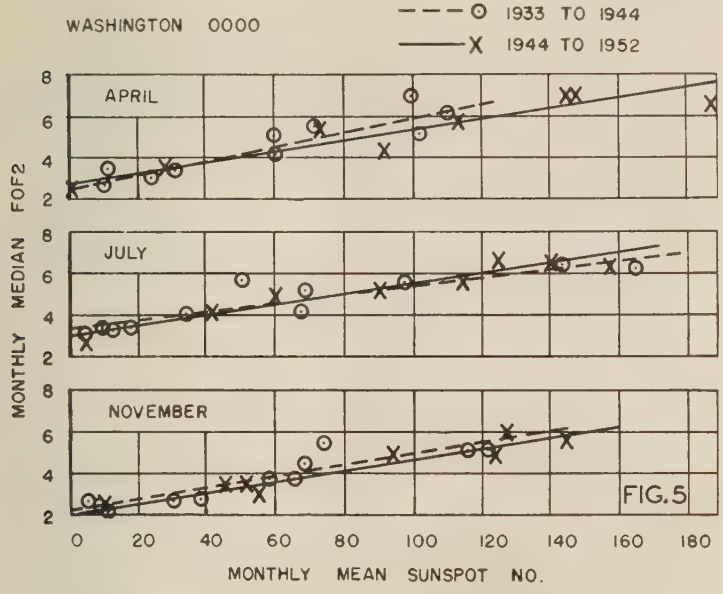

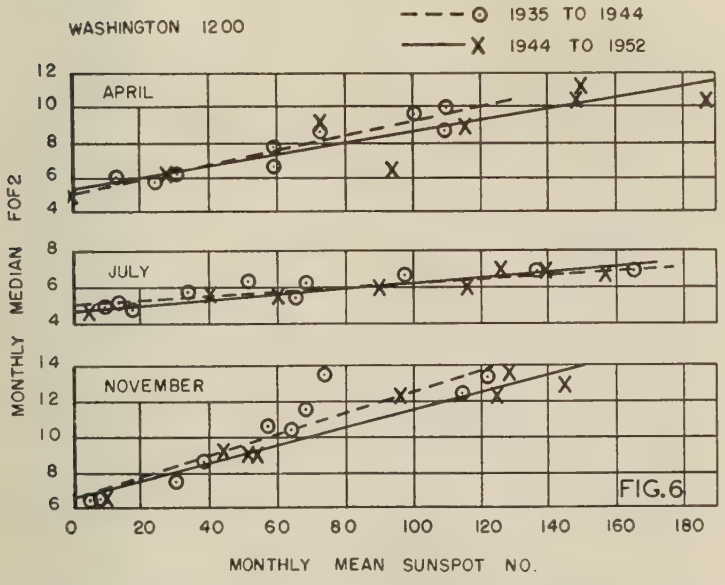

FIGS. 5 AND 6—LEAST SQUARES LINES OF REGRESSION OF MONTHLY MEDIAN $f^{\circ}F2$ AGAINST MONTHLY MEAN ZURICH SUNSPOT NUMBER FOR TWO SUNSPOT CYCLES, LOCAL TIME

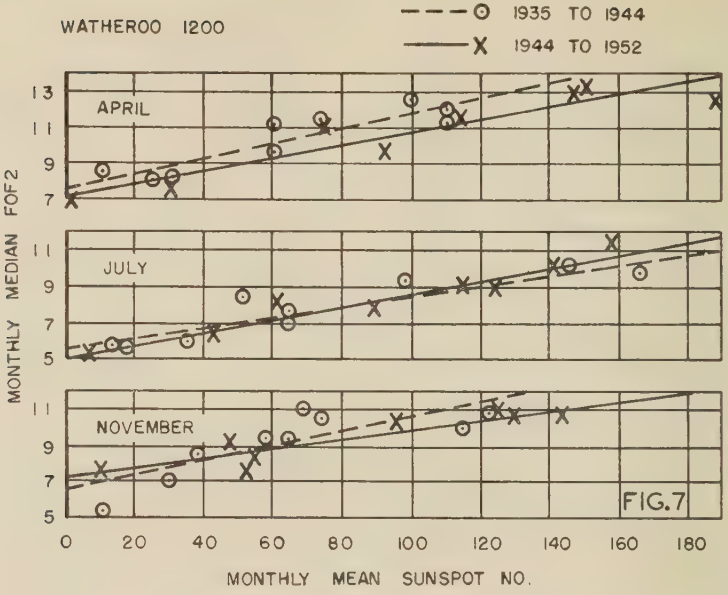

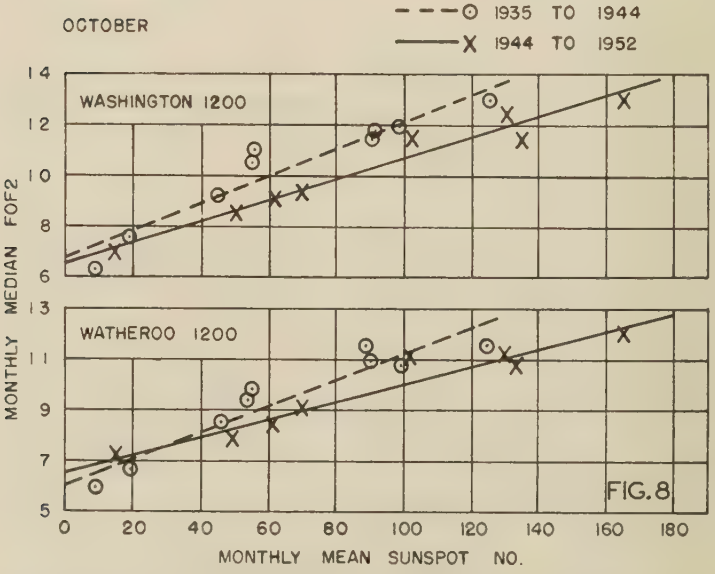

FIGS. 7 AND 8—LEAST SQUARES LINES OF REGRESSION OF MONTHLY MEDIAN $f^{0}F2$ AGAINST MONTHLY MEAN ZURICH SUNSPOT NUMBER FOR TWO SUNSPOT CYCLES, LOCAL TIME

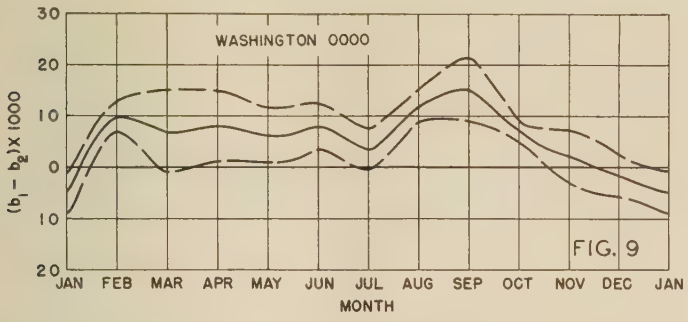

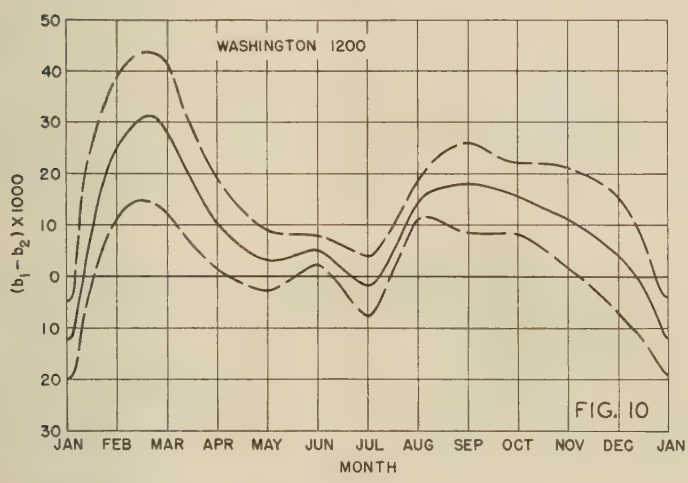

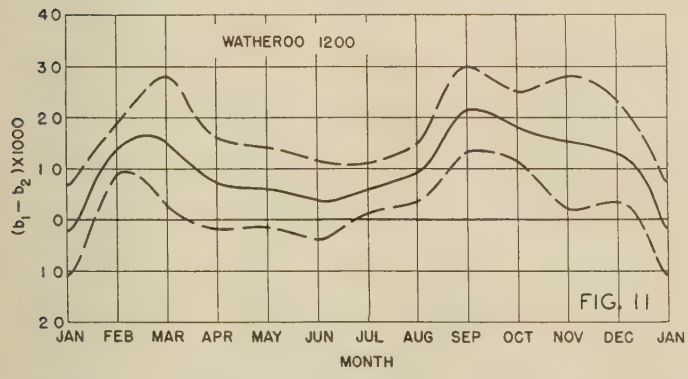

FIGS. 9, 10, AND 11—THE ANNUAL VARIATION OF THE DIFFERENCE BETWEEN SLOPES FOR TWO SUNSPOT CYCLES OF THE LINES OF REGRESSION OF MONTHLY MEDIAN $f^{o}F2$ AGAINST MONTHLY AVERAGE ZURICH SUNSPOT NUMBER, LOCAL TIME; UPPER AND LOWER DASHED CURVES SHOW STANDARD ERROR OF ESTIMATE

slopes for the two periods, we find that the differences of slopes are generally not of import at the 5 per cent level of significance except for a few months near the equinoxes. Plotting the difference in slopes, $(b_1 - b_2)$, month by month, where b_1 refers to the slope for the period March 1944 to the present, and b_2 refers to the slope for the period prior to March 1944, we get an interesting curve of the annual variation of this difference. Figures 9, 10, and 11 show this variation for 0000 and 1200 at Washington and for 1200 at Watheroo, the upper and lower dashed curves showing the standard error of estimate. The few months that showed statistically significant differences between the slopes by the t test were near the peaks of the curve.

The explanation of the seasonal variation of the differences of slopes is not clear. It may be that the slopes which are generally larger for months near the equinoxes than for other months of the year are therefore more sensitive to differences in solar activity for the same sunspot number.

Similar calculations and graphs were made to test the relationship between monthly median $f^{\circ}F2$ values and 12-month running averages of monthly Zurich sunspot numbers. These are not presented here, but they yielded essentially similar results.

3—CONCLUSIONS

The results of this study indicate that for most months of the year, the data show no statistically significant difference in the relationship between $F2$-layer critical frequency and sunspot number for the current and immediately preceding cycles. Months near the equinoxes do show significant differences between the two cycles. The authors believe that the relatively inconclusive statistical results for most of the year are due to the relatively small sample sizes and the variations of data quality discussed earlier. The significance of the differences for the months near the equinoxes and the seasonal variations shown in Figures 9, 10, and 11 indicates that small but real differences exist between sunspot cycles in the relationship between $F2$-layer critical frequencies and sunspot number. Therefore, the Zurich sunspot number is not an entirely satisfactory index of the solar activity responsible for ionospheric ionization. From the practical point of view, therefore, for use in radio propagation predictions, it seems advisable to use data for only the current cycle in establishing trends whenever possible.

The difficulties experienced with the data emphasize the importance in current and future work of continuing the efforts to achieve world-wide standardization of ionospheric observations and data. Reliable and consistent data are necessary for the derivation of valid results from statistical or other analyses.

4—ACKNOWLEDGMENTS

The authors wish to express their appreciation to Mr. J. M. Cameron for very helpful discussion and advice on the statistical aspects of this paper, and to the Department of Terrestrial Magnetism, Carnegie Institution of Washington, for making available original ionospheric records and data sheets from Watheroo.

Reference

[1] National Bureau of Standards, Ionospheric Radio Propagation, Washington, D. C., U. S. Dept. of Comm., Nation. Bur. Stand. Circular 462 (June 25, 1948).

THE ELECTRIC FIELDS OF A LONG CURRENT-CARRYING WIRE ON A STRATIFIED EARTH*

By James R. Wait

Defence Research Telecommunications Establishment (Radio Physics Laboratory), Defence Research Board, Ottawa, Ontario, Canada

(Received June 30, 1952)

ABSTRACT

A numerical solution is given for the problem of a long insulated wire carrying a uniform oscillating current over a stratified earth with a highly conducting lower layer. The resultant electrical field parallel to this wire is shown to be influenced to an appreciable extent by the presence of a conducting zone at a depth of 500 meters for a frequency of 500 cycles per second.

Introduction

The earth's crust may often be represented as a horizontally stratified medium with homogeneous electrical properties in each layer. The analysis of direct current flow in such a medium requires the solution of Laplace's equation. The necessary conditions at the boundaries and at the current sources or sinks are sufficient to determine the potential everywhere. When a source of time-varying current is situated in the vicinity of a layered earth, the problem becomes more complex. The fields must satisfy the Helmholtz wave equation, satisfy the boundary conditions at the interfaces, and behave in the proper manner near the current source and at infinity.

The discussion here will be limited only to two-dimensional problems which are suitable for the study of long straight wires lying on the surface of the earth. Such a condition may arise in methods of electrical prospecting. In this case, it is desirable to know under what conditions a subsurface layer of relatively high conductivity can be detected by measuring the resultant electric field of the wire at some other point on the surface.

Formulas for the fields of an overhead wire parallel to the surface of a flat homogeneous earth have been obtained by Carson [see 1 of "References" at end of paper] and by Price [2], who employed numerical methods of integration. The case where the conductivity varied exponentially with the depth was solved formally by Marion Gray [3], and some useful numerical results were presented. Riordan and Sunde [4] investigated the infinite wire lying on a two-layered earth and gave numerical results for cases of low conductivity contrasts between the layers. Evans [5] also studied the two-layered structure and gave a few numerical examples. In all these problems, the frequency of alteration of the primary current

*Presented at the Congress of the Canadian Association of Physicists, in Quebec City, May 30, 1952.

is such that all displacement currents can be neglected. This is justified for frequencies not over 10 kilocycles per second for normal earth materials.

The solution of the fields for the problem of an infinite wire carrying a uniform current over a flat earth is of value in estimating the field of a finite wire lying on the surface of the earth. In this case, the finite wire may be the side of a large rectangular loop or the wire may be grounded at its distant ends. It is here assumed that the infinite wire representation will be satisfactory to describe the behaviour of the finite wire if the electric field is measured relatively near the centre point of the finite wire. This consideration is discussed in more detail by Heiland [6, p. 774].

In this paper, results will be given for the value of the electric field parallel to the infinite current-carrying wire for the case when the earth may be represented as a two-layer structure with a relatively high conducting zone at depth.

Solution of problem

A Cartesian coordinate system (x, y, z) is chosen so that the wire is coincident with the z axis. The surface of the earth is taken to be the (x, z) plane. The earth medium between the surface $y = 0$ and $y = -d$ has a conductivity σ and magnetic permeability μ. The conductivity of the lower region for $y < -d$ is σ_0 and magnetic permeability μ. It is thus being assumed that there is no magnetic contrast between the media. The displacement currents in the air and the two lower media are assumed negligible. Evans [5] has given the formal integral solution for this problem. Using his result, the electric field E_z on the surface of the earth at $z = 0$ is given by

$$E_z = \frac{i\mu\omega I}{\pi} \int_0^\infty \frac{[(u + u_0) + (u - u_0)e^{-2du}] \cos \lambda x \, d\lambda}{(u + u_0)(\lambda + u) + (u - u_0)(\lambda - u_0)e^{-2du}} \quad \ldots\ldots(1)$$

where $u = (\lambda^2 + i\sigma\mu\omega)^{1/2}$ and $u_0 = (\lambda^2 + i\sigma_0\mu\omega)^{1/2}$.

The units are in the M. K. S. system. The current is given by the real part of $Ie^{i\omega t}$. The actual electric field is then given by the real part of $E_z e^{i\omega t}$.

The particular case to be investigated here is when the lower region is very highly conducting such that no appreciable error is introduced by setting $\sigma_0 = \infty$.

The electric field is then written

$$E_z = \frac{i\mu\omega I}{\pi} \int_0^\infty \frac{(1 - e^{-2du}) \cos \lambda x \, d\lambda}{(\lambda + u) - (\lambda - u)e^{-2du}} \quad \ldots\ldots(2)$$

This can be broken into two parts as follows:

$$E_z = \frac{i\mu\omega I}{\pi} [P(x) - 2Q(x)] \quad \ldots\ldots(3)$$

where

$$P(x) = \int_0^\infty \frac{\cos \lambda x}{\lambda + u} \, d\lambda \quad \ldots\ldots(4)$$

and

$$Q(x) = \int_0^\infty \frac{ue^{-2du} \cos \lambda x \, d\lambda}{(\lambda + u)^2 + i\sigma\mu\omega e^{-2du}} \quad \ldots\ldots(5)$$

It is evident that the second integral $Q(x)$ goes to zero when the depth d tends to infinity, leaving only the contribution from the integral $P(x)$.

The integral $P(x)$ will now be expressed in terms of tabulated functions. The numerator and denominator are multiplied by $(u - \lambda)$ to obtain

$$P(x) = \frac{1}{\gamma^2} \int_0^\infty [(\lambda^2 + \gamma^2)^{1/2} - \lambda] \cos \lambda x \, d\lambda \quad \ldots\ldots (6)$$

where $\lambda^2 = i\sigma\mu\omega$.

The factor $(\lambda^2 + \gamma^2)^{1/2} - \lambda$ in the intergrand can be replaced by an infinite integral with respect to another parameter g by employing a formula given by Watson [7, p. 386, No. 7] then

$$P(x) = \frac{1}{\gamma} \int_0^\infty \frac{J_1(\gamma g)}{g} \, dg \int_0^\infty e^{-\lambda g} \cos \lambda x \, d\lambda \quad \ldots\ldots (7)$$

The integration with respect λ can now be carried out employing the well-known Fourier-cosine integral as given by Pierce [8, p. 64, No. 506].

$$P(x) = \frac{1}{\gamma} \int_0^\infty \frac{J_1(\gamma g)}{g^2 + x^2} \, dg \quad \ldots\ldots (8)$$

The following integral, given by Watson [7, p. 434], is now employed:

$$\int_0^\infty \frac{g J_0(gh)}{1 + g^2} \, dg = K_0(h) \quad \ldots\ldots (9)$$

This equation is differential with respect to h on both sides to give

$$\int_0^\infty \frac{g^2 J_1(gh)}{1 + g^2} \, dg = K_1(h) \quad \ldots\ldots (10)$$

Another integral given by Watson [7, p. 386, No. 8 with $a = 0$] is given by

$$\int_0^\infty J_1(gh) \, dg = \frac{1}{h} \quad \ldots\ldots (11)$$

TABLE I—*Values of* $P(x)$

$\lvert \gamma x \rvert$	Real part of $P(x)$	Imaginary part of $P(x)$
0.0	∞	−0.392
0.2	1.115	−0.382
0.4	0.774	−0.370
0.6	0.579	−0.351
0.8	0.449	−0.328
1.0	0.350	−0.305
1.4	0.221	−0.259
2.0	0.111	−0.197
2.4	0.067	−0.197
3.0	0.031	−0.118

Employing equations (10) and (11), the integral $P(x)$ can be written

$$P(x) = \frac{1}{\gamma^2 x^2}\left[1 - \gamma x K_1(\gamma x)\right] \quad \ldots\ldots\ldots\ldots\ldots\ldots\ldots\ldots (12)$$

The Bessel function $K_1(\gamma x)$ is extensively tabulated [9] for the argument proportional to the square root of i. Values of $P(x)$ are given in Table 1.

The integral $Q(x)$ is simplified in form by making the substitutions

$$\lambda = (\sigma\mu\omega)^{1/2}s, \qquad 2d = (\sigma\mu\omega)^{-1/2}B, \qquad \text{and} \qquad x = (\sigma\mu\omega)^{-1/2}R$$

Then

$$Q(x) = \int_0^\infty \frac{(s^2 + i)^{1/2} e^{-B(s^2+i)^{1/2}} \cos sR \, ds}{[s + (s^2 + i)^{1/2}]^2 + ie^{-B(s^2+i)^{1/2}}} \quad \ldots\ldots\ldots\ldots\ldots\ldots (13)$$

The integral $Q(x)$ has been evaluated numerically for three specified values of B over a range of R. This work was performed by the staff of the Computation Centre of the University of Toronto during 1950. The numerical results are shown in Table 2. For a specified conductivity σ and angular frequency ω, the R values are proportional to the radical separation x, since $R = (\sigma\mu\omega)^{1/2}x$. The three sets of columns correspond to three values of the depth d, since $B = (\sigma\mu\omega)^{1/2}2d$.

TABLE 2—*Values of* $Q(x)$

$\lvert\gamma x\rvert = R$	$Q(x)$ for $B = 0.632455$		$Q(x)$ for $B = 2.000000$		$Q(x)$ for $B = 6.324550$	
	Real part	Imaginary part	Real part	Imaginary part	Real part	Imaginary part
0.0316238	0.2685	−0.1866	0.003855	−0.1068	0.0001071	0.003662
0.0474342	0.2681	−0.1866	0.003841	−0.1068	0.0001074	0.003662
0.0632455	0.2676	−0.1865	0.003820	−0.1068	0.0001075	0.003662
0.0790570	0.2669	−0.1864	0.003793	−0.1067	0.0001081	0.003661
0.0948635	0.2661	−0.1863	0.003761	−0.1067	0.0001085	0.003661
0.10	0.2659	−0.1862	0.003748	−0.1067	0.0001087	0.003661
0.15	0.2624	−0.1856	0.003601	−0.1065	0.0001107	0.003659
0.20	0.2578	−0.1847	0.003396	−0.1062	0.0001130	0.003656
0.25	0.2521	−0.1836	0.003135	−0.1059	0.0001161	0.003652
0.30	0.2455	−0.1823	0.002820	−0.1054	0.0001203	0.003648
0.316238	0.2432	−0.1819	0.002706	−0.1053	0.0001220	0.003647
0.474342	0.2182	−0.1763	0.001331	−0.1034	0.0001402	0.003629
0.632455	0.1913	−0.1695	−0.0004613	−0.1008	0.0001653	0.003604
0.790570	0.1653	−0.1616	−0.002561	−0.09767	0.0001966	0.003571
0.948635	0.1414	−0.1533	−0.004850	−0.09402	0.0002342	0.003531
1.0	0.1342	−0.1505	−0.005615	−0.09274	0.0002478	0.003517
1.5	0.07825	−0.1230	−0.01280	−0.7881	0.0004030	0.003339
2.0	0.04324	−0.09763	−0.01813	−0.06402	0.0005871	0.003098
2.5	0.02227	−0.07615	−0.02088	−0.05030	0.0007740	0.002803
3.0	0.009930	−0.05878	−0.02140	−0.03862	0.0009405	0.002471

A numerical example is quoted by employing the following typical values:

$$\sigma = 10^{-3} \text{ mho per meter}$$

$$\mu = 4\pi \times 10^{-7} \text{ henry per meter}$$

$$\omega/2\pi = 500 \text{ cycles per second}$$

$$x = 100 \text{ meters}$$

$$I = 0.78 \text{ ampere}$$

The complex electric field referred to the primary current corresponding to four different depths to the lower layer can then be easily calculated employing the results in Tables 1 and 2.

Depth d (*meters*)	Electric field E_z (*millivolts per meter*)
∞	$0.382 + i\,1.115$
1580	$0.384 + i\,1.115$
500	$0.160 + i\,1.112$
158	$0.012 + i\,0.599$

It is then quite evident that highly conducting stratified zones at depths of the order of 500 meters should be detectable by a geophysical prospecting scheme that measures the electric field components both in phase and in quadrature with the source current in the primary wire.

References

[1] J. R. Carson, Bell System Tech. J., **5**, 539–554 (1926).
[2] A. T. Price, Q. J. Mech. Appl. Math., **3**, 385–410 (1950).
[3] M. C. Gray, Physics, **4**, 76–80 (1933).
[4] J. Riordan and E. D. Sunde, Bell System Tech. J., **12**, 162–177 (1933).
[5] H. P. Evans, Phys. Rev., **36**, 1579–1588 (1930).
[6] C. A. Heiland, Geophysical exploration, New York, Prentice-Hall, Inc. (1946).
[7] G. N. Watson, Theory of Bessel functions, Cambridge, University Press (1944).
[8] B. O. Pierce, A short table of integrals, Boston, Ginn and Co. (1929).
[9] N. W. McLachlan, Bessel functions for engineers, London, Oxford University Press (1934).

OBLIQUE INCIDENCE PROPAGATION AT 300 KC USING THE PULSE TECHNIQUE

By J. M. Watts

Central Radio Propagation Laboratory, National Bureau of Standards, Washington 25, D. C.

(Received July 10, 1952)

ABSTRACT

The results of an oblique incidence pulse experiment at 300 kc, using a path length of 1,185 km over sea-water, are presented. These consist of median time delays of sky wave *vs* surface wave for March, April, and May, 1951, together with pulse envelope photographs of typical pulse groups, continuous film recordings of surface- and sky-wave pulses, a plot of sunrise transition times, and a discussion of the sunrise conditions.

In late 1950, an experiment was planned by the Central Radio Propagation Laboratory of the National Bureau of Standards and the United States Coast Guard for the purpose of studying radio wave propagation in the low frequency band. The pulse technique for separating the surface wave from the ionospherically propagated wave was chosen in order to supplement the work of other groups who have used continuous wave transmissions [see 1 of "References" at end of paper].

Other experimental conditions were as follows:

Frequency—300 kc. This was a frequency already used by the Coast Guard for coastal beacons, high enough to allow short, loran-type pulses with reasonable antenna efficiency, yet low enough to avoid duplicating information which is already available from years of operation of loran stations near 2 Mc.

Path—From Wildwood, New Jersey, to Bermuda. The length of this path was considered to be about the maximum which would allow good resolution of the ground or surface wave and the one-hop sky-wave pulses. An over-water path was chosen to obtain minimum attenuation of the surface wave.

Pulse length—50 microseconds or less. The actual pulse length depended on the signal-to-noise ratio at the receiver. During most of the experiment, a duration of about 35 microseconds was used. The receiver band width was about 80 kc for the shortest pulses, although a receiver with 20-kc band width was used occasionally.

Pulse repetition rates—Submultiples of 25 per second were available. Throughout the experiment 1.5625 per second was used, to minimize interference with other services.

Accuracy of timing—One part in 10^9 for short periods. This enabled automatic

film records to be made, since the pulse group time position did not drift too far in a few hours.

Duration of the experiment—March 5 to June 14, 1951, which interval included several periods of ionospheric disturbance as well as quiet periods.

Method of observation—Most information was obtained by photographing the pulse group envelope with an automatic single-frame camera, and by recording the pulse delays continuously with another camera providing slow film travel.

Transmitting apparatus was prepared and operated by the United States Coast Guard. It consisted of a transmitter capable of delivering 100-kw peak pulse power, a 300-ft top loaded antenna, and a loran timer with a supplementary frequency divider to provide pulse rates of 12.5, 6.25, 3.125, and 1.5625 pulses per second. The location of the transmitter at the Electronics Engineering Station of the Coast Guard at Wildwood, New Jersey, was ideal because of its proximity to the ocean.

Receiving apparatus was prepared by the Central Radio Propagation Laboratory of the National Bureau of Standards and operated at Town Hill, Bermuda. A standard loran receiver was modified by adding binary dividers to the fast sweep circuits. This allowed the fast sweep and pedestal to be triggered only at the transmitter rates selected. A camera designed for photographing radar PPI screens was procured and fitted to the loran oscilloscope, and a timer for making photographs automatically on a prearranged schedule was devised.

The pulse selected from the binary chain was also used to start the sweep of the continuously recording oscilloscope, which was photographed by another camera whose 35-mm film moved continuously at a speed of approximately one inch per hour. The 50-microsecond markers from the loran indicator, together with the receiver output, were applied to the grid of this oscilloscope. The brightening of the screen thus produced a pattern of fine lines marking time in 50-microsecond intervals, upon which was superimposed the pulse pattern of surface and sky waves from the receiver.

The receiver consisted of a low frequency push-pull grounded grid amplifier stage feeding a balanced converter, the oscillator of which was crystal controlled. The converter output at 2 Mc was fed into two regular loran receivers. One receiver was of conventionally wide band width (about 80 kc), and the other was made considerably narrower (20 kc) by the expedient of shunting additional condensers across the i-f coils to lower the i-f frequency from 1,600 to about 525 kc.

Two antennas were used at the receiver. One, a vertical wire about 75 feet high, proved to have an effective length of about 2.7 meters. This was arrived at by measuring the field intensity of a local 393-kc station and comparing it with the open circuit voltage delivered by the vertical wire due to the same station. The second antenna, used most of the time, was a single wire loop erected broadside to the local radio range station, which was the greatest source of interference. The effective length of this antenna was not measured.

Transmission was begun March 5, 1951, and continued through June 14, 1951. The system proved to be quite reliable, except for periods when the timing was faulty, due to either transmitter instability or line voltage interruptions. There

were usually two or more failures of synchronization per day, although there was one period of more than a week without a single failure. When failure occurred at night, great difficulty was experienced in relocating the signal, since the noise level was high and the low repetition rate made identification difficult.

The field intensity of the surface wave was too small to measure directly with a field intensity meter; therefore, a substitution method was used to determine the e.m.f. induced in the vertical wire receiving antenna. This was determined to be 300 microvolts ± 15 per cent, which indicated a field intensity of about 111 microvolts per meter, using the measured equivalent height of the vertical wire.

From simple geometry, a set of curves shown in Figure 1 was calculated. These show the layer heights which would account for surface-wave *vs* sky-wave delays up to 700 microseconds and for one-, two-, and three-hop modes, assuming the surface wave travels with the speed of light in free space.

Figure 2 presents reproductions of typical received pulse envelope photographs, which were made with a 50-microsecond transmitted pulse and the narrow band

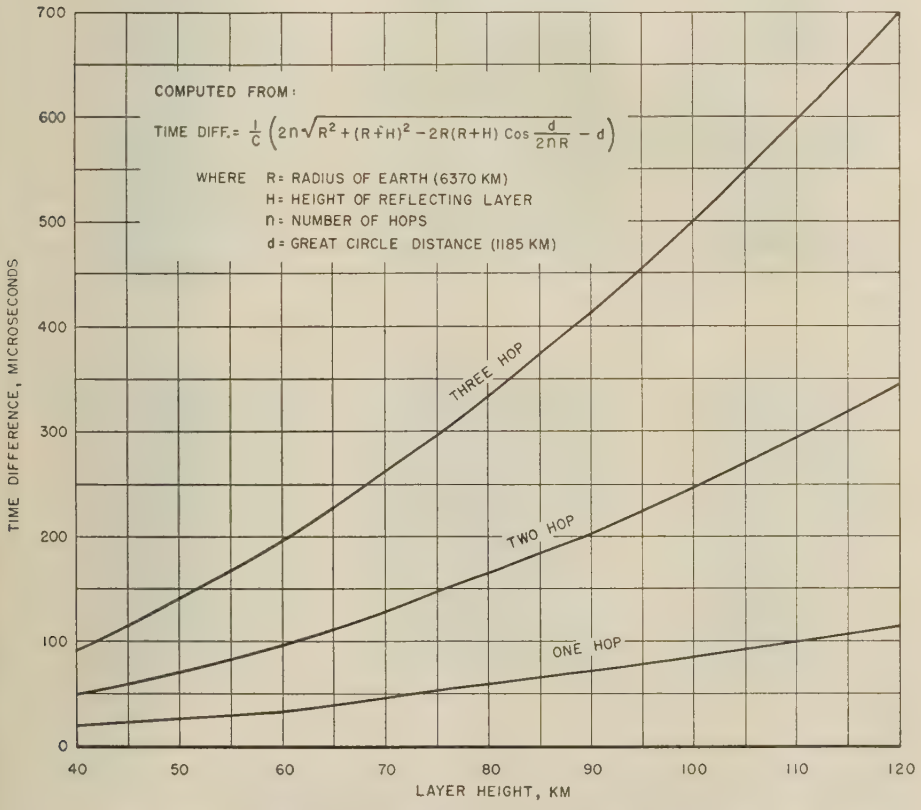

FIG. 1—TIME DIFFERENCE BETWEEN ARRIVAL OF SURFACE WAVE AND SKY WAVES FOR A GREAT CIRCLE DISTANCE OF 1185 KM

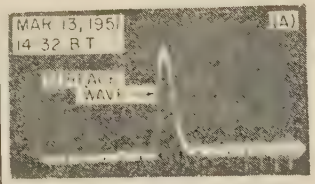

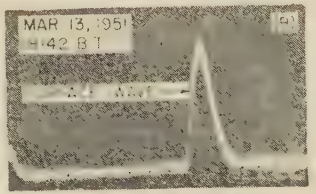

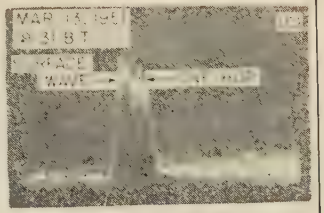

(A) TYPICAL DAYTIME RECEIVED PULSE CONSISTING OF SURFACE WAVE WITH PRACTICALLY NO SKY WAVE
(B) BASE OF SURFACE-WAVE PULSE SHOWS BROADENING DUE TO CONTAMINATION BY SMALL SKY-WAVE PULSE
(C) SKY-WAVE PULSE HAS INCREASED TO NEARLY THE AMPLITUDE OF THE SURFACE-WAVE PULSE

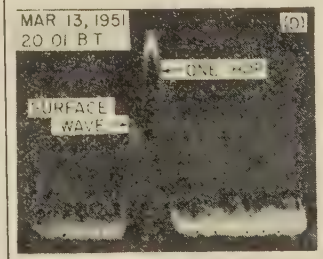

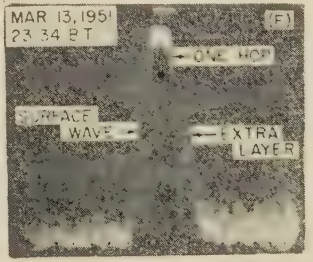

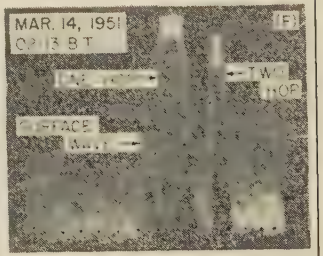

(D) LOW ABSORPTION AT NIGHT CAUSES ONE-HOP SKY WAVE TO BE THE MOST PROMINENT PULSE RECEIVED
(E) ONE EXAMPLE OF THE EFFECT OF EXTRA STRATIFICATION - A PULSE WHICH IS BETWEEN NORMAL ONE AND TWO HOP IN DELAY
(F) TYPICAL NIGHT-TIME RECEIVED PULSE GROUP

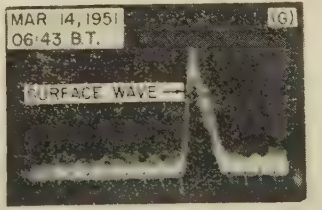

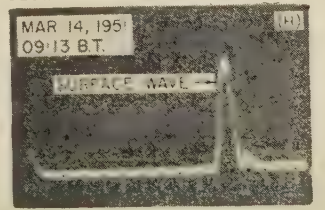

(G) SUNRISE, NOTE SIMILARITY TO (C)
(H) DIP BETWEEN TWO PULSES APPEARS TO BE PHASE INTERFERENCE, PREVENTING ACCURATE DELAY MEASUREMENT

FIG. 2—RECEIVED PULSES, MARCH 13-14, 1951

receiver. The narrow band width permitted excellent photographs to be made, but, as in Figure 2*B*, the resolution was not always sufficient to allow measurement of sky-wave delays. However, the series of photographs illustrates nicely the types of phenomena which were generally observed during the entire experiment.

One of the most obvious applications of the pulse envelope photographic data to basic ionospheric propagation work is its interpretation in terms of layer height. By using the curves of Figure 1 and one-hop time delays as measured from the film records, the data shown in Figure 3 were plotted. These show a considerable spread due to the inherent inaccuracies of this method of measuring reflecting height. However, the one-hop equivalent layer heights, which are typical of those observed throughout the period, are considerably lower than those virtual heights which have been observed at vertical incidence. Also, it should be noted that the equivalent layer heights derived from two- and three-hop pulse delays are different from those derived from one hop, and are usually higher with increasing number of hops. One possible explanation of this is that the layer possesses appreciable thickness, and the degree of penetration into the layer is a function of the angle of incidence. Another factor which might offer an explanation for the apparent discrepancy in height is the velocity of propagation of the surface-wave pulse, which is certainly not equal to the velocity in free space used in computing Figure 1, but somewhat less. The delay due to the refractive index of air would account for a maximum of 1.5 microseconds' differential for the path, and the additional delay due to the finite conductivity of sea-water and effects of the earth's curvature is estimated by K. A. Norton [2] to be another 1.5 microseconds, making a total of 3 microseconds. This is based on theoretical work still in progress.

However, examination of the curves of Figure 1 indicates this correction is not enough to account for the differences between one-, two-, and three-hop layer heights. As an example, the delays at $01^{h}\ 30^{m}$ Bermuda time, March 31, 1951, were 55, 185, and 415 microseconds for one, two, and three hops, respectively, corresponding to reflecting heights of 76, 86, and 90 km. The correction due to surface-wave retardation would have to be more than 15 microseconds to make the equivalent reflecting heights approximately equal. This leads to the conclusion that the reflecting height is markedly dependent on the angle of incidence.

A summary of the one-hop delay data obtained is shown in the form of median values for each hour of the day in Figure 4. The arrows indicate that the one-hop sky-wave pulse merged with the surface-wave pulse, so that the delay could only be estimated as being less than the value shown by the dot. Delays of 60 microseconds were observed quite consistently at night, although the medians for May nights deviated somewhat from that value. The daytime values of delay, however, show a progressive decrease, as if there were a seasonal trend.

The amplitude of the sky-wave pulse, when compared with that of the surface-wave pulse, gives a measure of ionospheric absorption which is to some degree independent of transmitter and receiver characteristics. To a fair degree of accuracy, the antenna responses were the same for both waves, and in most cases the sky-wave pulse was not elongated appreciably due to dispersion, so that the frequency spectra were the same. Therefore, the comparison was independent of receiver

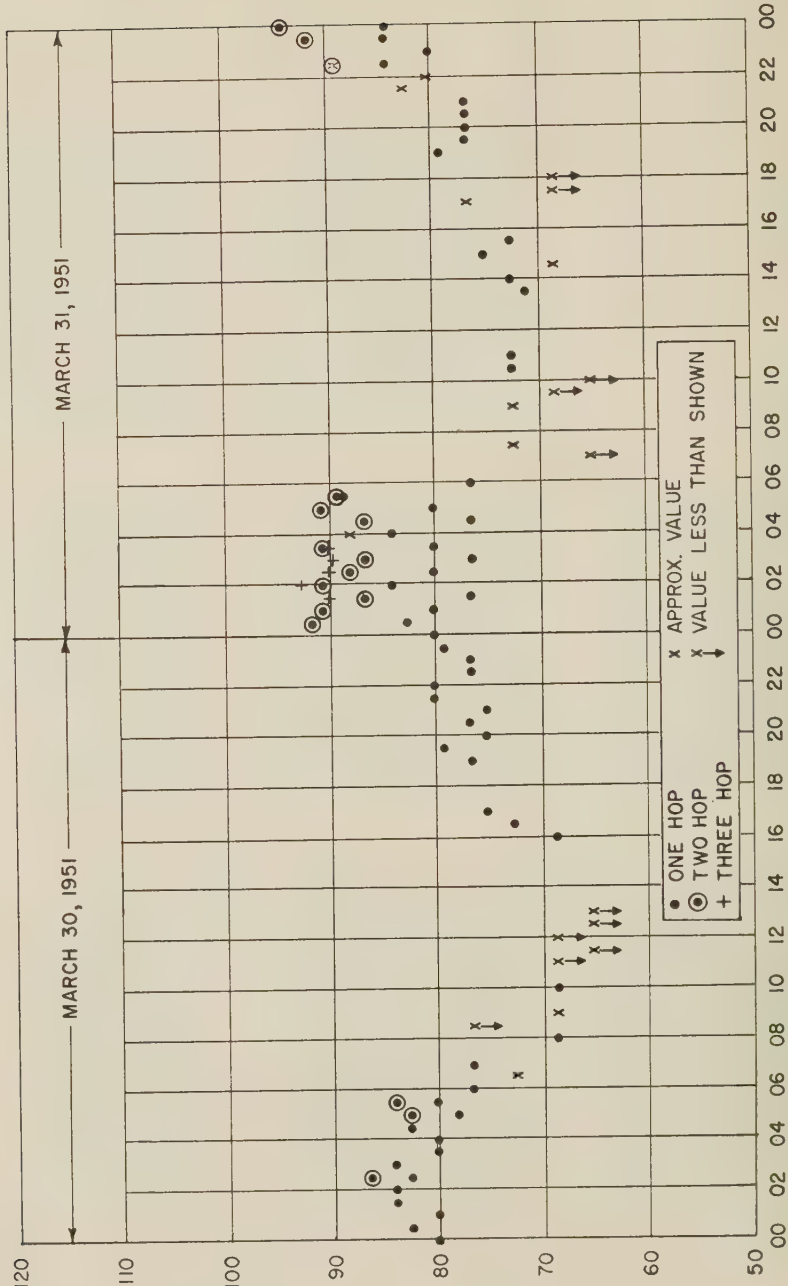

FIG. 3— EQUIVALENT LAYER HEIGHTS DURING TWO TYPICAL DAYS
(USING UNCORRECTED SURFACE-WAVE DELAY TIMES)

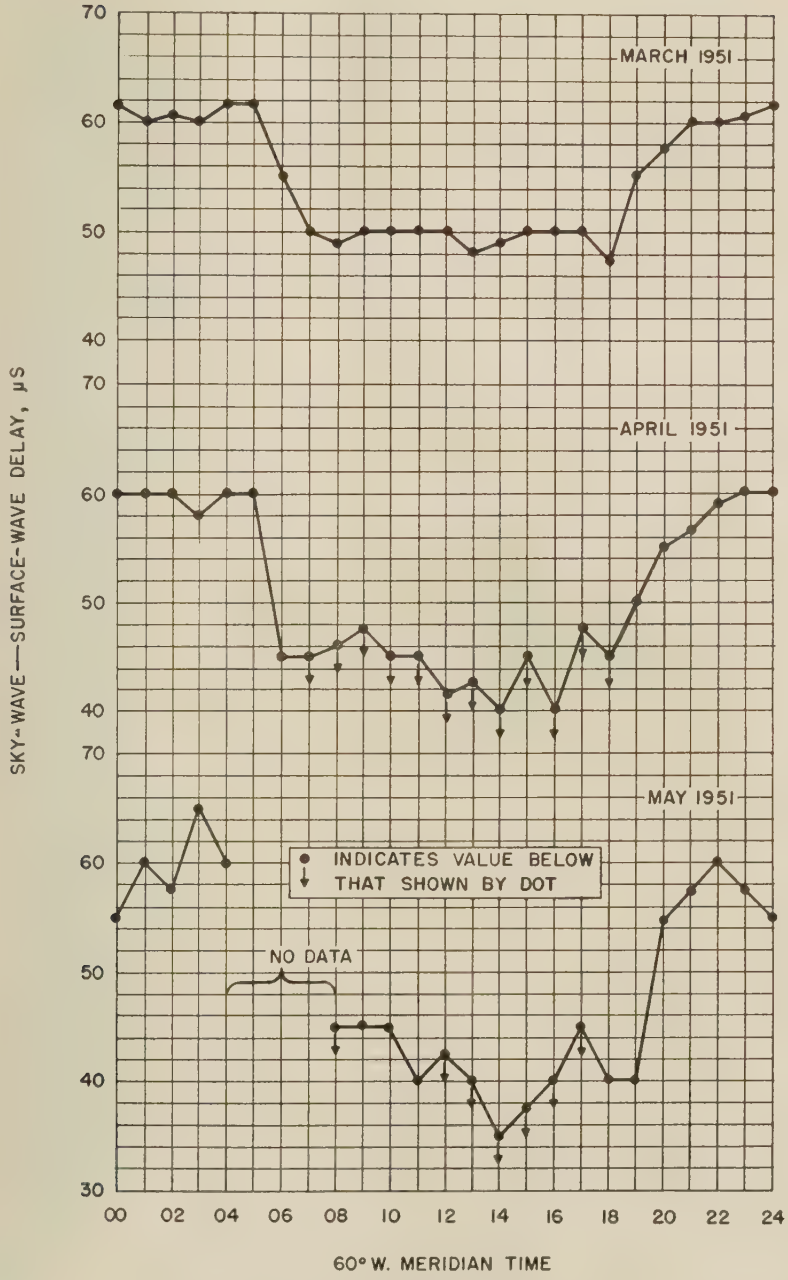

FIG. 4—HOURLY MEDIAN VALUES, SKY-WAVE VS SURFACE-WAVE DELAYS

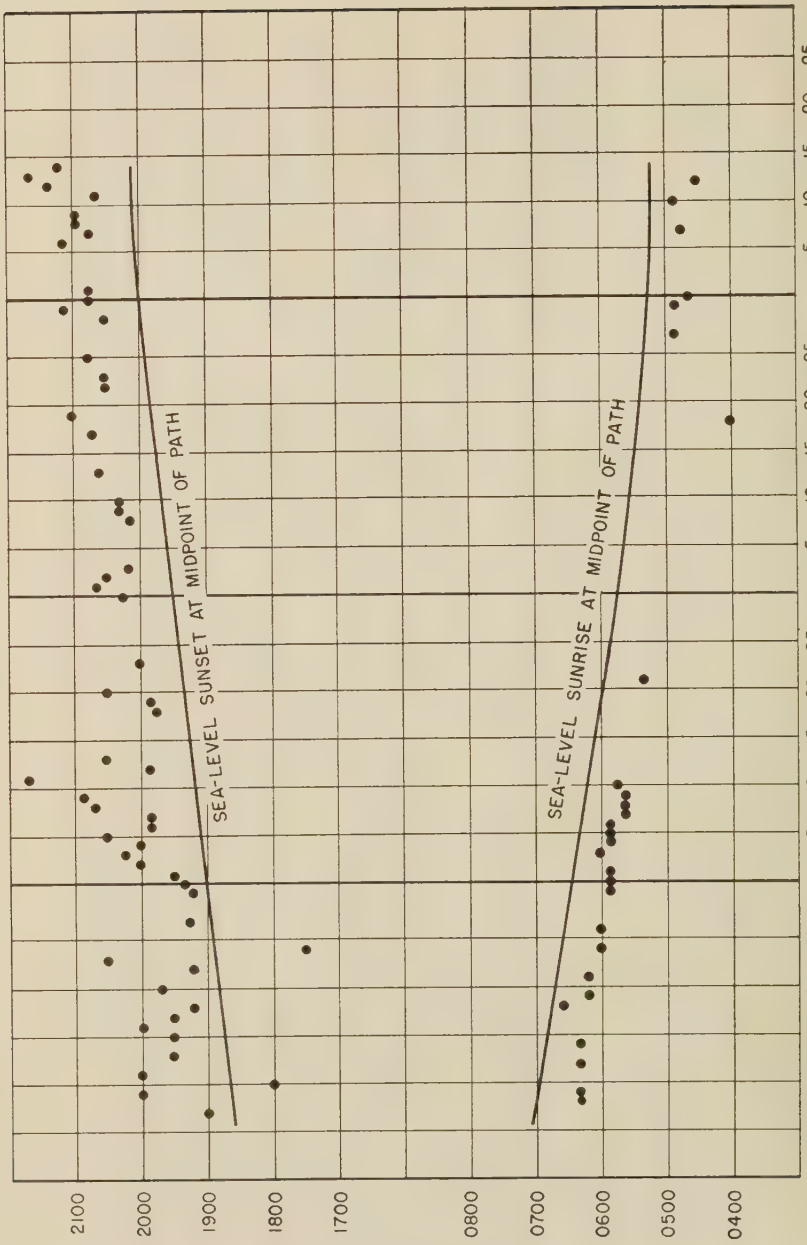

FIG. 5—AMPLITUDE CROSSOVER TIMES FOR SURFACE AND SKY WAVES

band width. Linearity of receiver output was, however, very important, since the amplitudes of sky- and surface-wave pulses differed greatly most of the time.

The daytime sky-wave pulse was much smaller than the surface-wave pulse. It was estimated that the ratio varied between 1/10 and 1/4 in March, and was still less in June. Moreover, the separation of surface- and sky-wave pulses was less in the daytime than at night, and therefore there was always some contamination of the small pulse by the large one during the day.

The night-time one-hop sky-wave pulse dominated the pulse group, causing the receiver to saturate most of the time. It was estimated that the ratio was 10:1, except during some of the fading cycle minima.

The transition from night to day amplitudes occurred in a very short time. On many mornings, the sky wave practically disappeared in a few minutes' time. The times at which the sky-wave pulse amplitude became equal to the surface-wave pulse amplitude, the "amplitude crossover times," are plotted in Figure 5. It is interesting to note the regularity of the crossover period in the mornings; also its relation to sea-level sunrise at the path midpoint. The corresponding period at sunset was not as well defined, but the same trend is evident. The dramatically sudden increase of absorption with sunrise and its regularity suggest that the relationship between the propagation path and the time of sunrise could be used to discover the true height of the absorbing region [3, 4]. It is shown in Figure 5 that the sunrise time as defined by the "amplitude crossover time" occurred approximately 35 minutes earlier than sea-level sunrise at the path midpoint. A series of great circle calculations based on the sunrise of March 21, 1951, shows that the ground tangent sun ray passed under the path midpoint at a height of approximately 50 km. The intersection point was decreasing in height at an approximate rate of 3-1/2 km per minute at that time. Therefore, if the crossover time can be determined from Figure 5 with an accuracy of ± 3 minutes, the height of intersection is accurate to within approximately ± 12 km. The corrected ground-wave *vs* sky-wave delay at that time was 58 microseconds, which, from Figure 1, corresponds to an equivalent reflecting height of 79 km. The accuracy of the time delay measurements is approximately ± 5 microseconds, producing an accuracy of ± 4 km in the equivalent reflecting height.

The solution for the true height of the absorbing region from these data is not complete, however, because of the effect of the filtering of the sun's radiant energy by the atmosphere at the point of tangency. The ground tangent ray, of course, contains only visible and infrared energy capable only of disassociating ions of very low binding energy. Miltra [5] has suggested that the negative ion of atomic oxygen would be disassociated by solar rays tangent to the ozone layer, which extends to a height of about 35 km. This solar ray would then first intersect the midpoint of the transmission path approximately 35 km higher than the ground tangent ray, or at about 85 km. This is 6 km higher than the observed equivalent reflecting height, but well within the probable error of observation. Therefore, a sun ray tangent to the ozone layer is sufficient to explain the observations, but only if the absorbing region is near the height of reflection.

The evidence, however, does not preclude the possibility that the absorbing region is below the height of 80 km if electrons could be liberated in that region by

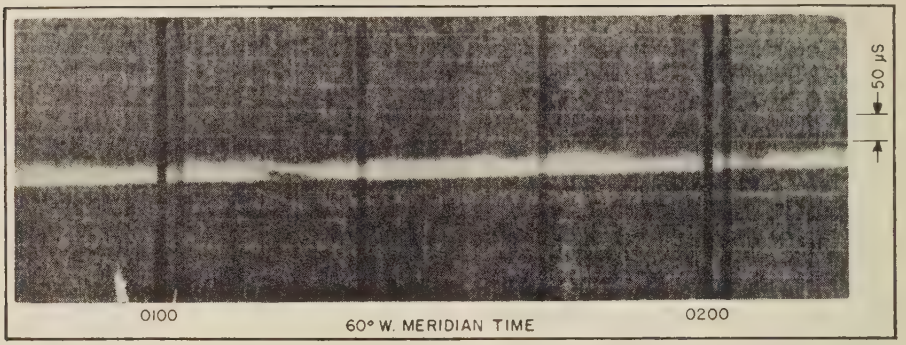

FIG 6—MOVING FILM RECORD, MAY 31, 1951 SURFACE-WAVE PULSE INVISIBLE IN NOISE. SKY-WAVE SPLIT SHOWN AT 01 15.

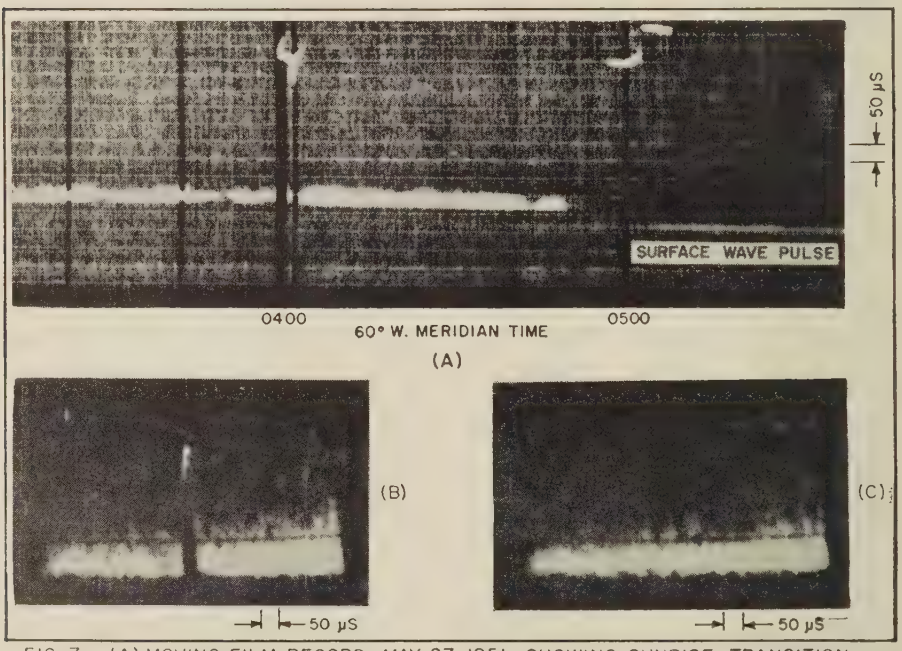

FIG. 7—(A) MOVING FILM RECORD, MAY 27, 1951, SHOWING SUNRISE TRANSITION
(B) PULSE ENVELOPE PHOTOGRAPH AT 04:42
(C) PULSE ENVELOPE PHOTOGRAPH 10 MINUTES LATER

visible light. At the instant being considered, the ground tangent ray actually intersected the propagation path at a height slightly less than 20 km and directly above a place about 191 km from the receiving station.

This means that at that time a portion of the path of propagation was illuminated to some degree by sunlight at all heights between 20 km and the reflecting region. Unfortunately, therefore, there are still two unknown factors which define the absorbing region, its physical location and the portion of the sun's radiant

energy responsible for its sudden excitation at the "amplitude crossover time."

The sharpness of the sunrise transition on the oblique incidence path suggested a further experiment at nearly vertical incidence. This was done by receiving the 300-kc pulses from Wildwood at Sterling, Virginia, for a short time. During this two-week interval, the short path sunrise transition was so erratic in time of occurrence that no corresponding data could be derived. In addition, 160-kc vertical incidence records made at Sterling, Virginia, during the same period were examined for sunrise effects. The effects seen on these records appeared to accompany ground sunrise, with certainly no effects regularly preceding ground sunrise by as much as 35 minutes. The measurements at or near vertical incidence all seemed to result from a more gradual transition than was observed on the oblique incidence path. A possible explanation is that absorption occurred in the entire region between 20 and 80 km, and the sunlight illuminated the entire region more suddenly in the oblique incidence case because the path of propagation and the rays of sunlight intersected at a small angle.

Figure 6 contains a typical example of the effect of stratification or turbulence in the reflecting region. It has been shown from vertical incidence recordings [6] that ionospherically disturbed periods are accompanied by distinctive effects upon the *E*-region at night. These effects appear to be a thinning of the lower level ionization so that it becomes transparent, and regions above it are recorded as scattered patches and miscellaneous strata of no continuity, many of them possibly from directions other than directly overhead. The oblique incidence records produced only minor manifestations of the same phenomena. The lower level, as evidenced by the leading edge of the sky-wave pulse, was continuous and uniform most of the time. Occasionally, a thickening of the trace occurred, but this was always at the trailing edge. The leading edge became indistinct or unreliable during periods similar to that of $01^h\ 15^m$ in Figure 6, but these were rare, and of short duration. Severe fading accompanied these periods. Examples of deep fades may be seen at $02^h\ 07^m$ in Figure 6, and at $03^h\ 50^m$ and $04^h\ 45^m$ in Figure 7. In the moving film records, hour marks are represented by complete blanking of the trace, but periodic weakening of the trace three times each hour for one minute was caused by an automatic reduction of receiver gain in an attempt to get pulse envelope photographs containing unsaturated sky wave. The apparent increase of time delay during these periods was caused by a weakening of the leading edge. This effect on the accuracy of the time delay measurements was minimized by checking the distance between the pulse peaks in the pulse envelope photographs and also by reconstructing the leading edges when they were indistinct. Nevertheless, this remains the largest source of error in the time delay measurements. It tended to cause an increase in measured daytime delay differences when the surface wave was larger than the sky wave, and to cause a decrease in the measured differences for night when the sky wave was larger than the surface wave.

The results derived from this experiment consist largely of the practical evidence contained in the measured time delay differences between the surface wave and the one-hop sky wave. They are, of course, valid only for the specific conditions of the experiment, that is, 300 kc, a path from Wildwood, New Jersey, to Bermuda, and the time period from March to June, 1951. The pulse envelope photographs in

Figure 2, together with numerous unpublished ones, constitute basic propagation data which can be used to derive the characteristics of this particular circuit, whether it is used for pulse type services or c-w communications.

References

[1] C. Williams, Low frequency radio wave propagation by the ionosphere, with particular reference to long-distance navigation, Proc. Inst. Elec. Eng. (London), **98**, Pt. 3, 81-99 (1951).

[2] K. A. Norton, A new source of systematic error in radio navigation systems requiring the measurement of the relative phases of the propagated waves, Proc. Inst. Radio Eng., **35**, 284 (1947).

[3] R. A. Helliwell, *et al.* (the sunrise effect), Interim Progress Report on Ionosphere Research, pp. 17-19, Electronics Research Laboratory, Stanford University (March 15, 1951).

[4] R. A. Helliwell, *et al.* (the sunrise effect), Pulse studies of the ionosphere at low frequencies, pp. 60-76, Report of Electronics Research Laboratory, Stanford University (March 15, 1951).

[5] S. K. Mitra, The upper atmosphere, pp. 219-222, Calcutta, Royal Asiatic Society of Bengal (1948).

[6] J. M. Watts and J. N. Brown, Effects of ionosphere disturbances on low frequency propagation, J. Geophys. Res., **56**, 403-408 (1951).

ON THE NATURAL RADIOACTIVITY IN THE AIR

By Irving H. Blifford, Luther B. Lockhart, Jr., and Herbert B. Rosenstock

United States Naval Research Laboratory, Washington 25, D. C.

(Received July 24, 1952)

ABSTRACT

The concentrations of the various radioactive decay products of radium in the air have been determined by observing the beta activity (1) of pieces of filter paper through which air has been passed, and (2) of chemically separated isotopes obtained from such filter papers. The relative amounts of long-lived and short-lived products found indicate that, besides the radioactive decay of the substances, some other process which removes radioactive particles from the air is active. The mean life of the particles with respect to this removing process is found to be about 10 days. The hypothesis that this process is the capture of the radioactive particles by rain droplets (clouds) is consistent with measurements made of the radioactive content of rain-water. On the other hand, the removal of the ionized radioactive particles by the electric field of the earth leads to a much smaller effect.

I—INTRODUCTION AND SUMMARY OF RESULTS

Radon from the soil diffuses into the air and with its decay products, the thallium, lead, bismuth, and polonium isotopes, radium A, B, C, D, E, and F, produces the bulk of the natural radioactivity of the atmosphere. The equilibrium amounts present of each substance should, in the absence of some special mechanism of depletion, be inversely proportional to the respective radioactive decay constants, and the rate of radioactive decay would, therefore, be the same for all substances [see 1 of "References" at end of paper], including the long-lived materials.

In this work, we have determined the relative amounts of the long-lived and short-lived decay products of radium in the air, and found a much smaller concentration of long-lived products than is expected from the above considerations. The short-lived substances were determined by measuring the activity of a filter paper through which air was drawn. The radioactive ions are known to be attached to comparatively large particles [2, 3] which are retained in the filter paper. To measure the long-lived products, it was necessary to separate them chemically from several large filter papers through which a much larger volume of air had passed.

This low concentration of the long-lived decay products indicates that some mechanism for their removal other than radioactive decay is, in fact, at work.

The usual decay constant λ_X is defined as the fraction of radioactive atoms of substance X lost out of a given volume by radioactive decay in unit time, as follows:

$$\lambda_X \, dt = -dX_{rad}/X$$

We can, by analogy, define a "decay constant" ξ as the fraction of atoms of substance X lost out of a given volume by this additional non-radioactive mechanism in unit time:

$$\xi \, dt = -dX_{non\text{-}rad}/X$$

If ξ is assumed to be the same for all substances A, B, C, $\cdots$ (in contrast to λ_A, λ_B, λ_C, $\cdots$ which are different from each other), then our data give an average value

$$\xi \cong 10^{-6} \text{ sec}^{-1}$$

We may express this by saying that the "mean life" of each substance due to non-radiative loss is $1/\xi \cong 10$ days. This should be compared, for example, to the radioactive mean lives $1/\lambda_B \cong 1$ hour for RaB and $1/\lambda_D \cong 32$ years for RaD. The mean life of any substance in question due to non-radioactive loss is thus long compared to the radioactive mean life of radium B and the other short-lived substances, but very short compared to the radioactive mean life of radium D.

To explain the nature of this non-radioactive loss, three possibilities come to mind, as follows: The particles, which are charged, might be pulled to the ground, either by the electric field of the earth [4], or by its gravitational field; or they might be swept out of the volume in question by rain.

It is reasonable to assume that the original distribution in height z of RaA will be exponential [5, 6], since it is due to the diffusion of radon out of the ground

$$A(z) = A^0 e^{-\alpha z}$$

On the assumption that any radioactive matter swept out of the air by moisture will eventually return to the earth in form of rain, the following simple formula may then be written (section III)

$$\xi = \alpha[f(\text{rain}) + v]$$

The $f(\text{rain})$, which involves measurable quantities such as the annual rainfall and the radioactivity of rain-water, can be computed; v, the velocity of the ions, impelled either by the electric or the gravitational field of the earth, is known [2, 3]; in fact, the gravitational contribution to the velocity is negligible compared to the electric one [7]. We find

$$f(\text{rain})/v \geq 40$$

The effect of the rain is thus the predominant one in causing the "loss" of radioactive particles in the air.

From the above, we also find

$$\alpha = 1.9 \times 10^{-6} \text{ cm}^{-1}$$

The height in which the radioactive content falls off to half its ground value is thus about 3.5 km, in reasonable agreement with measurements of Wigand and Wenk [5] in Berlin and Halle, Germany, and with semiempirical calculations of Priebsch [6].

II—EXPERIMENTAL PROCEDURE

Since the content of long-lived RaD, E, and F is quite low, the collection of a measurable amount of activity requires the processing of a large volume of air. In order to do this, a turbine-type blower, operating at about 2,000 cubic feet per minute, was used to draw air through a 400 square inch of ACC type 5 filter paper.* The flow rate was measured using a recording-type flow meter, compensated for pressure and temperature. It was found that the normal dust load in the air at Washington, D. C., plugged up the filter quite rapidly and, therefore, it was necessary to expose several papers over a period of about a week. The curves of flow rate *versus* time were integrated mechanically to obtain the total air flow for the whole period of operation. The volume of air processed was approximately 9.0×10^6 cubic feet.

Coincident with the large volume collection, a smaller pump operating at a constant rate drew air through a two-inch diameter MSA "Red All-Dust" filter. A beta-sensitive, end-window Geiger counter was suspended over the filter during collection and the counting rate recorded by a counting rate meter and pen recorder. The curve of counting rate *versus* collecting time is shown in Figure 1.

The small filter was changed every 24 hours, at which time a radioactive standard was run in place of the filter, and the rate meter calibration checked

*It has been found [8] that Mine Safety Appliances Company "Red All-Dust" filter paper and Army Chemical Corps type 5 filter paper are approximately equivalent for filtering naturally radioactive particulates from the air.

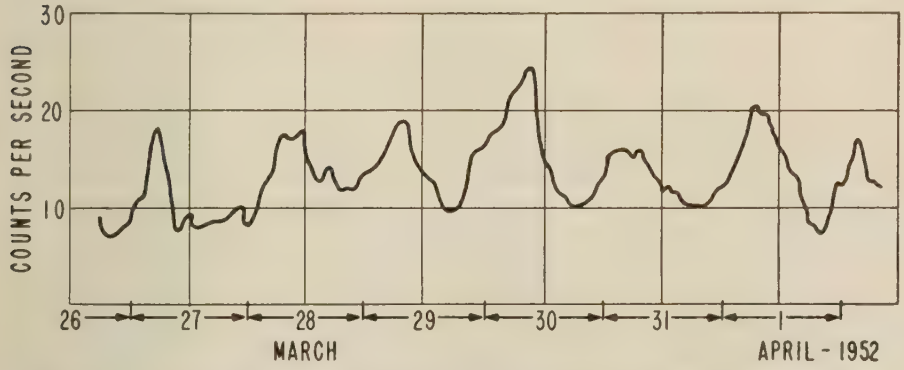

FIG. 1—COUNTING RATE FROM A FILTER WHILE AIR FLOWS THROUGH IT (EXPERIMENT A); FILTER PAPER WAS CHANGED DAILY; COUNTING RATE RETURNED TO NORMAL WITHIN TWO HOURS IN EACH CASE; EXPERIMENT B WAS RUN OVER THE SAME PERIOD

against the 60-cycle supply current. It has been found that after inserting a new filter, usually about two hours are required for the rate meter to reach a stable reading. This equilibrium time is determined mainly by the decay rates of RaB and RaC. In Figure 1, successive day's curves are connected together by neglecting the first two hours of collecting time. In passing, note that a maximum occurs in the morning of each day. This is a real effect, and not, as might be suspected, due to plugging up of the filter paper, since the flow rate remained approximately constant during the collecting time. These fluctuations are related primarily to the stability of the air and correspond to diurnal variations in meteorological parameters.

In order to obtain the long-lived products in a form suitable for quantitative measurement, a chemical separation of the total Pb, Bi, and Po was made from the 1,600 square inches of filter from the large blower.

The samples containing the collected activity were completely dissolved with acid treatment and fusions where necessary, boiled with lead and bismuth carriers to establish exchange, and then the lead and bismuth precipitated as sulfides. The sulfides were dissolved and lead precipitated as lead sulfate, leaving the bismuth in solution. Both elements were purified further and finally converted to lead sulfate and bismuth oxide for counting. Fifty milligram samples were mounted on plastic holders with collodion and counted immediately after drying. The lead was recounted after reaching equilibrium with the RaE (Bi^{210}). Considerable α-activity was obtained from these samples by carrying on tellurium and finally plating chemically onto silver plates to give weightless mounts of polonium (RaF).

III—DATA AND CALCULATIONS

Let $A_n = A_n(t)$ be the number of atoms of substance A_n in a unit volume at time t. Let the radioactive substances A_1, A_2, A_3, $\cdots$ A_n be related by the differential equations

$$\left.\begin{aligned} dA_1 &= [f(t) - (\lambda_1 + \xi)A_1]\,dt \\ dA_n &= [\lambda_{n-1}A_{n-1} - (\lambda_n + \xi)A_n]\,dt \qquad n > 1 \end{aligned}\right\} \quad \ldots\ldots\ldots\ldots (1)$$

That is, a fraction λ_n of each substance A_n is assumed to decay radioactively into A_{n+1} in unit time, and an additional fraction ξ of A_n is assumed to be lost in some non-radioactive fashion in unit time. $f(t)$ is the number of A_1 atoms created in unit time at time t in a unit volume. The solution of these equations is

$$\left.\begin{aligned} A_1(t) &= e^{-(\lambda_1+\xi)t}\int_{-\infty}^{t} f(t)e^{(\lambda_1+\xi)t}\,dt \\ A_n(t) &= e^{-(\lambda_n+\xi)t}\int_{-\infty}^{t} \lambda_{n-1}A_{n-1}(t)e^{(\lambda_n+\xi)t}\,dt \qquad n > 1 \end{aligned}\right\} \quad \ldots\ldots\ldots (2)$$

If the creation rate is constant (and has been constant since $t = -\infty$),

$$f(t)\,dt = K\,dt \ldots\ldots\ldots\ldots\ldots\ldots\ldots\ldots (3)$$

then (2) reduces to the "equilibrium" values

$$A_n(t)_{eo} \equiv a_n = \frac{K}{\lambda_1 + \xi}\left(\frac{\lambda_1}{\lambda_2 + \xi}\frac{\lambda_2}{\lambda_3 + \xi}\cdots\frac{\lambda_{n-1}}{\lambda_n + \xi}\right) \quad \ldots\ldots(4)$$

Parenthetically observe that for $\xi = 0$ (no non-radioactive loss) this reduces to the usual

$$a_n = K/\lambda_n \quad \ldots\ldots(5)$$

and that if we let dA_n^*/dt denote the rate of decay particles (α or β) resulting from the decay of substance A_n, then

$$dA_n^* = +\lambda_n A_n\, dt \quad \ldots\ldots(6)$$

so that (5) leads to

$$dA_n^*/dt = K \qquad n \geq 1 \quad \ldots\ldots(7)$$

That is, in the absence of non-radioactive loss, each substance emits the same number of decay particles per unit time after equilibrium has been reached. This is, of course, expected physically and is well known.

Next, consider the problem defined by requiring

$$f(t)\, dt = \begin{cases} K\, dt & t < 0 \\ 0 & 0 < t \end{cases} \quad \ldots\ldots(8)$$

instead of (3). Physically, this corresponds to removing the constant source of of material A_1 at $t = 0$. Equations (1) and (2) still hold, but for $t > 0$ we find instead of (4)

$$\overline{A}_n(t) = \sum_{k=1} \alpha_{nk} e^{-\lambda_k t} \qquad n \geq 1 \quad \ldots\ldots(9)$$

where

$$\alpha_{nk} = \begin{cases} 0 & n < k \\ a_1 & n = k = 1 \\ a_n - (\alpha_{n1} + \alpha_{n2} + \cdots \alpha_{n\,n-1}) & n = k \neq 1 \\ \lambda_{n-1}\alpha_{n-1\,k}/(\lambda_n - \lambda_{n-1}) & n > k \end{cases}$$

We have written $\overline{A}_n$ instead of A_n to indicate explicitly that we are referring to $f(t)$ with a cut-off at $t = 0$, as given by (8), and not (3).

From this we can compute the number of decay particles per second resulting at any time t from the decay of A_n collected by passing air through a filter paper at the rate of V cc/sec from the time $t = T < 0$ to $t = 0$:

$$\frac{dA_n^*}{V\, dt} = \begin{cases} \sum_{k=1} \beta_{nk}(1 - e^{-\lambda_k(t-T)}) & T < t < 0 \\ \sum_{k=1} \beta_{nk} e^{-\lambda_k t}(1 - e^{+\lambda_k T}) & 0 < t \end{cases} \quad \ldots\ldots(10)$$

where

$$\beta_{nk} = \alpha_{nk} \frac{\lambda_n}{\lambda_k}$$

The β_{nk}'s depend on ξ and the known λ_n and counting rates may be found experimentally. We can, therefore, calculate the loss coefficient from equation (10). To simplify the practical calculations, we replace the scheme

$$\mathrm{Rn} \rightarrow \mathrm{RaA} \underset{\lambda_A}{\rightarrow} \mathrm{RaB} \underset{\lambda_B}{\rightarrow} \mathrm{RaC} \underset{\lambda_C}{\rightarrow} \mathrm{RaD} \underset{\lambda_D}{\rightarrow} \mathrm{RaE} \rightarrow \mathrm{RaF}$$

by

$$A_1 \underset{\lambda_1}{\rightarrow} A_2 \underset{\lambda_2}{\rightarrow} A_3$$

where $A_1 = \mathrm{B} + \mathrm{C}$, $A_2 = \mathrm{D} + \mathrm{E}$; that is, assume that the process is equivalent to material A_1 , being created at a uniform rate, decaying, with decay constant λ_1 , with emission of two β's into A_2 , which in turn decays, with decay constant λ_2 with emission of two β's into A_3 . (This is feasible because the half lives of B and C are comparable with each other, but much smaller than that of D and because the half life of A is much smaller still, and because in the measurement of RaB, C, and E we restrict ourselves experimentally to time intervals long compared to the respective half lives.) Decay constants λ_1 and λ_2 are to be so adjusted that they lead to the correct "half lives" for the "substances" A_1 and A_2 . By this we mean that $ln\ 2/\lambda_1$ has been obtained in such a way that it is the time in which one-half of the total number of betas of the reaction $A_1 \overset{\lambda_1}{\rightarrow} A_2$ (which is one-half of two betas per B atom, or one beta per B atom) is given off.

Now consider two experiments, as follows:

(*A*) We determine the counting rate E_A while the pump is on. E_A is the sum of $\mathrm{d}A_1^*/\mathrm{d}t$ and $\mathrm{d}A_2^*/\mathrm{d}t$. The top line of equation (10) gives

$$E_A/V_A = \gamma_1[\beta_{11}(1 - e^{-\lambda_1\tau})] + \gamma_2[\beta_{21}(1 - e^{-\lambda_1\tau}) + \beta_{22}(1 - e^{-\lambda_2\tau})] \ldots . (11)$$

Here γ_1 and γ_2 are the number of β's in each reaction that are actually observed; they may differ from the expected number 2 on account of internal conversion, β-energies too low for detection, etc. $\tau = t - T$ has been written for the time the pump has been on.

(*B*) After collecting for a time $U = -T \sim 10^6$ seconds, A_2 is separated chemically and the counting rate $E_B = \mathrm{d}A_2^*/\mathrm{d}t$ is observed. (Note that if a few hours are permitted to elapse after shutting off the pump, the resulting counting rate would theoretically be nearly the same if no chemical separation were performed, as $\mathrm{d}A_1^*/\mathrm{d}t$ falls off rapidly. The chemical separation is an experimental convenience only, serving to collect in a small volume the radioactive lead spread out over several large pieces of filter paper.) Using the bottom line of equation (10), we have

$$E_B/V_B = \gamma_2[\beta_{21}e^{-\lambda_1 t}(1 - e^{-\lambda_1 U}) + \beta_{22}e^{-\lambda_2 t}(1 - e^{-\lambda_2 U})] \ldots \ldots . (12)$$

Equations (10), (11), and (12) can be greatly simplified if we note the following orders of magnitude:

$$\lambda_1 \sim 10^{-3}\ \text{sec}^{-1}$$

$$\lambda_2 \sim 10^{-9}\ \text{sec}^{-1}$$

$$\tau \sim 10^{6}\ \text{sec}$$

$$U \sim 10^{6}\ \text{sec}$$

$$t \sim 10^{6}\ \text{sec}$$

These permit the following approximations:

$$\lambda_1 + \lambda_2 \rightarrow \lambda_1$$

$$e^{-\lambda_1 t},\ e^{-\lambda_1 \tau},\ e^{-\lambda_1 U} \rightarrow 0$$

$$e^{-\lambda_2 t} \rightarrow 1 - \lambda_2 t$$

$$e^{-\lambda_2 \tau} \rightarrow 1 - \lambda_1 \tau$$

$$e^{-\lambda_2 U} \rightarrow 1 - \lambda_2 U$$

With these approximations, we obtain

$$\xi = (F\lambda_1 - \lambda_2)/(1 - F)$$

where

$$F = (DU - \tau)\gamma_2\lambda_2/\gamma_1 \qquad (13)$$

and

$$D = E_A V_B / E_B V_A$$

The symbols in the above equation have the following values and dimensions:

$\lambda_1 = 2.8 \times 10^{-4}\ \text{sec}^{-1}$

$\lambda_2 = 1.0 \times 10^{-9}\ \text{sec}^{-1}$

$V_A = 0.475\ \text{ft}^3/\text{sec}$ = small filter flow rate

$V_B \times U = 9.1 \times 10^{6}\ \text{ft}^3$ = total volume of air passed through large filter

$E_A = 119$ disintegrations per sec = small filter average disintegration rate

$E_B = 160$ disintegrations per sec = disintegration rate of RaD separated from large filters

$\gamma_1 = 2.3$ (reference [1], chapter 13)

$\gamma_2 = 1.0$ (reference [1], chapter 13)

$\tau \cong 10^{6}$ sec (negligible)

E_A was obtained from the integrated counting rate and the time of collection after correcting for the count due to thorium B in the air, and for the geometry of the counter tube in the small filter apparatus.

E_B was obtained from the counting rate of the RaE that built up in the Pb fraction separated from the large filter papers. The absolute disintegration rate of the separated sample was obtained by correcting the observed counting rate for geometry, absorption of beta particle in mica window, chemical yield, and sample absorption and back-scattering.

Substituting these values in the expression for ξ, we obtain

$$\xi = 7.6 \times 10^{-7}\ \text{sec}^{-1} \quad \ldots\ldots(14)$$

for Washington, D. C.

The "mean life" of natural radioactivity in the air due to non-radioactive loss is therefore

$$1/\xi = 1.3 \times 10^{6}\ \text{sec} \cong 15\ \text{days}$$

Values for ξ of 1.1×10^{-6} and 4.8×10^{-6} were obtained from similar measurements made in French Morocco and Alaska, respectively.

In attempting to determine the physical nature of the non-radioactive loss, we consider two possibilities. First, the particles may leave the entire volume, as if through a sink, that is, by precipitation sweeping the volume; second, the particles may flow from one volume element to an adjacent one in a continuous way, caused, say, by the electric or gravitational field of the earth. The creation function K must now be taken as a function of the height z. It is proportional to the density of radon at that height. Although this distribution function is not known in general, it seems reasonable to take $K(z) = K_0 e^{-\alpha z}$. The appropriate generalization of equation (1) for equilibrium conditions ($t \to \infty$) gives

$$\left.\begin{aligned} a_1 &= [K_0/(\eta + \alpha v + \lambda_1)]e^{-\alpha z} \\ a_2 &= [K_0/(\eta + \alpha v + \lambda_1)][\lambda_1/(\eta + \alpha v + \lambda_2)]e^{-\alpha z} \end{aligned}\right\} \quad \ldots\ldots(15)$$

η is the fraction of atoms lost per unit time out of a unit volume on account of the sink, and V is the downward velocity of the radioactive particles. Comparing equation (15) with equation (4) shows

$$\xi = \eta + \alpha v \quad \ldots\ldots(16)$$

Ions that are lost on account of being swept out of the air by moisture should be contained in the rain-water. On this assumption, we can show

$$\eta = VN\alpha/\lambda_2 A_2^0$$

where V = average rainfall (per sec) and N = number of disintegrations per sec of RaD contained in one cc of rain-water. Equation (16) thus becomes

$$\xi = \alpha[VN/\lambda_2 A_2^0 + v]$$

The downward velocity v of ions of this size in the electric field of the earth (which is [9] about 1 volt/cm) is known [2, 3] to be $\lesssim 10^{-2}$ cm sec^{-1}; the velocity due to gravity is much smaller [7] and may be neglected. We measured

$N = 8.8 \times 10^{-5}$ disintegrations of RaD per sec per cc of rain (Table 1) and

$V = 3.4 \times 10^{-6}$ cm^3 sec^{-1} cm^{-2}, the average rainfall in Washington, D. C., is known [10].

$\lambda_2 A_2^0 = 7.2 \times 10^{-10}$ disintegrations due to RaD per sec per cm^3 of air was determined from the previously described experiment with the large blower.

We thus find

$$\xi = \alpha\{[39 + 1] \times 10^{-2} \text{ cm sec}^{-1}\}$$

$$\alpha = 1.9 \times 10^{-6} \text{ cm}^{-1}$$

The average number of RaD disintegrations per second per cc of rain measured at a number of widely separated locations is given in Table 1.

TABLE 1

Location	Average ($\times 10^{-5}$)
Washington, D. C. . . .	8.8
Chicago, Ill.	9.2
Panama, C. Z.	1.8
Hawaiian Islands	4.0
Philippine Islands . . .	4.0
Samoan Islands	0.9
Alaska	2.9
Average	4.5×10^{-5}

These figures are averages of several measurements over a period of about a year. It may be noted that the inland stations showed the greatest activity, while the Samoan Islands with their small land mass and remoteness from continental areas gave the least. No particular correlation with season, relative cleanness of the rain-water, character of the rain, or time between rains was noted. In general, the first part of the rain contained the greatest amount of insoluble material and the highest concentration of activity.

It may be of some interest to consider whether in general, on a world-wide scale, rain is the primary agency for the removal of the long-lived radioactivity of the air. Rankama and Sahama [11] give the total rainfall over land as 99×10^3 km^3/year and the total area of the land surface as 149×10^6 km^2. From the above, the average rainfall over land is 67 cm/year, a figure comparable to that for Washington, D. C. If the average world-wide RaD activity in rain-water is taken to be that of Table 1 and $ln\ 2/\alpha = 1$ km, we obtain $\xi = 10^{-6}$ sec^{-1}, in good agreement with the measured value for Washington, D. C.

A word should be said concerning the correction of the observed counting rate for thorium B decay particles. In equation (13), E_A is the counting rate due to the decay of the radium series, but the air also contains thorium B atoms, which decay by beta emission with a half life of 10.6 hours. The data necessary for making this correction may be obtained by passing air through a filter for 24 hours and observing the count rate after air flow is cut off. This is illustrated in Figure 2.

It must be recognized that in the type of experiments reported in this paper, there may be many sources of error. Not the least of these is the lack of sufficient data collected over many years to allow the estimation of satisfactory average

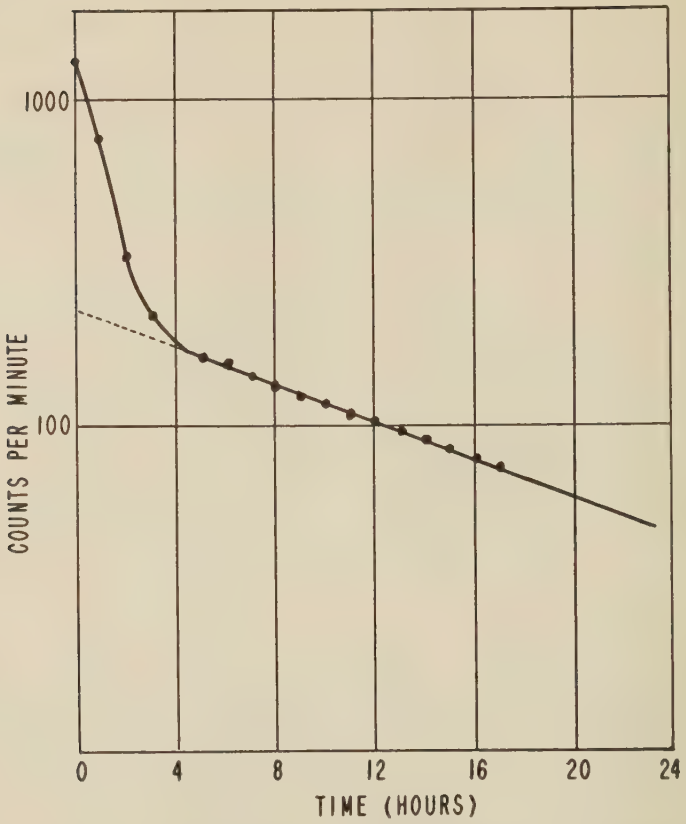

FIG. 2—COUNTING RATES FROM A FILTER PAPER AFTER AIRFLOW HAS BEEN CUT OFF; THE COUNTING RATE IS HIGH INITIALLY DUE TO RaB AND RaC, AND FINALLY DECREASES EXPONENTIALLY WITH THE DECAY CONSTANT OF ThB; THE FRACTION OF ThB MAY BE COMPUTED BY EXTRAPOLATING THE CURVE BACK TO ZERO TIME (DOTTED LINE)

conditions. Although the present work suffers in this respect, the theory and methods are sufficiently reliable that we feel the calculated results should be correct to well within an order of magnitude.

We should like to acknowledge the interest of Drs. H. Friedman and P. King in this work. We are also indebted for helpful discussions to Drs. T. A. Chubb and F. E. Geiger. We are particularly grateful to the Naval personnel who performed measurements for us at all the locations listed in Table 1.

References

[1] E. Rutherford, J. Chadwick, and C. D. Ellis, Radiations from radioactive substances, Cambridge, University Press (1930).
[2] V. F. Hess, Die elektrische Leitfähigkeit der Atmosphäre und ihre Ursachen, Braunschweig, Verlag von Friedr. Vieweg u. Sohn (1926); or English translation by L. W. Codd, London, Constable and Co., Ltd. (1928).
[3] M. H. Wilkening, Rev. Sci. Instr., **23**, 13 (1952).
[4] W. F. G. Swann, Terr. Mag., **9**, 13 (1915).
[5] A. Wigand and F. Wenk, Der Gehalt der Luft an Radium-Emanation, nach Messungen bei Flugzeugaufstiegen, Ann. Physik, **86**, 657 (1928).
[6] J. A. Priebsch, Zur Verteilung radioaktiver Stoffe in der freien Luft, Physik. Zs., **32**, 622 (1931).
[7] S. C. Blacktin, Dust, Cleveland, Sherwood Press, p. 166 (1934).
[8] I. H. Blifford, U.S. Naval Research Laboratory report (to be published).
[9] J. A. Fleming (Editor), Terrestrial magnetism and electricity, New York, Dover Publication, Inc., 2nd ed. (1949).
[10] Local climatological summary for Washington, D.C., U.S. Dept. Comm., Weather Bureau (1951).
[11] K. Rankama and Th. G. Sahama, Geochemistry, Chicago, University of Chicago Press (1950).

ON CURRENT SYSTEMS PROPOSED FOR S_D IN THE THEORY OF MAGNETIC STORMS

By C. B. Kirkpatrick

New South Wales University of Technology, Sydney, Australia

(Received July 1, 1952)

ABSTRACT

A theoretical current system, similar to the models proposed by Birkeland and Alfvén as sources of geomagnetic disturbance, is analysed, and the magnetic field produced by it is compared with the observational data and the fields of other theoretical models. The results indicate that the Birkeland model, which has been rejected by Vestine and Chapman, and Alfvén's model are unsatisfactory as sources of the daily variation (S_D) of geomagnetic disturbance. Some general principles are developed for use in the field analysis of current systems.

1—INTRODUCTION

Birkeland [see 1 of "References" at end of paper] and Chapman [2] have proposed two different systems of electric currents to account for the daily variation (S_D) of magnetic disturbance at high latitudes. The fields due to these two models have been compared with the observational data by Vestine and Chapman [3], who concluded that, whilst the Birkeland model was unsatisfactory, the Chapman model reproduced the average characteristics of the disturbance field with some success. In the idealized form of Birkeland's model, a straight line current, tangential to the earth's field in the auroral zone, represents flow of charged particles of solar origin into the upper atmosphere at auroral levels. This current divides into equal semicircular currents at a constant height (at about colatitude 23°) and recedes into outer space as a similar line current. This model lacks the polar cap current sheet of the Chapman model and consequently fails to produce the observed north-south component of S_D in the polar regions. Vestine and Chapman doubted whether even drastic modification of Birkeland's model could overcome this difficulty.

Alfvén [4, 5], in his theory of magnetic storms and aurorae, has derived a current sheet system which may be regarded as a modification of the Birkeland line system, and claims that measurements by a search coil method on such a model constructed by Malmfors are in fair agreement with the observational data. According to Alfvén's theory, an ionised stream from the sun gives rise to flow of currents and accumulation of charge around a forbidden region in the equatorial plane at a distance of several earth radii; from the boundary of the forbidden region a discharge along the lines of force of the terrestrial field constitutes a *sheet* current, the circuit being completed by an auroral ring line current.

A model similar to that of Alfvén has been selected for mathematical investigation in order to test the possibility of modifying the Birkeland model, and to provide a theoretical check on the experimental results of Alfvén.

In the course of the investigation, some principles of general interest were developed for use in the field analysis of current systems.

2—DESCRIPTION OF THE MODEL

The model investigated in this paper is illustrated in Figure 1, where O is the centre of the earth and ON (N denoting the North Pole) is normal to the paper in the upward sense. The shaded limbs on the outermost circle portray a line current encircling the earth in its equatorial plane at a distance of several earth

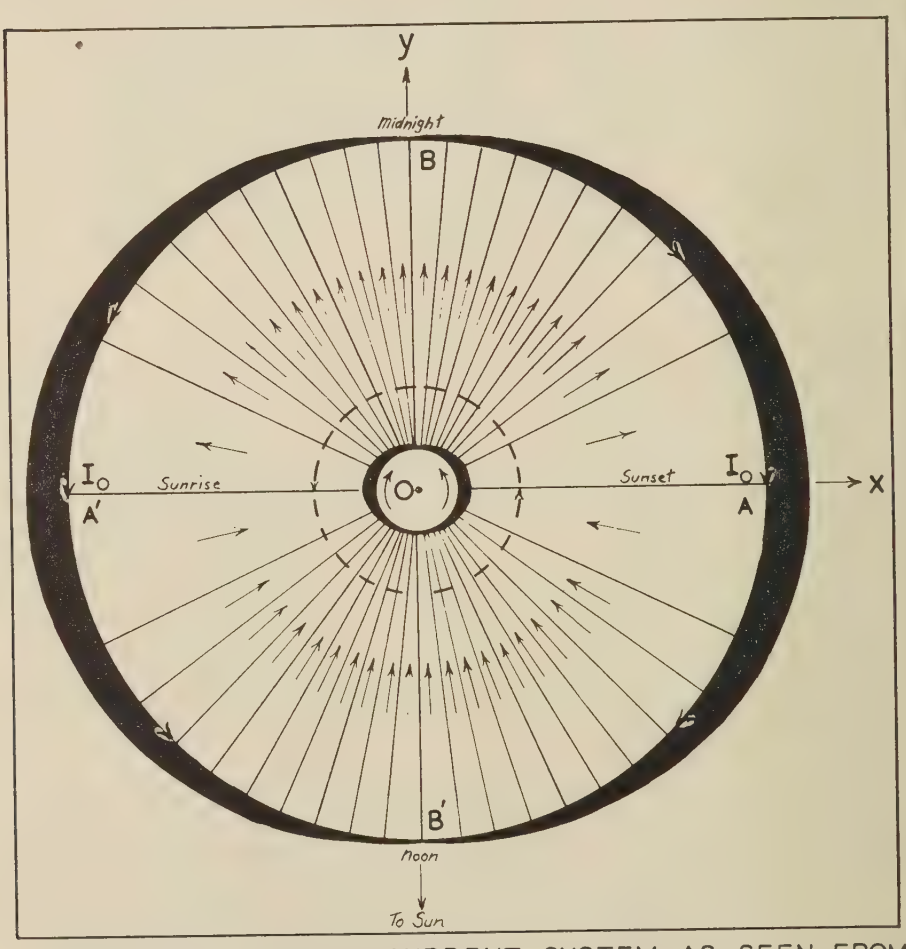

FIG. 1—PLAN VIEW OF CURRENT SYSTEM AS SEEN FROM ABOVE THE EARTH'S NORTH POLE; RADIAL ARROWS INDICATE CURRENTS OF AVERAGE STRENGTH 0.1 I_O

radii. In this equatorial circle, with a radius equal to K, currents of strength I_0 flow across the sunrise and sunset planes towards the sun. These currents decrease sinoidally to zero at the noon half-plane due to leakage along the lines of force of the earth's magnetic field. This leakage constitutes a sheet current which flows into the sunlit half of the auroral circle and produces a circular current which is the same as that in the equatorial circle except that it is of opposite sense. The circuit is completed by flow on the evening side from the auroral circle *via* the lines of force to the equatorial circle. It is probable that a constant current is present in the equatorial ring in addition to the sinoidal current, but it has been omitted from Figure 1, as it would contribute to the D_m-field and not to S_D .

The orientation of the reference axes $Oxyz$ (fixed relative to the sun) and the

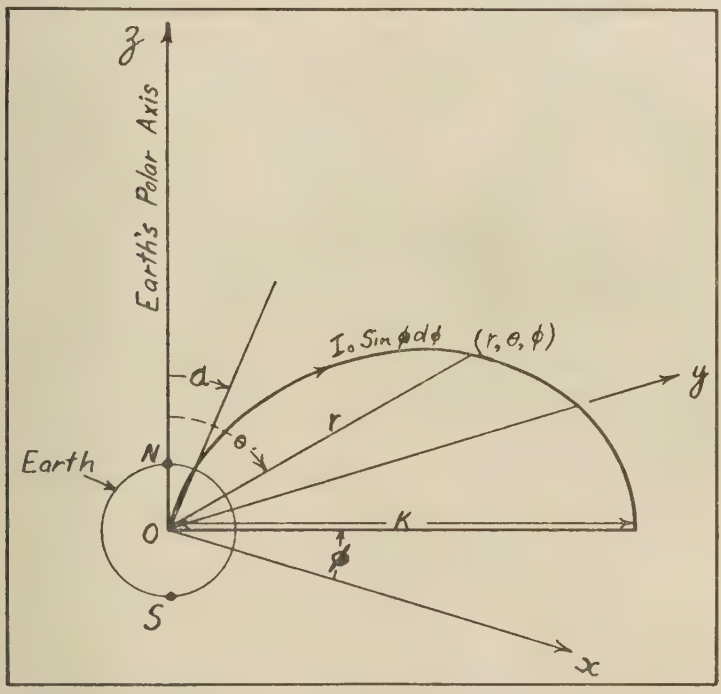

FIG. 2—LINE OF FLOW OF THE SHEET CURRENT

notation for the co-ordinates of a current element are apparent from Figures 1 and 2. The current system is comprised of

(i) A line current of strength $I_0 \cos(\pi + \phi)$ flowing in the equatorial circle of radius K ($\rho = K, z = 0$)

(ii) A sheet current of strength $I_0 \sin\phi$ per radian of ϕ flowing along the lines of force ($r = K \sin^2\theta, \phi = \text{const.}$) from the auroral circle into the equatorial circle

(iii) A line current of strength $I_0 \cos \phi$ flowing in the auroral circle ($\theta = \alpha$, $\rho = K \sin^3 \alpha$).

If the view that an extra-terrestrial current ring exists during magnetic storms is accepted (and there is considerable evidence to support this view), then this model is a plausible one, even if Alfvén's theory of magnetic storms is rejected.

Our model is not complicated by the asymmetrical features of Alfvén's model and is simpler to investigate by mathematical methods.

Prior to the analysis of the model, the magnetic field of a current is discussed along fairly general lines.

3—MAGNETIC FIELD OF A CURRENT SYSTEM

3.1 *General considerations*—In most problems involving complex spatial current systems, it is advantageous where possible to resolve the current system into simpler systems and then to superpose the effects of these simpler systems. Many current systems may be represented by currents flowing along the generators and the orthogonal circles on surfaces of revolution. In general, the currents flowing along these curves may vary from point to point along a given curve, but it is, nevertheless, convenient to regard these curves as lines of flow. Consider a surface of revolution described in cylindrical co-ordinates by the equation $z = z(\rho)$. The generator curves $z = z(\rho)$, $\phi = \text{const.}$, and the circles $\rho = \text{const.}$, $z = \text{const.}$, may be regarded as lines of flow for any system of currents flowing on this surface. The currents flowing in the zone between the circles of radius ρ and $(\rho + d\rho)$ constitute a current element for which it is possible to determine the associated magnetic field by analytical methods. In a magnetic field problem, therefore, considerable numerical work may be avoided by giving consideration to the possibility of determining the magnetic field arising from the currents in a zonal element on a surface of revolution (or in a solid of revolution of infinitesimal cross-section). Formulae are therefore developed here for determination of the magnetic field of a zonal current element. For convenience, the principal symbols used are listed, as follows:

$\mathbf{H}$ = the magnetic force

$\mathbf{J}$ = the current density

$\mathbf{ds} = \mathbf{s}\, ds$ = the vector element of arc on a line of current flow

$\mathbf{s}$ = unit vector in the direction and sense of $\mathbf{ds}$

$J = \mathbf{J} \cdot \mathbf{s}$ = the quantity specifying the magnitude and sense of the current density

(ρ, ϕ, z) = the cylindrical co-ordinates of the current element

(ρ_0, ϕ_0, z_0) = the cylindrical co-ordinates of the field point

R = distance from the current element to the field point

$\mathbf{R}$ = position vector of the current element relative to the field point; namely,

$\mathbf{R} = \mathbf{i}(x - x_0) + \mathbf{j}(y - y_0) + \mathbf{k}(z - z_0)$

(r, θ, ϕ) = spherical co-ordinates of the current element

(r_0, θ_0, ϕ_0) = spherical co-ordinates of the field point

$\psi = \phi - \phi_0$ = the azimuth of the current element relative to the field point

dS = the cross-section of a small tube of flow

$\mathbf{dS} = \mathbf{s}\, dS$; $d\tau$ = $\mathbf{ds} \cdot \mathbf{dS}$, a volume element of a tube of flow.

The magnetic vector potential at the field point (ρ_0 , ϕ_0 , z_0) of the tubular current element $\mathbf{J}\, d\tau$ at (ρ, ϕ, z) is

$$\frac{\mathbf{J}\, d\tau}{R}$$

The curl of the vector potential evaluated at the field point gives the magnetic force $\mathbf{dH}$ arising from $d\tau$, so that at the field point

$$\mathbf{dH} = J\, dS \cdot \frac{\mathbf{R} \times \mathbf{ds}}{R^3} \qquad (1)$$

where $J dS$ is the current flowing across dS in the same sense as $\mathbf{ds}$.

If $\mathbf{p}$, $\mathbf{n}$, $\mathbf{k}$ denote fixed unit vectors in the directions of increasing ρ_0 , ϕ_0 , and z_0 , respectively, the vector product $\mathbf{R} \times \mathbf{ds}$ is the sum of the vector differentials

$$[(z_0 - z)(\mathbf{p} \sin \psi - \mathbf{n} \cos \psi) - \mathbf{k}\rho_0 \sin \psi]\, d\rho,$$

$$[(z_0 - z)(\mathbf{p} \cos \psi + \mathbf{n} \sin \psi) + \mathbf{k}(\rho - \rho_0 \cos \psi)]\rho\, d\psi,$$

$$[\mathbf{p}(\rho \sin \psi) + \mathbf{n}(\rho_0 - \rho \cos \psi)]\, dz \qquad (2)$$

The lines of flow of a sheet current on a surface $z = z(\rho)$ may be represented by the circles $\rho =$ const. and the orthogonal generator curves $\phi =$ const. For each of these families of curves, z and ρ are independent of ϕ. This independence enhances the possibility of analytic integration with regard to ϕ in order to find the magnetic field of the currents in a zonal element.

In cylindrical co-ordinates

$$R^2 = \rho^2 + \rho_0^2 + (z - z_0)^2 - 2\rho\rho_0 \cos \psi, \qquad R > 0 \qquad (3)$$

Let

$$A^2 = \rho^2 + \rho_0^2 + (z - z_0)^2, \qquad A > 0 \qquad (4)$$

$$\xi^{1/2} = \frac{2\rho\rho_0}{A^2} \qquad (5)$$

Then

$$R^2 = A^2(1 - \xi^{1/2} \cos \psi)$$

and, by binomial expansion,

$$R^{-3} = A^{-3} \sum_{n=0}^{\infty} \frac{(2n + 1)!}{4^n (n!)^2} \xi^{n/2} \cos^n \psi \qquad (6)$$

so that we may write

$$R^{-3} = \sum_{n=0}^{\infty} \alpha_n \cos^n \psi \qquad (7)$$

where the coefficients α_n are independent of ϕ (and ψ) if the point (ρ, ϕ, z) lies on the surface of revolution. The current density function J is defined, for a given

current system, in the interval $0 \leq \phi < 2\pi$, and it is, therefore, possible to express J as a Fourier series, or, more conveniently, in the series form

$$J = \sum_{m=0}^{\infty} (a_m + b_m \sin \phi) \cos^m \phi \quad \ldots\ldots\ldots\ldots\ldots\ldots (8)$$

where the coefficients a_m , b_m are functions of ρ and z.

3.2 *Magnetic field of a circular current*—For a circular line of flow described by the equations

$$\rho = \text{const.}, \qquad z = \text{const.}$$

$\mathbf{R} \times \mathbf{ds}$ reduces to the second differential in (2); thus

$$\mathbf{R} \times \mathbf{ds} = [\mathbf{p}(z_0 - z) \cos \psi + \mathbf{n}(z_0 - z) \sin \psi + \mathbf{k}(\rho - \rho_0 \cos \psi)]\rho \, d\psi$$

The cylindrical components of the magnetic field at the point (ρ_0 , ϕ_0 , z_0), produced by a circular line current $I(\phi)$, flowing along the circle (ρ, z), in the sense of increasing ϕ, are therefore given by the equations

$$H_\rho = \rho(z_0 - z) \int_0^{2\pi} R^{-3} I(\phi) \cos \psi \, d\psi \quad \ldots\ldots\ldots\ldots\ldots\ldots (9.1)$$

$$H_\phi = \rho(z_0 - z) \int_0^{2\pi} R^{-3} I(\phi) \sin \psi \, d\psi \quad \ldots\ldots\ldots\ldots\ldots\ldots (9.2)$$

$$H_z = \rho \int_0^{2\pi} R^{-3} I(\phi)(\rho - \rho_0 \cos \psi) \, d\psi \quad \ldots\ldots\ldots\ldots\ldots\ldots (9.3)$$

It should be noted that $I(\phi)$ is substituted for $J \, dS$ in (1). For a continuous distribution of circular currents on the surface of revolution (that is, a sheet current with circular lines of flow), an expression containing $d\rho$ (or dz) replaces $J \, dS$ and the expressions for the field components of this sheet current are double integrals.

3.3 *Magnetic field of a zonal element with lines of flow along the generators of a surface of revolution*—The equations of the lines of flow are

$$z = z(\rho), \qquad \phi = \text{const.}$$

Noting that

$$z \, d\rho - \rho \, dz = r^2 \, d\theta$$

and putting $d\psi = 0$ in (2),

$$\mathbf{R} \times \mathbf{ds} = \mathbf{p}[(z_0 \, d\rho - r^2 \, d\theta) \sin \psi] + \mathbf{n}[\rho_0 \, dz - (z_0 \, d\rho - r^2 \, d\theta) \cos \psi] - \mathbf{k}\rho_0 \, d\rho \sin \psi$$

Let $I(\rho, \phi) \, d\phi$ denote the sheet current flowing between the generators ϕ and $\phi + d\phi$. Then in (1) $J \, dS$ may be replaced by $I(\rho, \phi) \, d\phi$; if a positive current flows in the same sense as $\mathbf{ds}$, $I(\rho, \phi)$ is positive. The equation (1) may now be used to

obtain expressions for the components of the magnetic field produced by the elements of current along the generators in the zone between the circles of radius ρ and $\rho + d\rho$.

The components of the magnetic field at the point (ρ_0 , ϕ_0 , z_0) produced by this zonal element are

$$dH_\rho = (z_0\, d\rho - r^2\, d\theta) \int_0^{2\pi} R^{-3} I(\rho, \phi) \sin \psi\, d\psi \quad \ldots\ldots (10.1)$$

$$dH_\phi = (r^2\, d\theta - z_0\, d\rho) \int_0^{2\pi} R^{-3} I(\rho, \phi) \cos \psi\, d\psi + \rho_0\, dz \int_0^{2\pi} R^{-3} I(\rho, \phi)\, d\phi \quad \ldots (10.2)$$

$$dH_z = -\rho_0\, d\rho \int_0^{2\pi} R^{-3} I(\rho, \phi) \sin \psi\, d\psi \quad \ldots\ldots (10.3)$$

3.4 *Formulae for the integrals*—The integrals appearing in equations (9) and (10) can be investigated with the aid of the expressions in equations (6) and (8), but the present discussion is limited to cases where the azimuthal distribution of current can be expressed in the form

$$I(\phi) = a_0 + b_0 \sin \phi + a_1 \cos \phi \quad \ldots\ldots (11)$$

where the coefficients a_0 , b_0 , a_1 may be functions of ρ.

Substitution of the expressions (6) and (11) in equations (9) and (10) leads to consideration of the integral

$$\int_0^{2\pi} \cos^p \psi \sin^q \psi\, d\psi$$

where p and q are positive integers. This integral vanishes if either p or q is odd, but, if k and l are also positive integers,

$$\int_0^{2\pi} \cos^{2k} \psi \sin^{2l} \psi\, d\psi = 2\pi \frac{(2k)!(2l)!}{4^{k+l}(k!)(l!)(k+l)!}$$

After determination of the integrals in equations (9) and (10), the expressions for the field components contain linear combinations of the infinite series

$$Q(\xi) = \sum_{k=0}^{\infty} u_k \xi^k \quad \ldots\ldots (12)$$

$$T(\xi) = \sum_{k=0}^{\infty} u_k \xi^k/(k+1) \quad \ldots\ldots (13)$$

where u_k is the sequence

$$u_k = \frac{(4k+1)!}{64^k (2k)!(k!)^2}, \qquad k = 0, 1, 2, \cdots \quad \ldots\ldots (14)$$

The formulae for the definite integrals occurring in (9) and (10) when the current distribution is given by (11) are listed below.

$$\int_0^{2\pi} R^{-3}\,d\phi = \frac{2\pi Q}{A^3} \quad (15.1)$$

$$\int_0^{2\pi} R^{-3}\cos\psi\,d\phi = \frac{\pi\rho\rho_0}{A^5}(4Q - T) \quad (15.2)$$

$$\int_0^{2\pi} R^{-3}\sin\psi\,d\phi = 0 \quad (15.3)$$

$$\int_0^{2\pi} R^{-3}\cos\phi\,d\phi = \frac{\pi\rho\rho_0}{A^5}(4Q - T)\cos\phi_0 \quad (15.4)$$

$$\int_0^{2\pi} R^{-3}\sin\phi\,d\phi = \frac{\pi\rho\rho_0}{A^5}(4Q - T)\sin\phi_0 \quad (15.5)$$

$$\int_0^{2\pi} R^{-3}\cos\psi\cos\phi\,d\phi = \frac{\pi}{A^3}(2Q - T)\cos\phi_0 \quad (15.6)$$

$$\int_0^{2\pi} R^{-3}\cos\psi\sin\phi\,d\phi = \frac{\pi}{A^3}(2Q - T)\sin\phi_0 \quad (15.7)$$

$$\int_0^{2\pi} R^{-3}\sin\psi\cos\phi\,d\phi = -\frac{\pi}{A^3}T\sin\phi_0 \quad (15.8)$$

$$\int_0^{2\pi} R^{-3}\sin\psi\sin\phi\,d\phi = \frac{\pi}{A^3}T\cos\phi_0 \quad (15.9)$$

The expressions for the integrals (15.1) to (15.9) have practical significance, because it is possible to evaluate Q and T without excessive labour, even though these series converge very slowly as ξ approaches unity.

This slow convergence is apparent on noting that, for $k > 0$,

$$u_k = \left(1 - \frac{1}{16}\right)\left(1 - \frac{1}{16 \times 4}\right)\cdots\left(1 - \frac{1}{16k^2}\right) \quad (16)$$

Applying Stirling's formula to (14),

$$u_\infty = \underset{k\to\infty}{Lt}\{u_k\} = \frac{2\sqrt{2}}{\pi} = 0.900316$$

Thus

$$0.9 < u_k \leq 1$$

It follows that $Q(\xi)$ approximates to the geometric series and $T(\xi)$ approximates to the series

$$L(\xi) = \sum_{k=0}^{\infty} \xi^k/(k+1) = \frac{1}{\xi}\log\left\{\frac{1}{1-\xi}\right\}$$

Accurate evaluation of $Q(\xi)$ is readily achieved with the aid of curves of the more rapidly convergent series

$$P(\xi) = (1 - \xi)Q(\xi)$$

It may be noted that

$$P(1) = u_\infty$$

so that

$$0.9 < P(\xi) \leq 1$$

Accurate evaluation of $T(\xi)$ is achieved by using the series (13) for small values of ξ (say $\xi < 0.05$), and using a formula such as

$$T(\xi) \simeq L(\xi) - 0.0825\{L(\xi) - 1\} + 0.01\xi + 0.0018\xi^2 - 10^{-3}\xi^4/(1 - \xi)$$

for other values of ξ. This approximate formula is derived from the relation

$$T(\xi) = A_0 L(\xi) + \sum_{k=0}^{\infty} (u_k - A_0)\xi^k/(k + 1)$$

where A_0 is any constant.

It is of interest to record that $P(\xi)$ may be expressed in terms of a complete elliptic integral; in fact,

$$P(\xi) = 4 \cdot E\left(\frac{\pi}{2}, \sqrt{\frac{2\xi^{1/2}}{1 + \xi^{1/2}}}\right)$$

The author is indebted to Mr. J. L. Griffith for establishing this relation.

3.5. *Magnetic field of a constant circular current*—Consider a circular line current of constant strength I flowing in the circle $\rho = \text{const.}$, $z = 0$.

Using the formulae (15), and substituting $I(\phi) = I$ in the equations (9), the cylindrical components of the field at any point on the circle (ρ_0 , z_0) are found to be

$$H_\rho = M \frac{\rho_0 z_0}{A^5}(4Q - T),$$

$$H_\phi = 0,$$

$$H_z = M\left\{\frac{2Q}{A^3} - \frac{\rho_0^2}{A^5}(4Q - T)\right\},$$

where $M = \pi\rho^2 I$ (the moment of the equivalent magnetic shell) and $A^2 = r_0^2 + \rho^2$.

If the current I increases and the radius ρ decreases so that

$$\lim_{\rho \to 0} [\pi\rho^2 I] = M_0$$

the field of a circulatory current at the origin is obtained; namely,

$$H_\rho = \frac{3M_0\rho_0 z_0}{r_0^5}, \qquad H_\phi = 0$$

$$H_z = \frac{M_0(3z_0^2 - r_0^2)}{r_0^5}$$

Clearly this field is identical with that of a magnetic dipole of strength $\mathbf{M} = \mathbf{k}M_0$ located at the origin.

4—ANALYSIS OF THE MODEL

With the aid of the formulae developed in section 3, the magnetic field of the current system described in section 2 can be calculated.

At this stage, some further notation is desirable, mainly because the radius (K) of the equatorial ring current is a convenient unit of length.

4.1 *Subsidiary notation—*

$$\mu = \cos\theta, \qquad \nu = r/K$$

$$a = \rho_0/K \geq 0, \qquad b = z_0/K$$

$$U = A/K > 0$$

$$L^2 = a^2 + b^2 = (r_0/K)^2, \qquad L > 0$$

$$H_0 = \frac{\pi I_0}{K}\left(\frac{\sqrt{\nu}}{U}\right)^3$$

Adopting this notation,

$$z = K\mu\nu$$

and

$$U^2 = \nu^2 + L^2 - 2b\mu\nu$$

Further, if all current elements lie on the surface $\nu = \sin^2\theta$ (as is the case for our model),

$$\rho = K\nu^{3/2}, \qquad \xi = 4a^2(\nu^3/U^4)$$

$$z_0\,\mathrm{d}\rho - r^2\,\mathrm{d}\theta = K^2\sqrt{\nu^3}\left(1 - 3b\,\frac{\mu}{\nu}\right)\mathrm{d}\mu$$

$$\rho\,\mathrm{d}z = -K^2\sqrt{\nu^3}\,(2 - 3\nu)\,\mathrm{d}\mu$$

and

$$\rho_0\,\mathrm{d}\rho = -K^2\sqrt{\nu}\cdot 3a\mu\,\mathrm{d}\mu$$

4.2 *Expressions for the field components*—Formulae for the magnetic field at the field point (a, ϕ_0, b) due to the current systems comprising the model are found with the aid of equations (9) and (10) and the formulae for the integrals. Thus,

for a circular current $I_0 \cos\phi$ flowing in a circle (ρ, z), the cylindrical components of the magnetic field are

$$H_\rho = H_0(b - \mu\nu)(2Q - T)\cos\phi_0$$
$$H_\phi = -H_0(b - \mu\nu)T\sin\phi_0$$
$$H_z = H_0 a\left\{\frac{\nu^3}{U^2}(4Q - T) - (2Q - T)\right\}\cos\phi_0$$

and, for a zonal element of the sheet current of strength $I_0 \sin\phi$ per radian,

$$dH_\rho = H_0\left\{1 - 3b\frac{\mu}{\nu}\right\}T\cos\phi_0\, d\mu$$
$$dH_\phi = -H_0\left\{\left(1 - 3b\frac{\mu}{\nu}\right)(2Q - T) + \frac{a^2}{U^2}(2 - 3\nu)(4Q - T)\right\}\sin\phi_0\, d\mu$$
$$dH_z = 3H_0 a\frac{\mu}{\nu}T\cos\phi_0\, d\mu$$

Writing H, Z, and E for the spherical field components towards the North Pole, the Nadir, and the East, respectively, we have

$$H = (aH_z - bH_\rho)/L$$
$$Z = -(aH_\rho + bH_z)/L$$
$$E = H_\phi$$

For the line current $(I_0 \cos\phi)$ flowing in the auroral circle,

$$H = \frac{H_0}{L}\left\{a^2\frac{\nu^3}{U^2}(4Q - T) - (L^2 - b\mu\nu)(2Q - T)\right\}\cos\phi_0$$
$$Z = \frac{a}{L}H_0\left\{\mu\nu(2Q - T) - b\frac{\nu^3}{U^2}(4Q - T)\right\}\cos\phi_0$$
$$E = H_0(\mu\nu - b)T\sin\phi_0$$

where

$$\mu = \cos\alpha, \qquad \nu = \sin^2\alpha$$

For the sheet current ($I_0 \sin\phi$ per radian) flowing along the lines of force,

$$H = \cos\phi_0\int_{\cos\alpha}^{0} H_0\left(3L\frac{\mu}{\nu} - \frac{b}{L}\right)T\, d\mu$$
$$Z = \cos\phi_0\int_{\cos\alpha}^{0} H_0\left(-\frac{a}{L}\right)T\, d\mu$$
$$E = \sin\phi_0\int_{0}^{\cos\alpha} H_0\left\{\left(1 - 3b\frac{\mu}{\nu}\right)(2Q - T) + a^2\left(\frac{2 - 3\nu}{U^2}\right)(4Q - T)\right\} d\mu$$

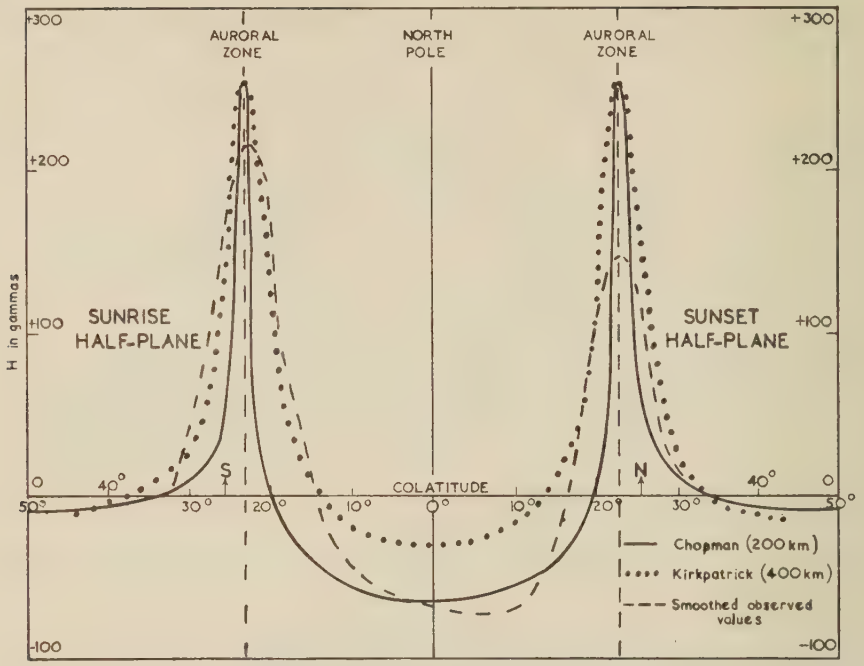

FIG. 3—CURVES SHOWING VARIATION WITH LATITUDE OF THE SOUTH-NORTH COMPONENT OF S_D

Finally, for the equatorial current $I_0 \cos(\pi + \phi)$ flowing in the circle $\rho = K$, $z = 0$,

$$H = H_0\left\{\frac{a^2}{LU^2}(4Q - T) - L(2Q - T)\right\}\cos(\pi + \phi_0)$$

$$Z = H_0 \frac{ab}{LU^2}(4Q - T)\cos\phi_0$$

$$E = -H_0 bT \sin\phi_0$$

where

$$U^2 = 1 + L^2, \qquad \xi = \frac{4a^2}{(1 + L^2)^2}$$

These expressions show that the total field components vary sinoidally with longitude, H and Z vanishing at points in the noon-midnight plane and E at points in the sunrise-sunset plane.

4.3 *The calculated field of the model*—Calculations were performed for the model with the auroral circle (iii) located at a height of 400 km and at colatitude $\alpha = \text{Arcos } (0.92)$; that is, approximately 23°. The earth's radius was taken to be 6,370 km. Adopting these values, $K = 6.91923$ earth radii and $L = 0.144525$ for points on the earth's surface.

For purposes of calculation, I_0 was taken equal to 10^6 amperes; then

$$\frac{\pi I_0}{K} = 7.13 \text{ gammas}$$

The parameter I_0 does not affect the shape of curves of the field and will be adjusted for purposes of comparison.

The value selected for α is the same as that used for the Chapman and Birkeland models and to a large degree α controls the value of K (if $\alpha = 23°$, $K > 6.5$). In Alfvén's model, the auroral current flows in a curve with colatitude (polar distance) between the limits 18° 45′ (at 06^h) and 25° 20′ (at 18^h), and his unit of length, which corresponds to K, is approximately 7.7 earth radii. A difference to be expected between the fields of Alfvén's and similar models is a latitude shift of marked features such as maxima.

The height selected for the auroral current is restricted by the extent of the ionosphere and cannot change the value of K by more than about 10 per cent. However, although it undoubtedly has a marked effect on the magnitude of the field produced at the surface of the earth, the height of the auroral current does not greatly influence the general features of field distribution, and the effects of varying this height can be inferred without difficulty. In the sequel, heights selected for the auroral current are indicated in parentheses, and H, Z, and E refer to the field components of the complete current system.

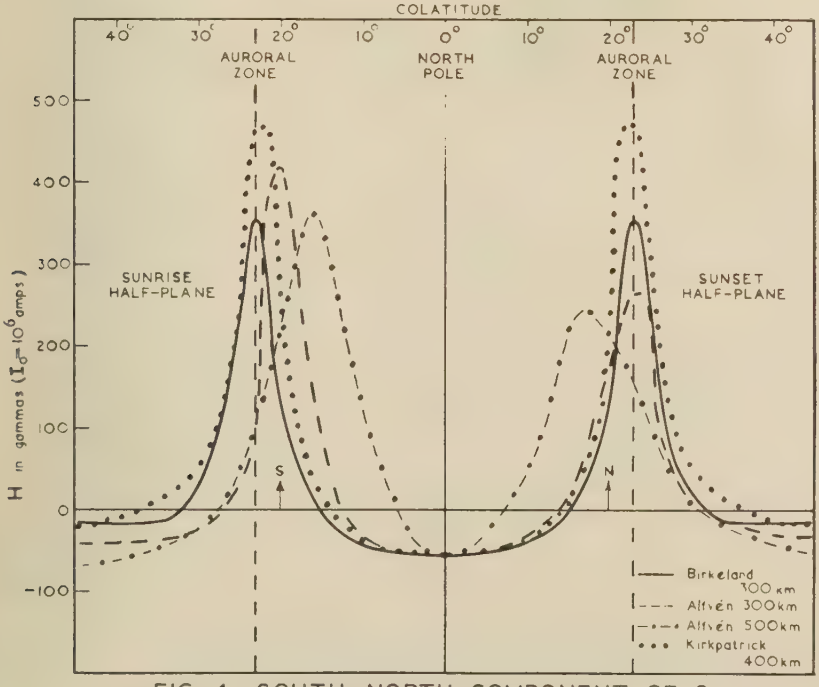

FIG. 4—SOUTH-NORTH COMPONENT OF S_D

5—DISCUSSION OF THE MODELS

In Figure 3, the variation of H with latitude in the sunrise-sunset plane is compared with the corresponding S_D variation for the Chapman model (200 km) and the observational data, the value of I_0 being adjusted so that both models have identical peak values of H at colatitude 23°. Our model fails to simulate the observational H-curve in the polar region if comparable values occur at the auroral peaks of H. This difficulty cannot be overcome by adjusting either the current I_0 or the value of K.

A comparison of our model (400 km) with those of Birkeland (300 km) and Alfvén (300 km, 500 km) is effected in Figures 4, 5, and 6, where the relative values of the parameter I_0 and its counterparts are adjusted so that all three models have the same value of H at the North Pole ($\theta_0 = 0$); for convenience, the absolute value of I_0 is set equal to 10^6 amperes. The left-hand vertical scales indicate the field components of our model in gammas per 10^6 amperes, and the right-hand scale in Figure 6 indicates the observed E-field in gammas.

In all three models, the variation with latitude is very similar. In particular, the ratios of the auroral value to the polar value of H are about 7 ± 2, whereas for the observational curve this ratio is about 2.5 ± 0.5. This discrepancy furnishes a strong objection to these models as possible sources of S_D . Furthermore, for our model, together with those of Birkeland and Alfvén, the relative polar and near-auroral values of E are incompatible with the observational values (see Fig. 6).

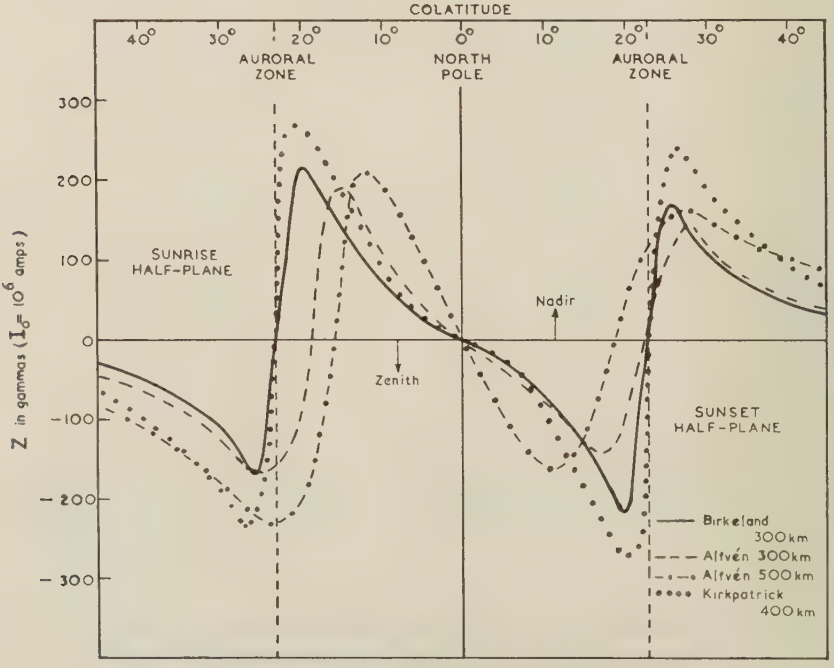

FIG. 5—VERTICAL COMPONENT OF S_D

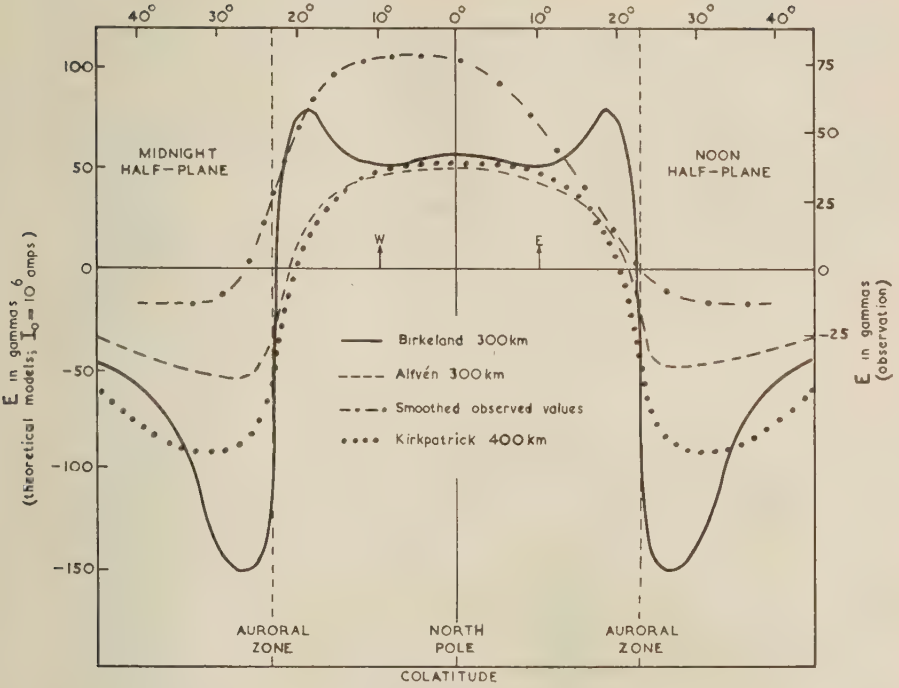

FIG. 6—WEST-EAST COMPONENT OF S_D

The Chapman curve for E is omitted from Figure 6, as it is in close agreement with the observational curve. The curves for Z (Fig. 5) resemble the observational curve and the Z-curve of Chapman's model.

Values of H and Z in accord with observation occur in the auroral zone if I_0 is about 0.4×10^6 amperes, whilst values of H and E accord in the polar region if I_0 is about 1.4×10^6 amperes. Estimates by Vestine and Chapman suggest that the latter value of I_0 should be rejected; then, for our model, the values of H and E are much too small in the polar region. A similar argument holds for the models of Birkeland and Alfvén.

In view of the above remarks, a more detailed examination of the models appears to be futile. Whilst the calculated field of our model supports the experimental measurements of the field of Alfvén's model, the results show that our model and that of Alfvén produce an S_D-field similar to that of the Birkeland model. These theoretical current systems should, therefore, be rejected as possible sources of the diurnal variation (S_D) of magnetic disturbance.

6—ACKNOWLEDGMENTS

The author has pleasure in acknowledging the helpful advice and encouragement of Dr. D. F. Martyn, and the valuable assistance of Miss B. Hardwick and the computing staff of the Radio Research Board, C.S.I.R.O., Australia. Facilities

for the work were made available through the courtesy of the Radio Research Board and the New South Wales University of Technology.

References

[1] Kr. Birkeland, Norwegian aurora polaris expedition, 1902–3, Christiana, **1**, Pt. 1 (1908) and Pt. 2 (1913).
[2] S. Chapman, Proc. R. Soc., A, **115**, 242 (1927).
[3] E. H. Vestine and S. Chapman, Terr. Mag., **43**, 351 (1938).
[4] H. Alfvén, Stockholm, Vet.-Ak. Handl., Pt. 3, **18**, No. 9 (1940).
[5] H. Alfvén, Cosmical electrodynamics, Oxford, Clarendon Press (1950).

GRAVITATION AND GYROMAGNETISM

BY GUSTAVE R. HOLM

4849 West Belden Avenue, Chicago 39, Illinois

(Received July 30, 1952)

ABSTRACT

This article seeks to develop a picture of the physical processes in space which are responsible for the existence of field phenomena, deriving certain relations between these phenomena outside the scope of the usual field theories.

Field phenomena represent processes on such a fine scale that details are, in general, unobservable (except insofar as the quantum aspect is concerned). We can, therefore, only classify and determine net *energy differences*, but this is all that is needed to account for field phenomena at the ordinary scale of magnitude.

I have discussed the derivation and interpretation of the electromagnetic field equations in published articles (American Journal of Physics, **18**, 509, Nov. 1950; also Journal of the Western Society of Engineers, **53**, 87, June 1948). The present article extends the same basic structure to include gravitation, and indicates a simple relationship between gravitation and electromagnetism.

There is considerable evidence of a connection between the rotation of any large mass and an associated magnetic field [see 1 of "References" at end of paper]. To explore the nature of this connection, we will need to go beyond conventional names and classifications of field phenomena and seek a more general approach. We can hardly hope to make progress if we regard gravitation and electromagnetism as mysterious fundamental forces not to be analyzed further. We will here consider the view that all field phenomena are manifestations of a single basic field structure in space. If we assume that field energy like thermal energy shows a trend toward uniformity, symmetry, then the energy of such a basic field structure must form a substantially uniform pattern at all times and places, while observable field phenomena are associated with small modifications of this structure.

We may infer the physical basis of gravitation and electromagnetism from some broad aspects of such a general energy field, without requiring a detailed specification of small-scale structure. We take the basic field pattern to be symmetrical and isotropic, so its energy is equally distributed with respect to three coordinate axes chosen arbitrarily. This energy can be associated with two kinds of motion, linear and rotational, just as energy on the ordinary scale of magnitude. We can thus divide the energy of our basic field structure into a total of six components. Energy differences in the field associated with these components individually give us the six components of the electromagnetic field. Three components

are associated with the energy of linear motion (electric field E), and three with the energy of rotational motion (magnetic field B). These components appear here as individual degrees of freedom.

In the region around an electric charge, the field energy along one line in space is modified with respect to the other five components, to form an electrostatic field. We can interpret an electric charge as a physical entity capable of producing such a modification. Magnetic fields involve differences in rotational energy, and are associated with the motion of electric charges (the curl of a vector potential) or with spin attributes at various orders of magnitude.

There is another way in which energy differences can be brought into our field structure. We can have differences in density of field energy, affecting all six components equally. Even though the density of field energy may vary from place to place, the six components may still maintain a *local* symmetry and equality, so that no electromagnetic effects appear. Such differences in energy density serve to account for gravitation.

In a gravitational field, the six components of field energy form a symmetrical small-scale structure; gravitational flux is equally distributed among the six field components. Electromagnetic effects cut across this small-scale structure, modifying individual components of the field over larger regions. We have here a consistent physical picture of both types of field phenomena in terms of a single basic field structure. The validity of a simple scalar potential in formulating field effects results from the fact that these effects can be added vectorially; such a potential is obviously not descriptive of the physical processes.

Gravitational flux may be defined in a manner quite analogous to electrostatic flux, the force between two masses being simply $\phi_1 \phi_2/r^2$, with ϕ_1 and ϕ_2 expressed in flux units. Here $\phi = g^{\frac{1}{2}}m$, where m is in grams and g is the usual gravitational constant 6.67×10^{-8}.

The gradient of a gravitational field is associated with energy differences uniformly distributed among the six field components. Only if we isolate the component along the line of gradient do we have a structure physically comparable to an electrostatic field. This component produces no electrostatic effect in an actual gravitational field as the local symmetry of the components is maintained. Yet the rotation of such a structure introduces differences in rotational energy, that is, a magnetic field, just as does the rotation of an electrostatic charge about its own axis. The radial component of gravitational flux is here analogous to an electrostatic flux with a magnitude equal to one-sixth of the gravitational flux; each gram mass corresponds to an equivalent negative charge of $g^{\frac{1}{2}}/6 = 4.3 \times 10^{-5}$ esu.

The magnetic field of such "spin" is twice that derived from a moving charge formula. To obtain this result for a uniform rotating sphere, we may picture the internal gradient as rotating with the body, using the expression $\nabla V \times \mathbf{v}/c$ for the local magnetizing field. This expression gives us the field of a moving charge in terms of external "lines of force" moving with the charge; we here apply it to the internal field. Only that portion of the gradient perpendicular to the axis of rotation is effective in producing a magnetic moment about this axis, so for a sphere of radius r, the axial magnetizing field H_z at a distance d from the axis is

$Q\omega d^2/r^3c$, where Q is the total equivalent charge. Making use of the classical "self-demagnetization factor," we set $\mathbf{H} = -(4\pi/3)\mathbf{M}$, where $\mathbf{M}$ is the magnetic moment per unit volume. The total magnetic moment is then $[(2/5)Q\omega r^2]/c$, or $[(1/15)g^{\frac{1}{2}}m\omega r^2]/c$, and the gyromagnetic ratio $\mu/J = Q/mc = g^{\frac{1}{2}}/6c$.

For a non-uniform density, we cannot, of course, set up a single spatial pattern of rotating flux in just this way. More generally, the contribution of an inner denser region can be superimposed on the result for a uniform sphere, so the distribution of magnetization will still correspond to that of angular momentum and the same gyromagnetic ratio will remain valid.

We have thus far taken no account of the quantum aspect of small-scale structure. It is here that we must seek limitations which distinguish gyromagnetism from familiar electromagnetic field laws. The earth's magnetic field appears far too weak to be quantized in terms of Bohr magnetons, but magnetization can appear at the nuclear level in terms of the smaller nuclear units, as a simple alignment of nuclear magnetic moments.

In the rotation of a large body, the change in momentum of each nucleus is governed by the structural forces of matter rather than by the acceleration which the field tends to produce. A continual interplay of energy exists between this mass and the surrounding field, which enables us to by-pass the quantization of the small-scale structure and form a statistically valid formulation in terms of large-scale quantities alone. With linear motion (or with free orbital motion), we cannot go this far.

The earth's gravitational flux is $g^{\frac{1}{2}}m$ or 1.55×10^{24}. Dividing by six gives us an equivalent charge of 2.58×10^{23} esu contributing to the gyromagnetic field. The gyromagnetic moment, $[(2/5)Q\omega r^2]/c$, is 1.02×10^{26} maxwell-centimeters. More simply, the earth's angular momentum of 7.1×10^{40} erg-seconds may be multiplied by $g^{\frac{1}{2}}/6c$ to give the magnetic moment directly.

The observed magnetic field of the earth is some 20 per cent less than the calculated gyromagnetic field. The difference appears reasonable, as we may attribute a demagnetizing effect to induced current in the earth's interior. The shift of the magnetic poles requires a current of about this same magnitude (sin 11°.5). The building up of such current is a long and rather complicated process; once established, it is maintained largely by self-induction, so actual transfer of energy is rather small [2]. Actual paths of current may be irregular, so the representation of the field by a dipole or simple current loop is better suited to the gyromagnetic portion alone.

Values of angular momentum and magnetic field for the sun are much less certain. Some experiments have indicated a general field near 55 gauss [3]. We can expect a smaller induced current component, so the shift of the magnetic axis is less than for the earth. If we take the sun's gyromagnetic field to be about 60 gauss (probably an upper limit), then the corresponding angular momentum is 7×10^{48} erg-seconds. This is 63 per cent of the value based on uniform density, and allows for a fairly high interior density, though not as extreme as some estimates.

It appears likely that at the level of magnetization existing beneath an equatorial belt in the sun, quantum jumps in terms of Bohr magnetons become possible,

introducing a degree of instability. The unstable magnetization manifests itself in the development of intense local fields (sunspots), showing a long period of oscillation and penetrating to the surface at either side of the equatorial belt. The magnetic field here appears as cause rather than effect.

References

[1] P. M. S. Blackett, Nature, **159**, 658 (1947).
[2] H. Lamb, On electrical motions in a spherical conductor, Phil. Trans. R. Soc., A, **174**, 519 (1883).
[3] G. E. Hale, Astroph. J., **38**, 27 (1913); **47**, 206 (1918).

GEOMAGNETIC AND SOLAR DATA

INTERNATIONAL DATA ON MAGNETIC DISTURBANCES, SECOND QUARTER, 1952

Preliminary Report on Sudden Commencements

S.c.'s given by five or more stations are in italics. Times given are mean values, with special weight on data from quick-run records.

Sudden commencements followed by a magnetic storm or a period of storminess (s.s.c.)

1952 April 14d 23h 49m: Am.—18d 11h 04: Ci Ka Tn.—18d 11h 21: SM.—*21d 11h 50:* thirty.—*27d 22h 14*: six.

1952 May 01d 16h 50m: So. –03d 14h 20: SM.—07d 13h 06: Es Wi. –17d 22h 20: Ci.—24d 10h 46: Ka El Ta.—26d 07h 40: SM.—26d 08h 28: Ci.—28d 11h 57: Ka.—29d 18h 50: So.

1952 June 08d 02h 12m: SM.—08d 16h 20: Ci SF.—10d 14h 58: Es Ab.—10d 15h 25: Es.—14d 04h 24: SM.—17d 10h 07: Es.—22d 07h 10: SM.—*25d 10h 49*: seven.—25d 20h 43: To Am.—*29d 19h 32*: twenty-three.

Sudden commencements of polar or pulsational disturbances (p.s.c.)

1952 April *02d 01h 07m*: five.—02d 19h 26: Eb SM.—02d 19h 48: Wn Eb Ci.—02d 22h 46: Ci Tl SF Hr.—03d 11h 23: Ka Am. –03d 19h 27: Tr So.—04d 01h 30: SM Va.—04d 18h 38: Wn Fu Eb Hr.—05d 02h 12: Ci Va.—05d 22h 13: Tr Fu Ci.—06d 00h 15: SM Ci.—*06d 23h 08*: eight.—*09d 17h 16*: five.—09d 21h 27: So Eb SM.—*10d 00h 33:* five.—11d 02h 25: SM Eb Tl Va.—*12d 01h 18:* eight.—12d 20h 27: Tr So.—13d 03h 35: SM Va.—*13d 18h 40:* six.—15d 02h 13: CF Va.—15d 19h 08: CF Fu.—15d 20h 26: So Eb.—16d 02h 16: Fu Tl Va.—17d 02h 39: SM Va.—*18d 18h 43:* five.—18d 21h 03: Tr SM Hr.—19d 22h 05: CF Fu SM Hr.—*20d 21h 30:* five.—23d 02h 08: CF SM Ci Eb.—*24d 16h 25:* nine.—24d 21h 00: Tr So CF Fu.—26d 16h 32: Es Ka.—26d 18h 29: Eb SM.—27d 17h 47: SM Va.—27d 18h 15: Ni Eb Va.—*28d 01h 09:* eight.—29d 17h 17: Tr Eb.—*29d 22h 20:* five.—30d 18h 35: Tr SM.—*30d 21h 04:* six.

1952 May 03d 18h 37m: Ci Tl SF Hr.—03d 21h 36: SM Ci Hr.—*05d 00h 47:* five.—*05d 22h 20:* five.—07d 02h 45: Va El Hr.—07d 06h 35: Eb Am.—07d 08h 52: Ka Am.—07d 21h 58: Es Eb SM.—08d 02h 56: SM Ci Hr.—08d 20h 14: Wn Fu Tl Hr.—*12d 00h 54:* eleven.—12d 19h 59: Wn Fu CF.—*13d 20h 44:* five.—*19d 00h 11:* seven.—19d 04h 00: Es SM Ka.—20d 20h 27: Tr So Wn Fu.—20d 21h 00: So Wn CF.—20d 21h 33: So Wn Eb Hr.—23d 18h 35: So Wn Fu. –24d 23h 44: Wn CF Eb Hr.—*26d 21h 10:* seven.—27d 00h 09: CF Fu.—27d 00h 35: SM Ci Hr.—*28d 19h 25:* fourteen.—29d 19h 15: So Hr.—*31d 20h 22:* six. –31d 20h 40: Le SM Eb.—31d 22h 30: Wn CF Hr.

1952 June *02d 18h 51m:* five.—*02d 19h 40:* five.—*03d 01h 13:* six.—*03d 18h 41:* eight.—03d 22h 56: CF Hr.—03d 23h 53: CF El.—05d 11h 17: To Am. –05d 23h 10: CF Hr.—06d 00h 10: CF SM Hr.—08d 02h 02: Wn Hr.—*08d 02h 32:* five.—*11d 21h 21:* eight.—18d 21h 59: So SM Hr.—19d 19h 16: Tr So Wn.

Geomagnetic planetary three-hour-range indices Kp, preliminary magnetic character-figures, C, and final selected days, April to June, 1952

April 1952

E	1	2	3	4	5	6	7	8	Sum
1	5 −	5o	5 −	5 −	6 −	5o	4o	2 −	35 +
2	6 +	5 +	5 +	7o	4 +	5 +	6 +	6 +	46 +
3	6o	6o	6 +	7 −	5 −	6 +	6 −	6 +	48o
4	5 +	4 +	6 −	5o	5o	4 +	6 +	6 −	42 −
5	5o	4 +	6 −	5o	5o	6 −	5o	6 −	41 +
6	6o	4 +	4 +	6 −	4 −	4o	5 −	6 +	39o
7	5o	4 +	5 +	4 +	4 −	4 −	5 −	4 +	35 +
8	5o	5 −	4 +	4o	4 +	4 −	5 −	4 +	35o
9	5o	4 −	4o	4o	3 +	5 −	4 +	5o	34o
10	7 −	5o	4 +	4o	3o	1 +	3 −	3 −	30 −
11	3o	2 +	3o	3o	3o	2 −	2o	1o	19o
12	4 −	3 −	2 +	2o	1 −	1 −	3 −	2o	17 −
13	4 −	5 +	2o	3o	3 −	2 −	3o	2o	23 +
14	2 −	1 −	2 −	3 +	3 −	4o	2 +	3o	19 +
15	3 +	3o	3 −	4 −	5 −	3 +	3 −	2 −	25o
16	3o	4 +	5 −	3 −	3 +	3 +	3o	3 −	27o
17	3o	5o	4o	3 −	1 +	1o	1 +	1 +	20 −
18	0 +	1o	1 +	2o	3 −	3 +	4o	5o	20 −
19	4o	4 −	3 −	2o	4 +	5 −	5 −	5 −	31 −
20	2 +	3o	2o	2 −	1o	2 −	1o	3o	16 −
21	3 −	3 +	4o	4o	8 +	8o	7o	6 +	44 −
22	5 −	5 +	6 −	5 +	3o	3o	3 −	3 −	32 +
23	4 −	4o	4 −	4o	2o	3 −	3o	2o	25o
24	1 +	1 +	0 +	1o	2 +	4 +	3 −	4 +	18 −
25	2 −	1 +	1 −	4 −	3 +	2 +	1o	2 −	16 −
26	1o	0 +	1o	2 −	2 −	3 −	3 +	2 +	14o
27	2o	1o	1 −	1o	1 +	1o	1o	3 −	11 −
28	4o	5 +	4o	4 +	4 +	4o	4 −	3 +	33o
29	4 +	6 −	6 +	4 +	5 +	7o	7o	7 +	47 +
30	7 −	5 +	5 +	5 +	5 −	5 +	5 +	6 +	44 +
31									

May 1952

1	2	3	4	5	6	7	8	Sum
6 +	5 +	5 +	6 −	5 −	4 +	5 +	6 −	43 −
6 +	6 −	5 −	5o	5o	5 −	5 +	6o	43 −
5 +	5 +	4 +	3 +	4o	4 +	6 +	7o	40o
7 −	5o	4o	4 −	4o	5 −	5o	5 +	38 +
5 +	4o	4o	4o	4 −	3 +	3o	5 −	32o
4 −	4 +	5 +	4 +	3o	4 −	3 −	3 +	30 +
4o	4 +	6 −	6 −	7 −	6o	6o	7o	45 +
6 −	5 −	5 −	4 −	4 −	4 −	3 +	2 +	32 −
2 −	1o	1 −	0o	0 +	0 +	0 +	2o	6 +
3o	2o	1o	2 −	2 +	0 +	1 −	0 +	11 +
0o	1 +	1 +	2o	4 −	4 +	4 −	2o	18 +
4o	3 +	3o	2o	2 −	1 +	3 −	2o	20o
1 +	1 +	1 +	2 +	4 +	2 −	3 +	4 −	19 +
4o	3 +	3 −	1o	1 −	1o	1o	1 −	14 +
1 +	0 +	0 +	1o	2 −	3 −	2 −	1 +	10 +
1o	1 −	1 −	1o	1 −	2 −	0 +	1o	7o
0 +	1o	1o	1 −	1 +	2 −	2 +	3o	11 +
5o	3o	4 +	5o	4o	6o	4o	3o	34 +
4o	6 −	5 −	6 −	3 +	4 −	3o	3 −	33 −
3o	4 −	3 +	3 +	4o	4 −	2o	4 −	27 −
3 −	3 −	3 +	4o	3 +	3 −	2o	2 −	22 +
1o	2 −	1 +	2 −	1 +	1 −	1 −	0 +	9 −
1 −	1 −	1o	2 −	2 +	3 −	3 −	2o	14 −
3 +	2 +	3 −	2 +	3o	3o	2 +	3 +	22 +
5 −	3 +	4o	3o	2 +	3o	1 +	1 −	22 +
0 +	1 −	4 −	6o	4o	5o	5 +	8 −	33 −
8o	6 −	5 −	5 +	4 +	5 +	6 −	5o	44o
5 −	3o	3o	4 +	5 −	6 −	5o	5o	35 +
5 −	5 +	4 +	5 +	4 −	5o	4o	4o	36 +
4o	5 −	4 −	3o	3o	2 +	4 −	3 +	28 −
5 −	5 −	4o	2 +	2 +	2o	3 +	4 +	28 −

June 1952

E	1	2	3	4	5	6	7	8	Sum
1	2o	3 +	3o	3 −	2 −	2o	2 +	2o	19o
2	2o	3 −	2o	1 +	2o	2o	3o	2 −	17 −
3	2 +	3 −	2 −	2 −	2 −	2 −	3o	3o	18 −
4	3o	1 +	1o	2o	1 +	1o	2 −	1 +	13 −
5	2o	3 −	2o	2o	2o	3o	2o	2 −	17 +
6	3 −	1 +	2o	1 +	1o	1 −	1o	1o	11o
7	1 +	1o	1o	2 −	1o	1 −	2o	1 +	10o
8	3o	3 +	3 +	4 +	3 +	4 +	4 +	4 +	30 +
9	3 +	4 +	4 −	3 +	6 −	5o	4 −	4 +	33 +
10	4 −	3o	3 −	3 −	4o	4 −	3 +	4 +	27 +
11	3 +	3o	4o	2 +	3o	4 −	3o	3 +	26 −
12	3o	2 +	3 −	2 −	2o	2o	2 −	2 −	17o
13	0 +	1o	2 +	0 +	1o	1o	2 +	2 +	11 −
14	2 −	3 −	5 −	4o	5 −	4 +	5 +	5o	32 +
15	3 −	4 +	4 −	4o	4o	3 −	3o	3o	27 +
16	3o	5 −	4 +	3 +	4 −	4 +	3o	2 −	28o
17	3 −	3 +	3 +	4 −	3 −	4 −	2 +	2 −	23 +
18	4 +	3 +	2 −	3 −	3o	2o	2o	3 +	22 +
19	2o	1 +	1 +	1 +	3 −	2o	2 −	1 +	14 −
20	2o	1 +	1o	1 +	2 −	1 +	1 +	1 +	11 +
21	1 +	1o	0 +	2 −	2 −	2 −	1 +	1 +	10 +
22	1o	1 +	3 +	3 −	5o	5 −	5 −	4 +	27o
23	4 +	4 −	5 −	5 −	5o	4 −	3 +	4 +	34 −
24	5 +	6 −	4 −	4o	5o	5 −	3 +	4 −	35 +
25	2 −	2 −	2o	3 −	4 −	3 +	4 −	4 +	23o
26	4 +	3o	3o	4o	4 −	4o	2 +	2 −	26o
27	3 −	3 +	3o	2 +	3 −	3 +	3 +	3o	24 −
28	3 −	1o	1 +	3 +	3o	2 −	1o	1o	15o
29	2 −	1 +	2 +	2 −	1 +	1o	4o	6o	19 +
30	5 +	8o	8 −	7o	4 −	2 +	2 −	2 +	38o
31									

Preliminary C, 1952

Apr.	May	June
1.2	1.5	0.5
1.6	1.4	0.4
1.7	1.5	0.6
1.5	1.4	0.4
1.4	1.2	0.6
1.5	1.0	0.2
1.2	1.6	0.1
1.3	1.1	1.2
1.1	0.0	1.2
1.0	0.2	1.0
0.3	0.8	0.8
0.3	0.5	0.4
0.7	0.6	0.3
0.6	0.4	1.3
0 8	0.3	0.9
0.8	0.1	0.9
0.6	0.4	0.8
0.9	1.4	0.8
1.2	1.3	0.3
0.4	0.9	0.1
1.8	0.6	0.2
1.2	0.0	1.1
0.7	0.4	1.3
0.8	0.8	1.2
0.2	0.8	0.9
0.4	1.5	1.0
0.2	1.6	0.8
1.1	1.3	0.4
1.7	1.3	0.9
1 6	1.0	1.7
	1.0	

Final selected days

Apr.	May	June
Five quiet		
12	9	6
20	10	7
25	15	13
26	16	20
27	22	21
Five disturbed		
2	1	9
3	2	14
21	3	23
29	7	24
30	27	30
Ten quiet		
11	9	2
12	10	4
14	12	6
17	13	7
20	14	12
23	15	13
24	16	19
25	17	20
26	22	21
27	23	28

Sudden impulses found in the magnetograms (s.i.)

1952 April 02d 06h 24m: Es Fu Ci.—03d 22h 44: Wn.—05d 10h 32: Es.—05d 17h 07: Fu.—05d 20h 15: Ci.—05d 20h 46: Wn Hr.—06d 19h 21: Fu. -06d 22h 02: Ci.—08d 03h 50: SM.—09d 15h 17: Es.—10d 00h 44: Eb Tl SF.—10d 07h 21: So SM.—13d 23h 15: Ka.—14d 15h 26: Fu.—15d 17h 06: SM.—21d 14h 56: Ab Ci SM Eb.—21d 15h 29: Ab CF Eb.—22d 12h 11: Es.—26d 18h 47: Ci.—28d 06h 31: Hr.—28d 10h 52: To Am.—30d 15h 51: Ci.

1952 May 01d 07h 35m: SM El Ta.—02d 11h 33: Ma Va.—04d 00h 28: Ci.—04d 10h 32: So.—*04d 17h 20:* five. *–08d 12h 36:* fourteen. -13d 20h 16: So.—*17d 23h 59:* nineteen.—18d 14h 34: Es SM.—*18d 15h 19:* eight.—18d 16h 09: Es Ci.—20d 04h 20: So.—24d 11h 47: Hr.—26d 23h 11: CF. –27d 16h 24: Fu.—27d 21h 29: Es.—28d 00h 03: Fu.—29d 04h 51: Eb SF Ka.—29d 15h 03: Fu.—29d 19h 45: Ci.

1952 June 08d 06h 24m: Ta. –08d 19h 47: Ci. -09d 07h 46: Ta.—09d 09h 07: Ta.—09d 14h 07: Do Ci.—11d 20h 24: Eb.—17d 09h 35: So.—17d 16h 09: Wi Ni SM.—18d 11h 48: So.—19d 14h 02: So.—19d 20h 11: Tr.—*22d 07h 36:* five.—*23d 18h 18:* six.—25d 20h 34: Te Ta.—30d 03h 18: Hr.

Preliminary Report on Solar-flare Effects

Effects confirmed by ionospheric or solar observations are in italics.

1952 April 02d 06h 24–31m: Eb (?).—03d 23h 51–24h 11: Te.—05d 10h 26–32: Eb (?).—06d 00h 15–01h 48: Te.—06d 22h 54–23h 55: Te.—08d 00h 37–01h 24: Te.—09d 06h 22–29: Eb (?).—10d 07h 18–24: Eb (?).—10d 10h 04–11: SM.—11d 15h 54–16h 00: Tu. –13d 16h 09–21h 00: Tu.—15d 13h 00: El. –16d 09h 45–53: SM.—20d 15h 39–49: Tu.—22d 12h 10–17: CF Eb.

1952 May 01d 00h 42m–01h 15m: Te.—01d 01h 15–02h 08: Te.—03d 21h 38–22h 45: Ch.—04d 20h 42–21h 05: Ch.—06d 07h 10: El.—07d 21h 03–22h 40: Ch.—12d 20h 00: Do.—16d 15h 33 -18h 00: Tu.—25d 09h 45–55: SM.—25d 15h 11–24h 00: Tu.—28d 15h 08: El.

1952 June 05d 10h 05–12m: SM.—07d 08h 37–44: SM.—09d 21h 32–51: Ch.—17d 13h 15: Hu.—17d 16h 03: Tu Hu.—21d 16h 41–51: SJ.—21d 17h 39–19h 00: Tu.—*22d 20h 40:* Hu.—23d 16h 03–19: Eb (?).—23d 18h 16–26: EB SJ.

Ionospheric or solar disturbances without clear geomagnetic effect

None.

Minor disturbances reported by one station only are listed in the De Bilt quarterly circular, but omitted here.

Committee on Characterization of Magnetic Disturbances

J. Bartels, *Chairman*
University
Göttingen, Germany

J. Veldkamp
Kon. Nederlandsch Meteorologisch Instituut
De Bilt, Holland

PROVISIONAL SUNSPOT-NUMBERS FOR JULY TO SEPTEMBER, 1952

(Dependent on observations at Zurich Observatory and its stations at Locarno and Arosa)

Day	July	Aug.	Sep.
1	59	62	89
2	55	42	75
3	39	35	55
4	31	44	35
5	26	46	32
6	12	43	30
7	13	51	20
8	19	49	7
9	44	57	15
10	52	59	16
11	70	43	7
12	66	54	0
13	72	66	7
14	93	50	0
15	90	44	8
16	85	45	8
17	53	50	11
18	43	43	23
19	23	30	17
20	30	22	20
21	25	28	27
22	9	30	29
23	9	54	42
24	9	69	45
25	17	84	38
26	11	74	38
27	19	90	37
28	23	85	31
29	26	89	28
30	36	83	19
31	60	85	
Means.....	39.3	55.0	27.0
No. days.....	31	31	30

Mean for quarter: 40.6 (92 days)

M. Waldmeier

Swiss Federal Observatory
Zurich, Switzerland

CHELTENHAM THREE-HOUR-RANGE INDICES K FOR JULY TO SEPTEMBER, 1952

[$K9 = 500\gamma$; scale-values of variometers in γ/mm: $D = 5.4$; $H = 2.5$; $Z = 4.1$]

day	July 1952		August 1952		September 1952	
	Values K	Sum	Values K	Sum	Values K	Sum
1	2211 1256	20	3332 2132	19	6555 3445	37
2	3323 2223	20	3332 2232	20	4564 3334	32
3	2222 3333	20	2565 4432	31	4544 2323	27
4	2323 2322	19	3332 2244	23	3333 2232	21
5	3454 4465	35	3333 1334	23	2243 3334	24
6	3463 2232	25	4553 2233	27	4442 1222	21
7	3343 1222	20	4354 2124	25	1541 2355	26
8	1332 3222	18	3333 2223	21	5665 3446	39
9	4345 3333	28	2322 2233	19	5555 3435	35
10	2543 3343	27	4323 3323	23	5463 3223	28
11	3442 2121	19	5223 3234	24	4333 2233	23
12	3333 1223	20	5334 3333	27	4432 3343	26
13	2222 3332	19	2322 2211	15	1212 2223	15
14	3322 2433	22	2221 1132	14	3533 3433	27
15	3434 2223	23	3001 1133	12	2222 2233	18
16	3333 2123	20	3211 0111	10	3312 2223	18
17	1321 2234	18	3344 4353	29	2222 2111	13
18	2311 2222	15	4532 3345	29	2231 0122	13
19	1111 2223	13	4434 2333	26	1011 2222	11
20	3335 4444	30	4533 3333	27	2221 2144	18
21	4654 4444	35	3223 3222	19	5322 1233	21
22	4333 2243	24	1122 1124	14	3332 2112	17
23	3332 2233	21	4321 2222	18	1222 2120	12
24	3212 2233	18	2323 2222	18	2242 2324	21
25	2232 2233	19	0121 2122	11	2111 1235	16
26	4332 2222	20	1211 1223	13	4531 1221	19
27	3001 2224	14	3353 2223	23	2543 3221	22
28	2321 2231	16	2311 1121	12	3344 3344	28
29	0110 1121	7	2222 2344	21	5555 4357	39
30	1111 2122	11	4442 1333	24	7546 2333	33
31	3343 2222	21	2422 3124	20		

Ralph R. Bodle
Observer-in-Charge

Cheltenham Magnetic Observatory
Cheltenham, Maryland, U. S. A.

PRINCIPAL MAGNETIC STORMS

(Advance knowledge of the character of the records at some observatories as regards disturbances)

Observatory (Observer-in-Charge)	Greenwich date	Storm-time		Sudden commencement				C-figure, degree of activity[4]	Maximal activity on K-scale 0 to 9			Ranges		
		GMT of begin.	GMT of ending[1]	Type[2]	Amplitudes[3]				Gr. day	Gr. 3-hr. period	K-index			
					D	H	Z					D	H	Z
(1)	(2)	(3)	(4)	(5)	(6)	(7)	(8)	(9)	(10)	(11)	(12)	(13)	(14)	(15)
	1952	h m	d h		′	γ	γ					′	γ	γ
College (M. L. Cleven)	July 5	04 00	5 21	.....	.....	.....	.....	ms	5	3	7	250	1400	930
	Sep. 1	01 00	3 18	.....	.....	.....	.....	ms	1	3,4	7	220	1520	1360
	Sep. 7	17 00	10 15	.....	.....	.....	.....	s	9	4	8	270	2280	990
	Sep. 27	04 00	30 17	.....	.....	.....	.....	ms	27	3	7	280	2050	1310
									28	4	7			
									29	4,5	7			
									30	4	7			
Sitka (T. L. Skillman)	July 5	03 30	6 13	.....	.....	.....	.....	s	5	3	8	72	725	634
	July 20	10 00	22 12	.....	.....	.....	.....	ms	21	2,5	7	83	866	543
	Aug. 3	03 09	5 13	.....	.....	.....	.....	ms	3	3	7	102	460	556
	Aug. 29	14 05	31 13	.....	.....	.....	.....	ms	30	2	6	34	462	381
	Aug. 31	22 00	3 11	.....	.....	.....	.....	ms	1	4	7	76	761	663
	Sep. 7	04 00	10 15	.....	.....	.....	.....	ms	9	2,3,4	7	106	1290	838
	Sep. 28	04 00	30 14	.....	.....	.....	.....	s	29	4,5	8	185	1800	1167
Witteveen (D. van Sabben)	Mar. 30	10 00	10 12	.....	.....	.....	.....	ms	30	8	7	50	290	185
									31	1	7			
									3	6	7			
	Apr. 21	11 50	23 12	s.c.	−2	+8	−3	ms	21	5,6,7	7	85	320	195
	Apr. 27	22 00	6 18	.....	.....	.....	.....	ms	3	7,8	7	45	295	165
	May 7	03 00	8 24	.....	.....	.....	.....	ms	7	8	7	40	225	135
	May 17	15 00	19 22	.....	.....	.....	.....	ms	18	6	6	25	180	80
	May 26	08 00	31 24	.....	.....	.....	.....	ms	26	8	7	50	295	210
	June 22	12 00	24 24	.....	.....	.....	.....	m	22	5,6	5	25	180	120
									23	5,8	5			
									24	1,2,5	5			
	June 29	19 32	30 24	s.c.	−2	+53	−2	ms	30	2	7	45	420	205
Cheltenham (R. R. Bodle)	July 1	20 32	2 00	s.c.	1	62	12	ms	1	8	6	6	10	230
	July 5	04 ..	6 13	.....	.....	.....	.....	ms	5	7	6	13	152	37
	July 9	02 ..	11 08	.....	.....	.....	.....	m	9	4	5	20	40	25
	July 20	10 ..	22 01	.....	.....	.....	.....	ms	21	2	6	24	58	50
	Aug. 3	04 ..	3 17	.....	.....	.....	.....	ms	3	3	6	26	35	20
	Aug. 6	00 ..	7 15	.....	.....	.....	.....	m	6	3	5	14	28	12
	Aug. 12	00 ..	13 07	.....	.....	.....	.....	m	12	1	5	17	64	34
	Aug. 17	07 ..	21 04	.....	.....	.....	.....	m	17	7	5	6	80	36
	Aug. 31	22 ..	5 09	.....	.....	.....	.....	ms	1	1	6	32	192	40
	Sep. 7	04 ..	10 15	.....	.....	.....	.....	ms	8	2	6	11	56	65
	Sep. 28	18 ..	1 06	.....	.....	.....	.....	ms	30	1	7	40	108	146
Tucson (J.B.Campbell)	July 5	00 ..	7 11	.....	.....	.....	.....	ms	6	3	6	14	218	39
	July 20	07 ..	22 15	.....	.....	.....	.....	ms	21	2	6	17	116	33
	Aug. 17	01 24	19 10	.....	.....	.....	.....	m	17	3,5,7	5	18	135	17
									18	8	5			
	Aug. 31	21 ..	4 15	.....	.....	.....	.....	ms	1	2	6	17	135	14
	Sep. 7	03 ..	10 11	.....	.....	.....	.....	ms	8	3	6	24	132	20
									9	2,4	6			
	Sep. 25	12 ..	1 15	.....	.....	.....	.....	ms	30	1	7	24	167	49
	(*Note:* The last mentioned probably two or more separate storms)													
San Juan (P. G. Ledig)	Sep. 28	15 25	30 12	.....	.....	.....	.....	ms	28	7	6	13	121	28

[1]Approximate time of ending of storm construed as the time of cessation of reasonably marked disturbance movements in the traces; more specifically, when the *K*-index measure diminished to 2 or less for a reasonable period.

[2]s.c. = sudden commencement; s.c.* = small initial impulse followed by main impulse (the amplitude in this case is that of the *main impulse only*, neglecting the initial brief pulse); . . . = gradual commencement.

[3]Signs of amplitudes of *D* and *Z* taken algebraically; *D* reckoned positive if towards the east and *Z* reckoned positive if verically downwards.

[4]Storm described by three degrees of activity: *m* for moderate (when *K*-index as great as 5); *ms* for moderately severe (when K = 6 or 7); *s* for severe (when *K* = 8 or 9).

PRINCIPAL MAGNETIC STORMS—Concluded

Observatory (Observer-in-Charge)	Greenwich date	Storm-time GMT of begin.	Storm-time GMT of ending[1]	Sudden commencement Type[2]	Amplitudes[3] D	H	Z	C-figure, degree of activity[4]	Maximal activity on K-scale 0 to 9 Gr. day	Gr. 3-hr. period	K-index	Ranges D	H	Z
(1)	(2)	(3)	(4)	(5)	(6)	(7)	(8)	(9)	(10)	(11)	(12)	(13)	(14)	(15)
	1952	*h m*	*d h*		′	γ	γ					′	γ	γ
Honolulu	Aug. 17	01 24	19 10	.....	.....	.....	.....	m	18	8	5	14	65	6
(R. F. White)	Sep. 7	07 12	10 13	.....	.....	.....	.....	m	8	3	5	9	101	4
	Sep. 28	15 27	30 15	.....	.....	.....	.....	m	29	4,5	5	7	129	4
Hermanus	July 5	00 ..	6 16	.....	.....	.....	.....	ms	5	7	6	25	104	10
(A. M. van Wijk)	July 20	00 56	23 00	p.s.c.	.....	.....	.....	m	20	4,8	5	21	118	9
									21	2,5,6	5			
	Aug. 17	01 21	19 18	p.s.c.	.....	.....	.....	m	17	4	5	17	128	8
									18	6,8	5			
	Aug. 29	09 ..	30 22	.....	.....	.....	.....	m	30	6	5	17	80	6
	Aug. 31	20 ..	4 02	.....	.....	.....	.....	m	1	1,4,8	5	12	94	6
									2	4,5	5			
	Sep. 5	04 ..	6 12	.....	.....	.....	.....	m	5	6	5	15	125	8
	Sep. 7	17 ..	10 15	.....	.....	.....	.....	m	8	1,7	5	17	72	6
	Sep. 13	20 ..	15 01	.....	.....	.....	.....	m	14	6	5	15	91	7
	Sep. 20	19 ..	21 03	.....	.....	.....	.....	m	21	1	5	10	55	5
	Sep. 24	22 40	25 01	p.s.c.	.....	.....	.....	m	24	8	5	.....	.....	.....
				(*Note:* Large bay.)										
	Sep. 25	15 15	26 14	s.c.?	.....	.....	.....	m	25	8	5	14	69	6
	Sep. 28	15 ..	30 20	.....	.....	.....	.....	ms	29	7,8	6	22	127	14
									30	1	6			
Watheroo	Apr. 2	00 00	6 18	.....	.....	.....	.....	ms	2	4	6	25	153	14
(L. S. Prior, 2nd quarter;									3	4,6	6			
J. E. Webb,									5	3	6			
3rd quarter)	Apr. 21	11 50	22 13	s.c.	+1	+21	?	ms	21	5,6	7	24	229	16
	Apr. 29	03 00	2 18	.....	.....	.....	.....	ms	29	6	6	23	170	19
	May 7	03 00	8 17	.....	.....	.....	.....	ms	7	5	6	21	148	16
	May 17	23 59	18 18	s.c.	−1	−10	−7	m	18	4,6	5	11	98	9
	May 26	08 00	28 04	.....	.....	.....	.....	ms	26	8	6	29	175	16
									27	1	6			
	June 29	19 34	30 16	s.c.	+2	+7	+7	ms	30	2,3,4	6	20	255	16
	Aug. 15	20 04	. . .	s.c.	+1	+10	+5	.....	.....	.....	.....	.....	.....	.....
				(*Note:* No appreciable disturbance followed)										
	Aug. 17	04 58	18 09	.....	.....	.....	.....	m	17	4,6,7	5	16	95	12
Toolangi	July 5	00 25	6 14	.....	.....	.....	.....	ms	5	5	6	28	160	6
(R. E. Ervin)									6	3	6			
	July 9	00 00	11 09	.....	.....	.....	.....	m	9	4	5	17	85	2
									10	4	5			
	July 20	07 00	22 13	.....	.....	.....	.....	ms	21	5	6	20	161	4
	Aug. 17	01 24	19 21	s.c.	....	3	....	ms	17	4	6	30	102	3
	Aug. 31	20 20	3 19	.....	.....	.....	.....	ms	1	4	6	22	176	5
	Sep. 7	17 45	10 15	.....	.....	.....	.....	ms	9	4	6	22	178	5
	Sep. 14	01 05	15 04	.....	.....	.....	.....	m	14	2,6	5	13	102	3
	Sep. 25	17 35	26 15	.....	.....	.....	.....	m	25	8	5	16	143	4
	Sep. 27	01 00	27 18	.....	.....	.....	.....	m	27	3	5	19	105	3
	Sep. 28	02 20	30 20	.....	.....	.....	.....	ms	29	5	6	27	155	5
Amberley	July 5	00 28	6 14	.....	.....	.....	.....	ms	6	3	6	38	102	6
(H. F. Baird)	July 20	00 56	22 12	.....	.....	.....	.....	m	21	3,4,5	5	18	132	5
	July 31	01 30	31 19	.....	.....	.....	.....	m	31	3	5	12	76	2
	Aug. 3	03 17	3 18	s.c.	0	4	−1	ms	3	3	6	20	49	3
	Aug. 17	01 20	19 18	s.c.	1	6	−2	m	17	4	5	22	114	3
	Aug. 30	01 00	30 09	.....	.....	.....	.....	m	30	3	5	14	92	4
	Sep. 1	00 ..	3 12	.....	.....	.....	.....	m	1	3,4	5	21	123	4
									2	3	5			
									3	3	5			
	Sep. 7	18 ..	10 15	.....	.....	.....	.....	m	8	3,4	5	23	147	5
									9	2,3,4	5			
	Sep. 13	22 10	15 05	.....	.....	.....	.....	m	14	2	5	12	75	3
	Sep. 25	18 ..	26 13	.....	.....	.....	.....	m	25	8	5	17	121	4
	Sep. 27	01 14	30 21	.....	.....	.....	.....	ms	27	3	6	20	180	8

ANNOUNCEMENT

Effective January 1, 1953, subscription matters will be handled by the editorial office of the Journal of Geophysical Research, instead of the Johns Hopkins Press, Baltimore, Maryland, as heretofore. Subscriptions and payments should accordingly be sent direct to the Journal of Geophysical Research, 5241 Broad Branch Road, Washington 15, D.C., U.S.A.

NOTES

(25) *Issuance of Bulletin of Information, I.U.G.G.*—The General Secretary of the International Union of Geodesy and Geophysics, Col. George Laclavère (30 Avenue Rapp, Paris, 7°, France), has announced the issuance of the initial number of the I.U.G.G. News Letter. It contains the resolutions adopted by the Union, as well as those adopted by the Associations, at the last General Assembly of the Union. It contains also various information of general interest to geophysicists. This publication, which is in the course of being distributed, will be sent at no cost to geophysicists, geodesists, and institutions all over the world. It is expected that the News Letter will be issued four times a year.

(26) *New officers of the International Council of Scientific Unions*—The following new officers of the I.C.S.U. were elected at the General Assembly of October 1–3, 1952, at Amsterdam: *President*, Prof. Bertil Lindblad (Stockholm); *Vice-Presidents*, Prof. H. Solberg (Oslo) and Col. E. Herbays (Brussels); *General Secretary*, Prof. A. V. Hill, Foreign Secretary of the Royal Society (London); *Treasurer*, Dr. W. A. Noyes, Jr., Chairman of Division of Chemistry and Chemical Technology of the National Research Council (Washington); *Members*, Prof. J. Pérès (Paris), Prof. H. Kamayama, Tôhoku University (Japan), and Prof. A. von Muralt, past President (Berne).

(27) *Release of two aeromagnetic maps of southwestern Washington*—Two preliminary total-intensity aeromagnetic maps of part of Grays Harbor, Pacific, Thurston, and Lewis counties, State of Washington, have been released in open file and may be examined at various offices of the United States Geological Survey. The southwestern part of Washington has long been regarded as a potential petroleum province of the United States, but the few wells drilled so far have not yet yielded oil in commercial quantities. It is expected that these maps, covering 1,300 square miles, will be of material benefit in future exploration for oil and gas, because an unusually good correlation appears to exist between the the magnetic contour maps and geologic structural features, such as folds and faults. These may form traps in which oil and gas have accumulated.

(28) *Meeting of Society of Exploration Geophysicists in Toronto, Canada*—Mining exploration was the subject of a two-day conference of the Society in Toronto, Canada, on October 27 and 28, 1952. Some 18 papers were presented by exploration scientists from many sections of the United States and Canada. A featured paper on exploration for natural gas in Ontario was "A gravity case history: Dawn No. 156, Ontario" by Richard A. Pohly, manager of the gravity division of Seismograph Service Corporation, Tulsa, Oklahoma. He described an Ontario gas pool found by drilling on a "gravity maximum," which now supplies

natural gas for the people of Chatham, Ontario, and surrounding towns at the rate of 6-1/2 million cubic feet per day. It is estimated that the pool from which the well is producing contains 13-1/2 billion cubic feet of gas, and is located on one of five Niagaran reefs which have been discovered through gravitational exploration methods in the southwest peninsula of Ontario, about 50 miles northeast of Detroit, Michigan, and 150 miles west of Toronto, Canada.

(29) *Department of Meteorology and Oceanography, New York University*—The Department of Meteorology of New York University's College of Engineering has been redesignated the Department of Meteorology and Oceanography. Formal curricula leading to the master's and doctor's degrees became effective at the opening of the academic year this past September. In announcing the new program, Dr. Thorndike Saville, dean of the College, pointed out that New York University is the first American university officially to combine meteorology and oceanography. "The arrangement is unusual but logical," he explained. "The atmosphere is greatly influenced by the properties of the ocean, while the ocean is affected by the properties of the atmosphere. Moreover, research methods in meteorology and oceanography are similar, since both disciplines deal with media which are fluids, subject to the same physical laws." The curricula will stress physical oceanography and the relationships between oceanography and meteorology.

(30) *Magnetic observations, islands of the Pacific*—Hamilton F. Baird, of the Magnetic Survey, New Zealand, reported that the publication "Resurvey of New Zealand 1945.5" will soon be distributed from Wellington. Arrangements have been made for a Pacific flight which promises to yield secular-variation stations, and if possible reoccupations, at Norfolk Island, Fiji, Samoa, Aitutaki, Rarotonga, and Bora Bora airfields. At Fiji, a new station was established at Nadi airfield, and an approximate reoccupation carried out at Lauthala Bay. The Civil Aviation Branch expects to make radio calibration flights to these islands perhaps twice yearly, and thus the stations may become international repeat stations with magnetic observations at intervals of two years. Tentative inquiries have been made as to the possibility of observations at Nauru and Ocean Islands in mid-1953. Later it is hoped to reach further islands, even to Pitcairn.

(31) *Geomagnetic activities of the United States Coast and Geodetic Survey*—Mr. Leonard R. Southwick and Mr. Clyde J. Beers completed observations at magnetic repeat stations in the western and east-central United States, respectively.

Mr. Richard G. Green completed observations at magnetic repeat stations in the southeastern States in August 1952, and is now making similar observations in the northeastern States.

"Magnetic Observatory Manual," by H. E. McComb, Special Publication No. 283 of the United States Coast and Geodetic Survey, is in the hands of the printer and is expected to be published early in the year 1953. It will be sold by the Superintendent of Documents, Government Printing Office, Washington 25, D. C.

(32) *A new series of books, "Advances in Geophysics"*—The Academic Press, Inc., New York, N.Y., plans to publish from time to time a series of books designed to serve geophysicists and meteorologists who desire to keep abreast of research results in hydrology, seismology, volcanology, and tectonophysics. Volume 1, now

available, was edited by H. E. Landsberg, of the Geophysics Research Directorate, Air Force Cambridge Research Center, Cambridge, Massachusetts. It consists of monographic treatises by outstanding investigators. A special feature of the first volume is the evaluation of geophysical data. Recent progress in some of the most active fields is reviewed and the way is pointed to new phases which need to be investigated. Volume 1, containing 362 pages, costs about $8.50.

(33) *Corrigenda*—The following corrigenda are noted in the September 1952 number of the JOURNAL: On page 426, Lewis D. Kaplan's "Letter to Editor," in fourth line of second paragraph, following the phrase "These values were determined," should be inserted the words "from Elterman's data"; in seventh line of the same paragraph the phrase "August sounding" should be replaced by "November sounding" while in the tenth line "November sounding" should read "August sounding."

(34) *Personalia*—Prof. Dr. *Julius Bartels*, of the Geophysikalisches Institut der Universität, Göttingen, Germany, visited the Dominion Observatory, Ottawa, Canada, from August 5 to the middle of October 1952, on the invitation of Dr. C. S. Beals, Dominion Astronomer.

Mr. *J. H. Nelson* has been appointed to succeed the late Mr. H. E. McComb as Chief of the Geomagnetism Branch, Division of Geophysics, of the United States Coast and Geodetic Survey. Mr. Nelson has been with the Coast Survey since 1936. He was reassigned to the Washington office in 1951, after ten years of duty at the magnetic observatories at Tucson and Sitka.

The United States was represented at the sixth general assembly of the International Council of Scientific Unions (I.C.S.U.), held at Amsterdam, Netherlands, October 1–3, 1952, by the following delegation: Dr. W. Albert Noyes (Chairman), Dr. Wallace W. Atwood, Jr., Lloyd V. Berkner, Dr. Dirk Brouwer, Dr. Walter H. Bucher, Donald B. Eddy, Dr. James Wallace Joyce, and Dr. C. Eugene Sunderlin. As a result of these meetings, some action is expected to be taken soon by the special committee appointed by the Council towards the organization of the third International Polar Year, or the Geophysical Year, as it is generally called.

Prof. *V. Laursen*, Secretary of the Association of Terrestrial Magnetism and Electricity, International Union of Geodesy and Geophysics, has returned from an inspection trip to the Thule Magnetic Observatory, where artificial disturbances, which could not be foreseen when the observatory was set up in 1946, have now made it necessary to move the installations to a new site.

HAROLD EDGAR McCOMB, 1886-1952

Our readers who have been acquainted personally or through his scientific activities with H. E. McComb of the United States Coast and Geodetic Survey will be sorry to learn of his death on October 11, 1952, the result of a brain tumor. His illness had a sudden onset in late August, just a week before he was to retire from active duty after a long and fruitful career.

Harold Edgar McComb was born at Wilsonville, Nebraska, on November 25, 1886, the son of James Patterson and Lola (Bradbury) McComb. He attended public schools there, and subsequently the University of Nebraska, where he specialized in geology, chemistry, and physics, receiving the B. Sc. degree in 1907 and the M. A. in 1909. He was appointed magnetic observer in the U.S. Coast and Geodetic Survey in June 1909 and in this capacity traveled throughout the United States during many seasons of the field work that was then under way pursuant to the general magnetic survey of the country. In 1918 he entered the military service, where his training was put to good use in the inspection of navigating equipment. Soon after the close of World War I, upon his return to duty at the Coast and Geodetic Survey, he was placed in charge of the magnetic observatory at Honolulu, Territory of Hawaii, remaining there throughout most of the ensuing nine years. One of his accomplishments was a magnetic survey of the Island of Oahu. Returning to Washington in 1927, he was entrusted with instrumental studies and developments in geomagnetism and seismology, and was designated as Chief of the newly formed Section of Observatories and Equipment. His important contributions to these fields are well known to many of our readers. He conducted exhaustive studies, some of them in a seismological laboratory which he set up in the basement of his home. He pushed the quality of magnetic observatory and field operations to new heights, through his meticulous attention to side effects too often neglected. Meanwhile, his administrative responsibilities repeatedly broadened, until in 1948 he became Chief of the Geomagnetism Branch. His final important work was the completion of his "Magnetic Observatory Manual," which had been in preparation for some time and is now in the course of publication.

Mr. McComb had a wholesome range of interests, both scientific and otherwise. He had served, for example, as Chairman of the Eastern Section, Seismological Society of America; as President of the Section of Seismology of the American Geophysical Union; as President of the Philosophical Society of Washington; as Vice-President of the Washington Academy of Sciences; as deputy member on a panel of the Research and Development Board; as Chairman of the Committee on Observational Technique, International Association of Terrestrial Magnetism and Electricity; and as District Commissioner of the National Capital Area Council, Boy Scouts of America. His outstanding services were recognized in 1950 by bestowal of the Exceptional Service Award of the U.S. Department of Commerce, and in 1947 he received the Silver Beaver Award of the Boy Scouts of America. He became highly proficient in legerdemain, and was active in the American Society of Magicians.

Mr. McComb never did anything by halves. Each activity that engaged his

attention profited by his whole-hearted participation,* and each study was pursued relentlessly to a conclusion. His many friends mourn the loss of a stalwart and true companion, and the example of his unfailing good humor and selfless devotion to the common weal must long serve as a guide to all who were privileged to have contact with some phase of his career.

Mr. McComb was married in 1924 to Lucille M. Wight, who, together with their two sons and Mr. McComb's aged mother, survives him. He was buried in Arlington National Cemetery.

Published writings of H. E. McComb

[1] Dispersion of electric double refraction and ordinary dispersion in liquids, Phys. Rev., **29**, 525-540 (1909). [Researches and thesis submitted for degree of Master of Arts at the University of Nebraska.]

[2] Laboratory manual in mechanics and heat, University of Nebraska (1912).

[3] Electric double refraction in liquids, Phys. Rev., Ser. 2, **6**, 180-183 (1915).

[4] An investigation of the Milne-Shaw seismograph, Bull. Seis. Soc. Amer., **12**, 220-226 (1922).

[5] The sensitivity of magnetic variometers, Terr. Mag., **33**, 65-78 (1928).

[6] A new method of marking time on magnetograms, Terr. Mag., **33**, 159-161 (1928).

[7] Comment on "Note on a vertical-intensity variometer," Terr. Mag., **33**, 166 (1928).

[8] Distribution-coefficients for vertical-intensity magnetic variometers, Terr. Mag., **34**, 59-61 (1929).

[9] The magneto-chronograph and its application to magnetic measurements (with C. Huff), Terr. Mag., **34**, 123-141 (1929); also abstract of same, **34**, 54 (1929).

[10] Induction-coefficients for magnetometer-magnets, Terr. Mag., **34**, 241-247 (1929).

[11] Scale-values of magnetic variometers, Terr. Mag., **34**, 260-261 (1929). [Letter to Editor.]

[12] Some recent instrumental investigations in terrestrial magnetism and seismology, J. Wash. Acad. Sci., **20**, 149-150 (1930).

[13] Temperature-compensation and adjustment of magnetic variometers (with A. K. Ludy), Terr. Mag., **35**, 29-34 (1930).

[14] A tilt-compensation seismometer, Trans. Amer. Geophys. Union, **11**, 159-161 (1930).

[15] List of seismological stations of the world, 2nd ed. (with Clarence J. West), Bull. Nat. Res. Council, No. 82, 119 pp. (1931).

[16] A tilt-compensation seismometer, Bull. Seis. Soc. Amer., **21**, 25-27 (1931).

[17] Progress-reports on development of instruments (with F. Wenner), Trans. Amer. Geophys. Union, **12**, 71-72 (1931).

[18] Progress-report on development of seismological instruments, Trans. Amer. Geophys. Union, **12**, 74-75 (1931).

[19] Testing of photographic recorders, Bull. Seis. Soc. Amer., **22**, 56-59 (1932).

[20] Improvements in magnetic instruments and methods adopted by the Coast and Geodetic Survey, Terr. Mag. **37**, 321-328 (1932).

[21] Strong-motion seismograph equipment and installations, Trans. Amer. Geophys. Union, **14**, 268-272 (1933).

[22] Analysis of rates of rotation of recording drums (with A. Blake), Trans. Amer. Geophys. Union, **14**, 324-329 (1933).

[23] A tilt-compensation seismometer, Proc. Fifth Pacific Sci. Cong., **3**, 2489-2494 (1934).

[24] Report of the Section of Seismology of the American Geophysical Union to the Association of Seismology of the International Union of Geodesy and Geophysics, 1933, Internat. Assoc. Seis., Travaux Scientifiques, No. 10, 54-76 (1935).

[25] Selection, installation, and operation of seismographs, U. S. Coast Geod. Surv., Spec. Pub. No. 206, 43 pp. (1936).

*As an interesting example, his collaboration on a study of the light of the night sky might be cited; see Lord Rayleigh, Proc. R. Soc., **119**, 11-33 (1928).

[26] Improved instruments and methods for magnetic measurements, Trans. Amer. Geophys. Union, **17**, 170-172 (1936).
[27] Shaking-table investigations of teleseismic seismometers (with F. Wenner), Bull. Seis. Soc. Amer., **26**, 291-316 (1936).
[28] The Galitzin seismometer: discrepancies between the Galitzin theory and the performance of a Wilip-Galitzin seismometer (with F. Wenner), Bull. Seis. Soc. Amer., **26**, 317-322 (1936).
[29] Strong-motion program and tiltmeters (with N. H. Heck and F. P. Ulrich), *in* Earthquake investigations in California, U. S. Coast Geod. Surv. Spec. Pub. No. 201, 4-30 (1936).
[30] Preliminary report on a photoelectric pendulum control for recorder clocks (with A. C. Ruge), Bull. Seis. Soc. Amer., **27**, 331-335 (1937).
[31] Tests of earthquake accelerometers on a shaking table (with A. C. Ruge), Bull. Seis. Soc. Amer., **27**, 325-329 (1937).
[32] Recherches a la Plate-forme d'essai sur les séismomètres téléséismiques (with F. Wenner), Internat. Assoc. Seis., Travaux Scientifiques, No. 15, 165-199 (1937).
[33] Le séismomètre Galitzine; sur les divergences entra la theorie de Galitzine et les résultats expérimentaux d'un séismomètre Wilip-Galitzine (with F. Wenner), Internat. Assoc. Seis., Travaux Scientifiques, No. 15, 200-207 (1937).
[34] Magnetic instruments (with H. F. Johnston and J. A. Fleming), *in* Terrestrial Magnetism and Electricity, New York, McGraw-Hill Book Co., Inc., 59-109 (1939); New York, Dover Publications, 2nd ed. (1949).
[35] The application of new instruments to magnetic field work (with J. W. Joyce), Trans. Amer. Geophys. Union, **20**, 364-366 (1939).
[36] Improvements in methods of field observations in the United States of America (with J. W. Joyce), Internat. Assoc. Terr. Mag. Electr., Bull. 11, 393-404 (1940).
[37] Improvements in technique at magnetic observatories in the United States of America (with J. W. Joyce), Internat. Assoc. Terr. Mag. Electr. Bull. 11, 404-413 (1940).
[38] Directions for operating a magnetic observatory in the Antarctic (with George Hartnell), 28 pp. (processed, 1939).
[39] New instruments and equipment at cooperative seismograph stations of the United States Coast and Geodetic Survey (with J. H. Nelson), Bull. Seis. Soc. Amer., **29**, 549-557 (1939).
[40] A dynamic tester for galvanometric seismographs (with J. H. Nelson), Trans. Amer. Geophys. Union, **21**, 236-237 (1940). [Abstract only.]
[41] Report of the Special Committee on Time Signal Service, Trans. Amer. Geophys. Union, **21**, 723 (1940); also **22**, 562 (1941), **23**, 724 (1942), **24**, 310 (1943), and **25**, 370 (1944).
[42] Geomagnetic observatories and instruments, Proc. Amer. Phil. Soc., **84**, 239-255 (1941).
[43] Comparison of P-phases as registered by high and low magnification seismographs, Trans. Amer. Geophys. Union, **22**, 374 (1941). [Abstract only.]
[44] Geophysical measurements in the laboratory and in the field, J. Wash. Acad. Sci., **32**, 65-79 (1942). [Address as retiring president of the Philosophical Society of Washington; portrait.]
[45] The determination of true ground motion from seismograph records (with F. Neumann and A. C. Ruge), Bull. Seis. Soc. Amer., **33**, 1-63 (1943); reprinted by U. S. Coast and Geodetic Survey as their Spec. Pub. 250 (1949).
[46] A general-purpose vibration-meter (with F. Neumann), Trans. Amer. Geophys. Union, **25**, 313-315 (1944).
[47] The seismological installation at the South Dakota State School of Mines and Technology, Rapid City, South Dakota (with R. E. Gebhardt and David Wark), Trans. Amer. Geophys. Union, **25**, 309-313 (1944).
[48] A two-component shock recorder, Trans. Amer. Geophys. Union, **29**, 461-463 (1948).
[49] Report of Committee on Observational Technique, Internat. Assoc. Terr. Mag. Electr., Bull. 13, 336-338 (1950).
[50] Report of Committee on Observational Technique, Internat. Assoc. Terr. Magn. Electr., Transactions of the Brussels meeting, 1951 (in press).
[51] Application of alignment charts to the design of magnetic variometer suspension systems, Internat. Assoc. Terr. Mag. Electr., Transactions of the Brussels meeting, 1951 (in press).
[52] Magnetic Observatory Manual, U. S. Coast Geod. Surv., Spec. Pub. No. 283 (in press).

LIST OF RECENT PUBLICATIONS

By W. E. Scott

Department of Terrestrial Magnetism,
Carnegie Institution of Washington,
Washington 15, D. C.

(Received September 24, 1952)

A—*Terrestrial Magnetism*

Bartels, J., and J. Veldkamp. International data on magnetic disturbances, first quarter, 1952. J. Geophys. Res., **57**, No. 3, 416-418 (1952).

Beagley, J. W. Geomagnetic sudden commencement analysis—Amberley. N. Z. J. Sci. Tech., B, **33**, No. 6, 460-470 (1952).

Chapman, S. The calculation of the probable error of determinations of lunar daily harmonic component variations in geophysical data: A correction. Aust. J. Sci. Res., A, **5**, No. 1, 218-222 (1952).

Coimbra. Observacões meteorológicas, magnéticas e sismológicas feitas no Instituto Geofisico (Observatório Meteorológico, Magnético e Sismológico). 2ª Partie—Magnetismo terrestre. Vol. LXXXI, contendo os valores das componentes do campo magnético de 1942 a 1951. Coimbra, Tip. da Atlântida, 16 pp. (1952).

Comité National Français de Géodésie et Géophysique. Comité National Français. Année, 1950. Comptes rendus publiés par le Secrétaire Général du Comité Français, P. Tardi. Paris, Secrétariat Général du Comité Français, 239 pp. (1951). [Pages 149-159 contain the reports of the Section of Terrestrial Magnetism and Electricity to the General Assembly of January 22, 1951.]

Geographical Survey Institute. Magnetic survey of Japan, 1948-1951. Bull. Geog. Surv. Inst. Japan, **2** Pts. 2-3, 121-166 (1951).

Geographical Survey Institute. The observations of the vertical deflection in Japan (1947-1950). Bull. Geog. Surv. Inst. Japan, **2**, Pts. 2-3, 167-237 (1951).

Graham, J. W. Note on the significance of inverse magnetizations of rocks. J. Geophys. Res., **57**, No. 3, 429-431 (1952). [Letter to Editor.]

Greenwich, Royal Observatory. Results of the magnetic and meteorological observations made at the Abinger magnetic station, Surrey, and the Royal Observatory, Greenwich, respectively, in the year 1938. London, H. M. Stationery Office, xx + 83 + 10 pls. (1951). 30 cm.

Haalck, H. Über die Ursachen des magnetischen Rindenfeldes der Erde. Beitr. Geophysik., **62**, Heft 3, 208-221 (1952).

Hasegawa, M. and H. Maeda. A suggestion for the electric conductivity of the upper atmosphere from an analysis of diurnal variations of terrestrial magnetism. Rep. Ionosphere Res. Japan, **5**, No. 4, 167-178 (1951); **6**, No. 3, 159-161 (1952).

Hermanus Magnetic Observatory. Magnetic observations, 1947-1948. Govt. Printer, Pretoria, 121 pp. (1952).

Kakioka Magnetic Observatory. Report of the Kakioka Magnetic Observatory, Geomagnetism 1936, 1937. Kakioka, 103 pp. with 19 pls. (1952).

Kato, Y., and J. Ossaka. Time variation of the earth's magnetic field at the time of bay-disturbance. Rep. Ionosphere Res. Japan, **6**, No. 1, 37-41 (1952).

Koenigsfeld, L. Observations magnétique faites à Manhay (Belgique) pendant l'année 1950. Liege, Les Presses de "Lejeunia" (40 pp., 1952). [Université de l'Liege, Institut d'Astronomie et de Géodésie, Physique du Globe, No. 14.]

Macht, H. G. Die Potentialanteile zweiter und höherer Ordnung des Erdmagnetfeldes—II. Beitr. Geophysik, 62, Heft 3, 222-247, and Heft 4, 288-301 (1952).

Mooney, H. M. Magnetic susceptibility measurements in Minnesota. Part I: Technique of measurement. Geophysics, 17, No. 3, 531-543 (1952).

Nagata, T. Distribution of SC* of magnetic storms. Rep. Ionosphere Res. Japan, 6, No. 1, 13-30 (1952)

Nagata, T., S. Uyeda, and S. Akimoto. Self-reversal of thermo-remanent magnetism of igneous rocks. Kyoto, J. Geomag. Geoelectr., 4, No. 1, 22-37 (1952).

Néel, L. Théorie du traînage magnétique de diffusion. J. Phys. Radium, 13, No. 5, 249-264 (1952).

Pramanik, S. K. Secular variation of the magnetic field at Colaba and Alibag. J. Geophys. Res., 57, No. 3, 339-355 (1952).

Press, F., and M. Ewing. Magnetic anomalies over oceanic structures. Trans. Amer. Geophys. Union, 33, No. 3, 349-355 (1952).

Teoloyucan, Observatorio Magnetico de. Valores magnéticos para 1948, 1949 y 1950. Universidad Nacional de Mexico, 42 pp. (1951).

Teoloyucan, Observatorio Magnetico de. Valores magnéticos correspondientes al 1er· Semestre de 1951. Universidad Nacional de Mexico, 21 pp. (1951).

Teoloyucan, Observatorio Magnetico de. Valores magnéticos correspondientes al 2°· Semestre de 1951. Universidad Nacional de Mexico, 23 pp. (1952).

Tromsö, Auroral Observatory. Results of magnetic observations for the year 1950. Bergen, Pub. Inst. Kosmisk Fysikk, No. 33, 31 pp. (1952).

United States Coast and Geodetic Survey. Magnetic hourly values, Cheltenham, 1949. Washington, D. C., U. S. Coast Geod. Surv., No. HV-Ch49, 44 pp. (1952).

United States Coast and Geodetic Survey. Magnetograms, San Juan, Puerto Rico, July-December 1949. Washington, D. C., U. S. Coast Geod. Surv., No. MG-J49.2, 54 pp. (1952).

B—*Terrestrial Electricity*

Cochet, R. Évolution d'une gouttelette d'eau chargée dans un nuage à temperature positive. Ann. Géophys., 8, No. 1, 33-54 (1952).

Dessens, H., C. Lafargue, et P. Stahl. Nouvelles recherches sur les noyaux de condensation. Ann. Géophys., 8, No. 1, 21-32 (1952).

Fritsch, V. Geoelektrische Untersuchungen an Blitzerdern. Beitr. Geophysik., 62, Heft 3, 164-207 (1952).

Israel, H., und H. W. Kasemir. Studien über das atmosphärische Potentialgefälle VI: Beispiele für das Verhalten luftelektrischer Elemente bei Nebel. Arch. Met. Geophys. Biokl., A, 5, Heft 1, 71-85 (1952)

Kasemir, H. W. Studien über das atmosphärische Potentialgefälle V: Zur Stromungstheorie des luftelektrischen Feldes II. Arch. Met. Geophys. Biokl., A, 5, Heft 1, 56-70 (1952).

O'Donnell, G. A. Electric conductivity and small ion concentration of the atmosphere at one metre above ground and conductivity at ground level. J. Atmos. Terr. Phys., 2, No. 4, 201-215 (1952).

Pollak, L. W., and T. Murphy. Sampling of condensation nuclei by means of a mobile photo-electric counter. Arch. Met. Geophys. Biokl., A, 5, Heft 1, 100-119 (1952).

Sucksdorff, E. Vom Polarlicht. Helsinki, SitzBer. Finn. Akad. Wiss., 1951, 97-109 (1952).

C—*Cosmic Rays*

Burbury, D. W. P., and K. P. Fenton. The high latitude east-west asymmetry of cosmic rays. Aust. J. Sci. Res., A, 5, No. 1, 47-58 (1952).

Clark, M. A. The hard component of cosmic rays in the upper atmosphere. Phys. Rev., 87, No. 1, 87-90 (1952).

Rollosson, G. W. A study of penetrating cosmic-ray showers in water. Phys. Rev., 87, No. 1, 71-74 (1952).

Singer, S. F. Diurnal variation of cosmic rays and the sun's magnetic field. Nature, 170, 63-64 (July 12, 1952).

D—*Upper Air Research*

Appleton, E. V., and W. R. Piggott. The morphology of storms in the F_2 layer of the ionosphere. I—Some statistical relationships. J. Atmos. Terr. Phys., **2**, No. 4, 236-252 (1952).

Bailey, V. A., R. A. Smith, K. Landecker, A. J. Higgs, and F. H. Hibberd. Resonance in gyro-interaction of radio waves. Nature, **169**, 911-913 (May 31, 1952).

Banerji, R. B. On the origin of the third ionospheric echo. Indian J. Phys., **26**, No. 1, and Proc. Indian Assoc. Cultivation Science, **35**, No. 1, 28-37 (1952).

Bates, D. R. Absorption of radiation by an atmosphere of H, H^+, and H_2^+. Mon. Not. R. Astr. Soc., **112**, No. 1, 40-44 (1952).

Bates, D. R., and H. S. W. Massey. On negative ions of molecular oxygen in the *D*-Layer. J. Atmos. Terr. Phys., **2**, No. 4, 253-254 (1952).

Bracewell, R. N. Theory of formation of an ionospheric layer below *E* layer based on eclipse and solar flare effects at 16 kc/sec. J. Atmos. Terr. Phys., **2**, No. 4, 226-235 (1952).

Bracewell, R. N., and W. C. Bain. An explanation of radio propagation at 16 kc/sec in terms of two layers below *E* layer. J. Atmos. Terr. Phys., **2**, No. 4, 216-225 (1952).

Chapman, S. Meteors and meteorites. J. Wash. Acad. Sci., **42**, No. 9, 273-282 (1952).

Ehmert, A. Gleichzeitige Messungen des Ozongehaltes bodennaher Luft an mehreren Stationen mit einem einfachen absoluten Verfahren. J. Atmos. Terr. Phys., **2**, No. 3, 189-195 (1952).

Elterman, L. A reply to Lewis D. Kaplan's comments on density measurements with the searchlight technique. J. Geophys. Res., **57**, No. 3, 428-429 (1952). [Letter to Editor.]

Geophysical Research Division, Air Force Cambridge Research Center. Proceedings of the conference on ionospheric physics (July 1950), Part A (edited by N. C. Gerson and R. J. Donaldson, Jr.). Geophysical Research Papers, No. 11, 285 pp. (April 1952).

Geophysical Research Division, Air Force Cambridge Research Center. Proceedings of the conference on ionospheric physics (July 1950), Part B (edited by L. Katz and N. C. Gerson). Geophysical Research Papers, No. 12, 114 pp. (April 1952).

Gibbons, J. J., and R. J. Nertney. Wave solutions, including coupling, of ionospherically reflected long waves for a particular *E*-region model. J. Geophys. Res., **57**, No. 3, 323-338 1952).

Graffi, D. Meccanica, ottica geometrica e propagazione ionosferica. Nuovo Cimento, supplemento al **8**, No. 2, 156-167 (1952).

Hirono, M. On the influence of the Hall current to the electrical conductivity of the ionosphere. Rep. Ionosphere Res. Japan, **6**, No. 1, 44-45 (1952).

Johnson, M. H. The relation between electrical and diffusion currents. J. Geophys. Res., **57**, No. 3, 405-412 (1952).

Kaplan, L. D. Some comments on L. Elterman's "The measurement of stratospheric density distribution with the searchlight technique." J. Geophys. Res., **57**, No. 3, 426-427 (1952). [Letter to Editor.]

Kelso, J. M. A procedure for the determination of the vertical distribution of the electron density in the ionosphere. J. Geophys. Res., **57**, No. 3, 357-367 (1952).

Koomen, M. J., C. Lock, D. M. Packer, R. Scolnik, R. Tousey, and E. O. Hulburt. Measurements of the brightness of the twilight sky. J. Optical Soc. Amer., **42**, No. 5, 353-356 (1952).

Lange-Hesse, G. Vergleich der Doppelbrechung im Kristall und in der Ionosphäre. Archiv Elektr. Uebertrag., **6**, Heft 4, 149-158 (1952).

Manning, L. A., O. G. Villard, Jr., and A. M. Peterson. Double-Doppler study of meteoric echoes. J. Geophys. Res., **57**, No. 3, 387-403 (1952).

Mitra, A. P. Effects of the variations of recombination coefficient and scale height on the structures of the ionized regions. Indian J. Phys., **26**, No. 2, and Proc. Indian Assoc. Cultivation Science, **35**, No. 2, 79-102 (1952).

Nagata, T. The solar flare type variation in geomagnetic field and the integrated electric conductivity of the ionosphere. (IV) The conductivity of the ionosphere over Japan. Rep. Ionosphere Res. Japan, **5**, No. 3, 123-128 (1951).

Nagata, T., and M. Tazima. The solar flare type variation in geomagnetic field and the integrated electric conductivity of the ionosphere. (III) Effect of the earth. Rep. Ionosphere Res. Japan, **5**, No. 3, 113-121 (1951).

Nertney, R. J. Reply to [preceding] note of J. B. Smyth. J. Geophys. Res., 57, No. 3, 423-425 (1952). [Letter to Editor.]

Paetzold, H. K. Erfassung der vertikalen Ozonverteilung in verschiedenen geographischen Breiten bei Mond fin sternissen. J. Atmos. Terr. Phys., 2, No. 3, 183-188 (1952).

Payne-Scott, R., and A. G. Little. The position and movement on the solar disk of sources of radiation at a frequency of 97 Mc/s. III—Outbursts. Aust. J. Sci. Res., A, 5, No. 1, 32-46 (1952).

Petrie, W. Rotational temperatures of Vegard-Kaplan auroral bands. Phys. Rev., 86, No. 5, 790-791 (1952).

Phillips, G. J. Measurement of winds in the ionosphere. J. Atmos. Terr. Phys., 2, No. 3, 141-154 (1952).

Piddington, J. H., and H. C. Minnett. Radio-frequency radiation from the constellation of Cygnus. Aust. J. Sci. Res., A, 5, No. 1, 17-31 (1952).

Regener, E. Über Schwankungen des Ozons in der Troposphäre und Stratosphäre. J. Atmos. Terr. Phys., 2, No. 3, 173-182 (1952).

Scott, J. C. W. The solar control of the E and $F1$ layers at high latitudes. J. Geophys. Res., 57, No. 3, 369-386 (1952).

Smyth, J. B. Note on Gibbons-Nertney paper, "A method for obtaining the wave solutions of ionospherically reflected long waves, including all variables and their height variation." J. Geophys. Res., 57, No. 3, 423 (1952). [Letter to Editor; see also *ibid.*, pp. 425-426 for concluding comments.]

Vegard, L. Recent advances in auroral spectroscopy and in our knowledge of the upper atmosphere. Ann. Géophys., 8, No. 1, 91-99 (1952).

E—*Earth's Crust and Interior*

Denson, M. E., Jr. Longitudinal waves through the earth's core. Bull. Seis. Soc. Amer., 42, No. 2, 119-134 (1952).

Eskola, P. The problems of the beginning of the earth and the universe. Helsinki, SitzBer. Finn. Akad. Wiss., 1951, 93-95 (1952).

Evans, P. Mountains and gravity. Nature, 169, 1079-1080 (June 28, 1952).

Gutenberg, B. Waves from blasts recorded in southern California. Trans. Amer. Geophys. Union, 33, No. 3, 427-431 (1952).

Jeffreys, H. Problems of thermal instability in a sphere. Mon. Not. R. Astr. Soc., 6, No. 5, 272-277 (1952).

Rikitake, T. Electromagnetic induction within the earth and its relation to the electrical state of the earth's interior. Part IV (in English). Bull. Earthquake Res. Inst., Tokyo Univ., 29, Pt. 4, 539-547 (1952).

Rodgers, J. Absolute ages of radioactive minerals from the Appalachian region. Amer. J. Sci., 250, No. 6, 411-427 (1952).

Stoyko, N. Sur les relations entre la variation de la rotation, l'oscillation libre et les tremblements de Terre. Paris, C.-R. Acad. sci., 234, No. 26, 2550-2552 (1952).

Valle, P. E. Sul gradient adiabatico di temperatura nell'interno della Terra. Ann. Geofis., Roma, 5, No. 1, 41-53 (1952).

F—*Miscellaneous*

Azambuja, L. d'., et R. Servajeans. Cartes synoptiques de la chromosphère solaire et catalogue des filaments de la couche supérieure (Vol. 1, Fasc. 9, années 1940 a 1944). Orléans, Impremerie Nouvelle, 142 pp. (1952). 32 cm. [Observatoire de Paris, Section d'Astrophysique, à Meudon.]

Barbier, D. Les atmosphères stellaires. Paris, E. Flammarion, 238 pp. (1952). 19 cm.

Douglas, A. V. The origin of the planets. J. R. Astr. Soc. Can., 46, No. 3, 105-109 (1952).

Newton, H. W., and H. Howe. Area changes in sunspots and solar flare incidence. Observatory, 72, No. 868, 111-117 (1952).

INDEX OF AUTHORS

Volume 57, 1952

NOTICE

When available, single unbound volumes can be supplied at $3.50 each and single numbers at $1 each, postpaid.

Charges for reprints and covers

Reprints can be supplied, but prices have increased considerably and costs depend on the number of articles per issue for which reprints are requested. It is no longer possible to publish a schedule of reprint charges, but if reprints are requested approximate estimates will be given when galley proofs are sent to authors. Reprints without covers are least expensive; standard covers (with title and author) can be supplied at an additional charge. Special printing on covers can also be supplied at further additional charge.

Fifty reprints, without covers, will be given to institutions paying the publication charge of $4.00 per page.

Alterations

Major alterations made by authors in proof will be charged at cost. Authors are requested, therefore, to make final revisions on their typewritten manuscripts.

Orders for back issues and reprints should be sent to Editorial Office, 5241 Broad Branch Road, N.W., Washington 15, D.C., U.S.A.

Subscriptions only are handled by The Johns Hopkins Press, Baltimore 18, Maryland, U.S.A.

CONTENTS—Concluded

JOURNAL OF GEOPHYSICAL RESEARCH